Modular and Cyclic Structure in a Vertebrate Sensorimotor Neuronal Circuit

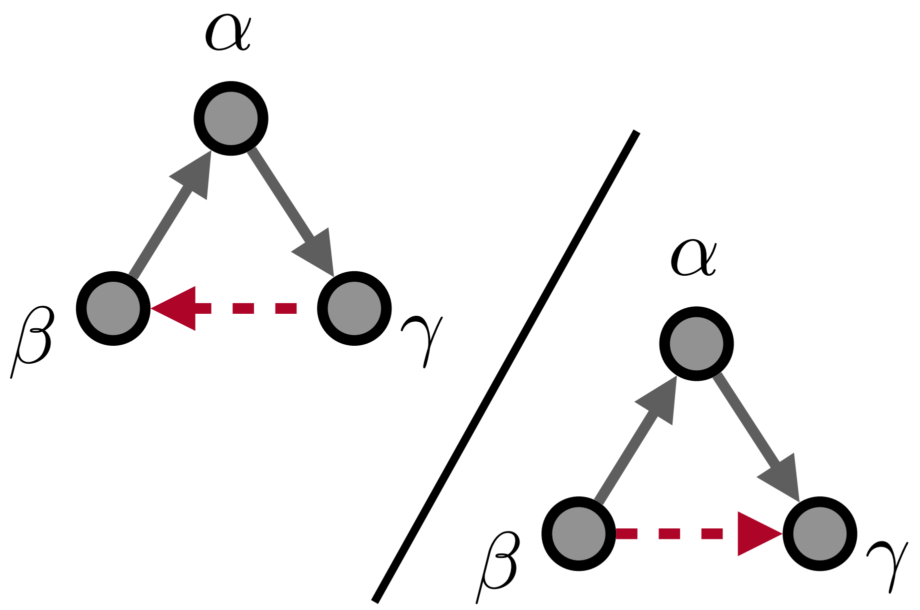

"Tony" Runzhe Yang

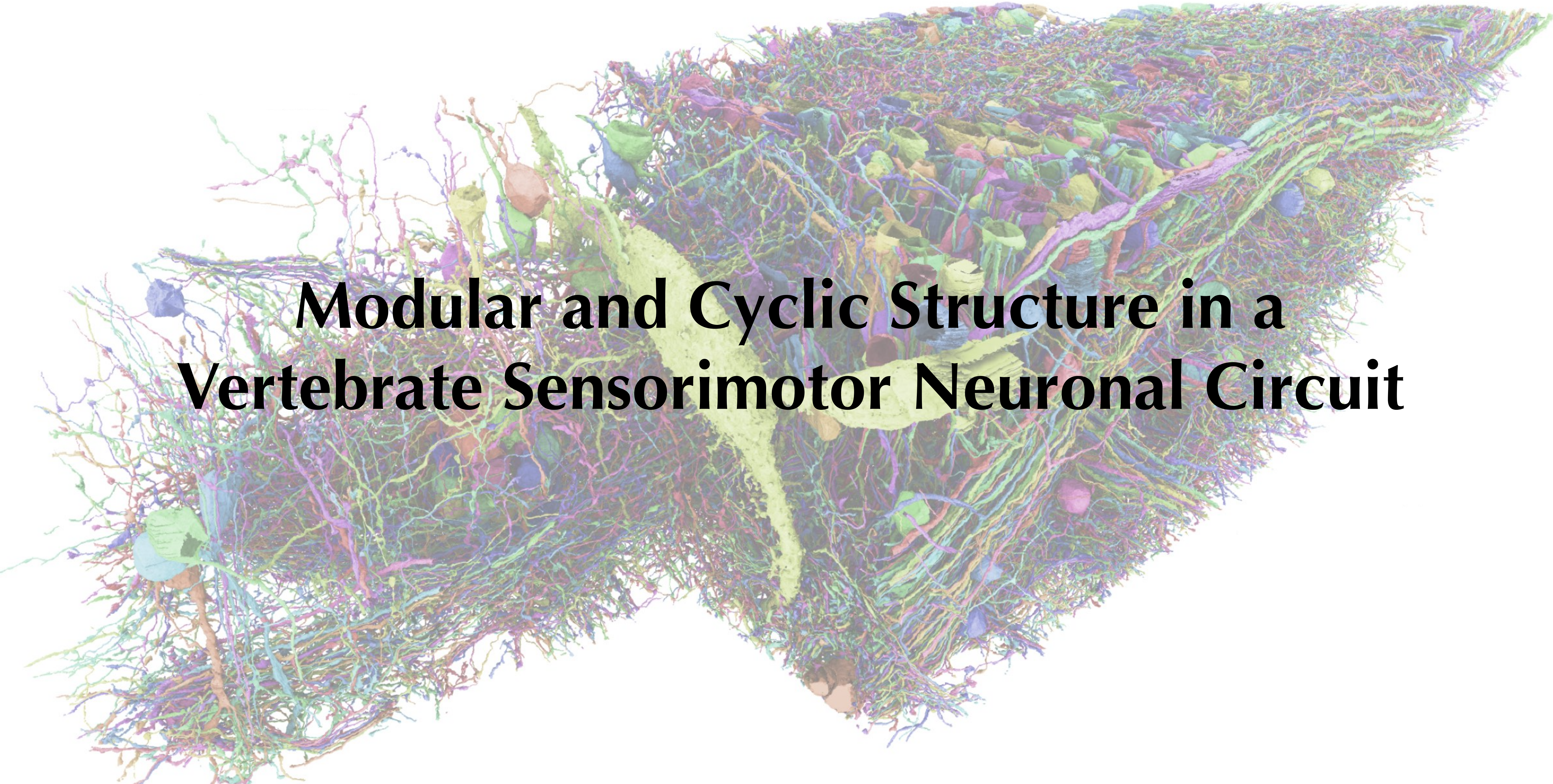

Modular and Cyclic Structure in a Vertebrate Sensorimotor Neuronal Circuit

“Tony” Runzhe Yang

Dr. Ashwin Vishwanathan

Prof. Emre Aksay

Prof. Mark Goldman

Prof. Sebastian Seung

The Connectomic Era has come

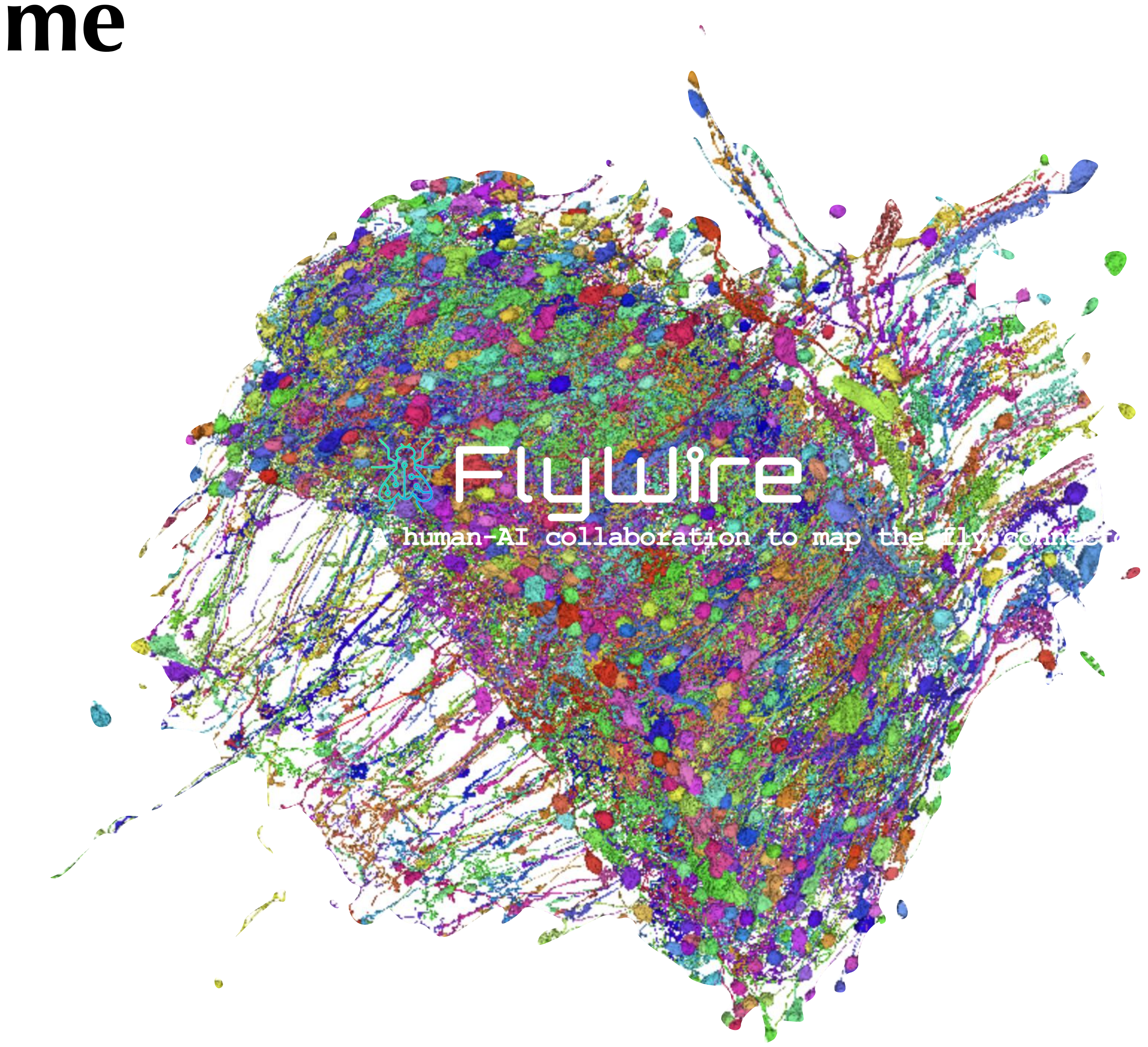

https://flywire.ai

adult *Drosophila, whole brain*

……

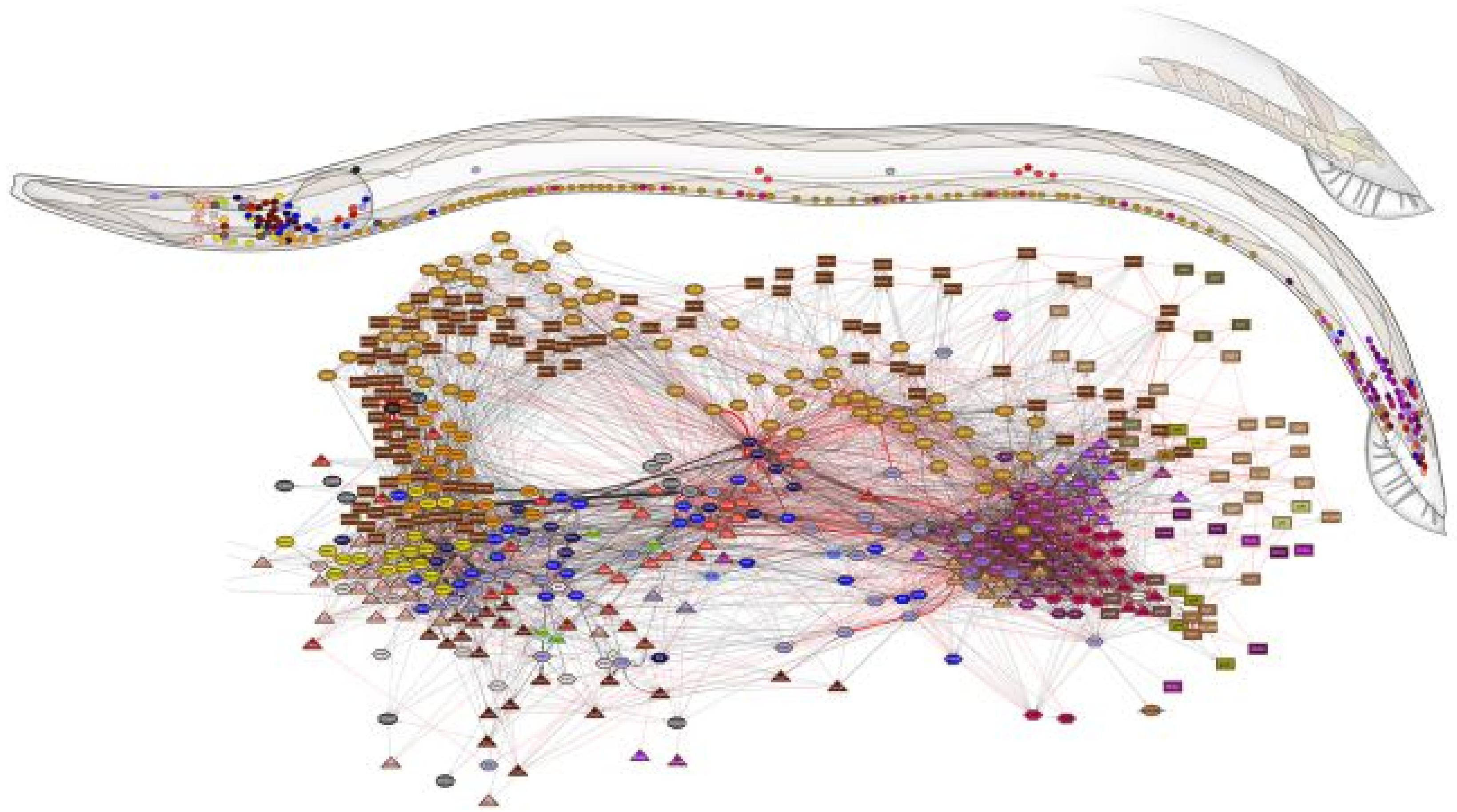

https://wormwiring.org

C. elegans, whole connectomes

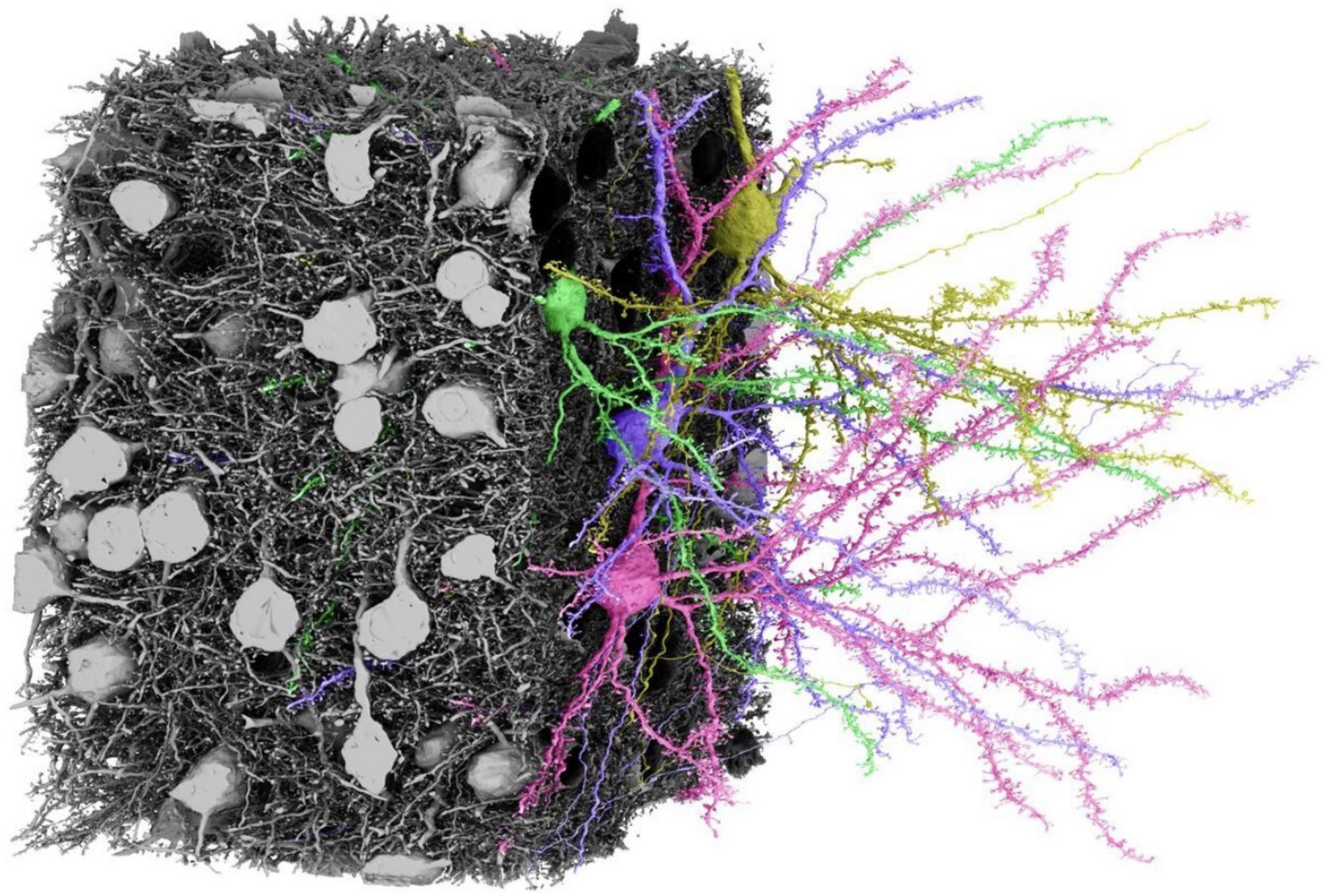

https://www.microns-explorer.org/

1mm^3 mouse visual cortex

EM reconstruction of a larval zebrafish brainstem

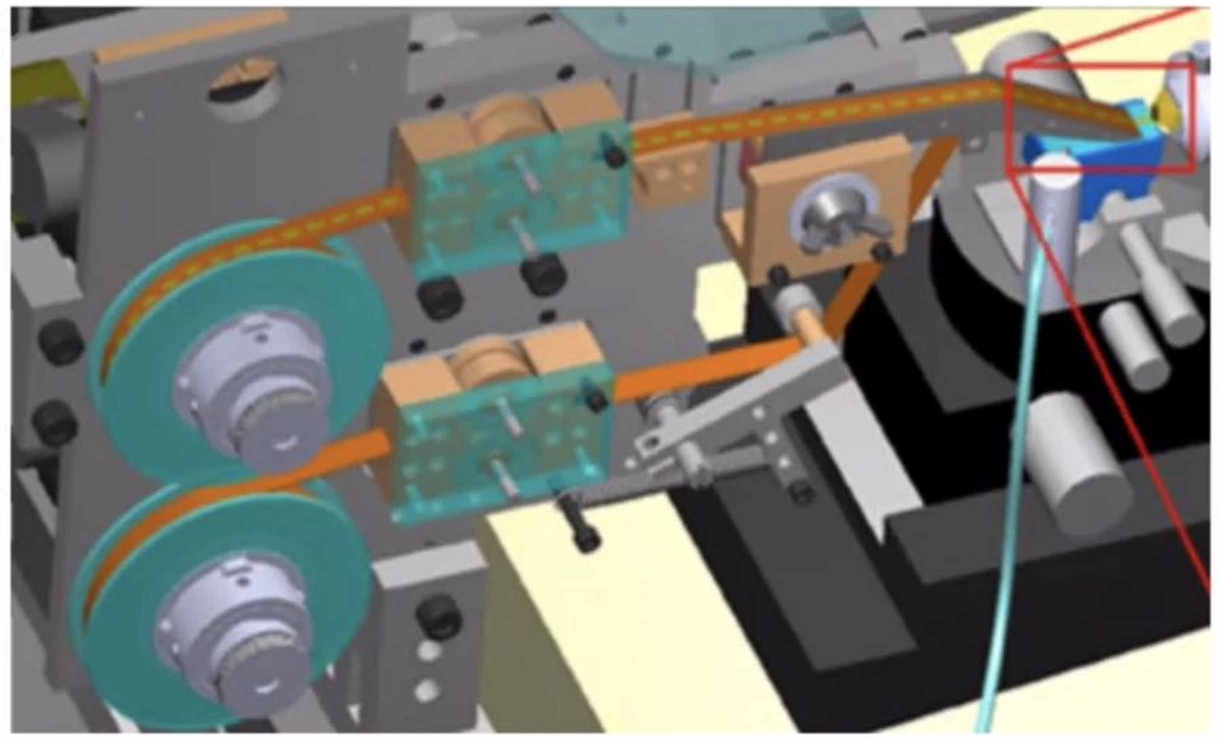

Hayworth et. al. 2014

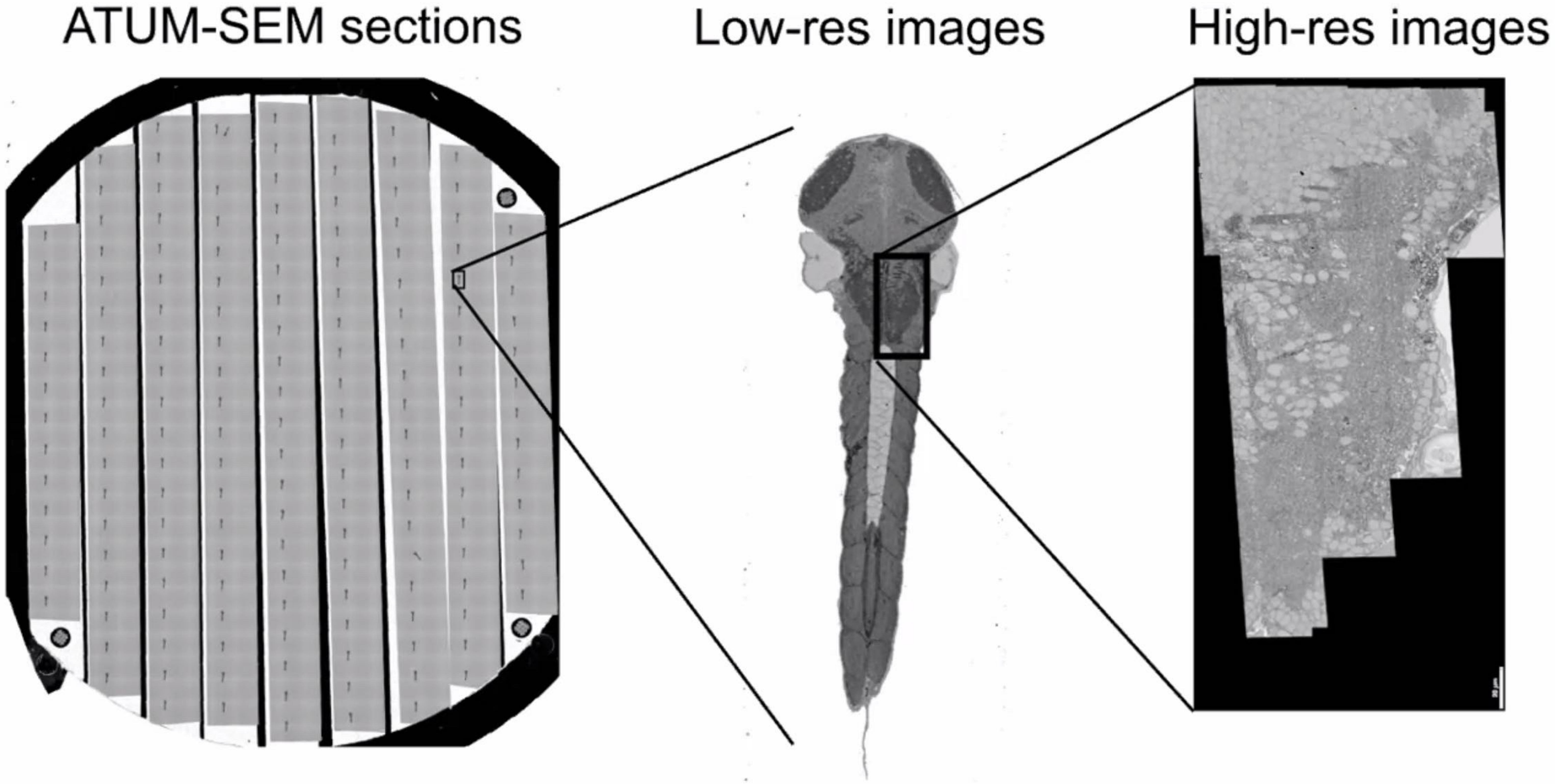

Varshney et. al. 2017

Each voxel: 5x5x45 nm^3

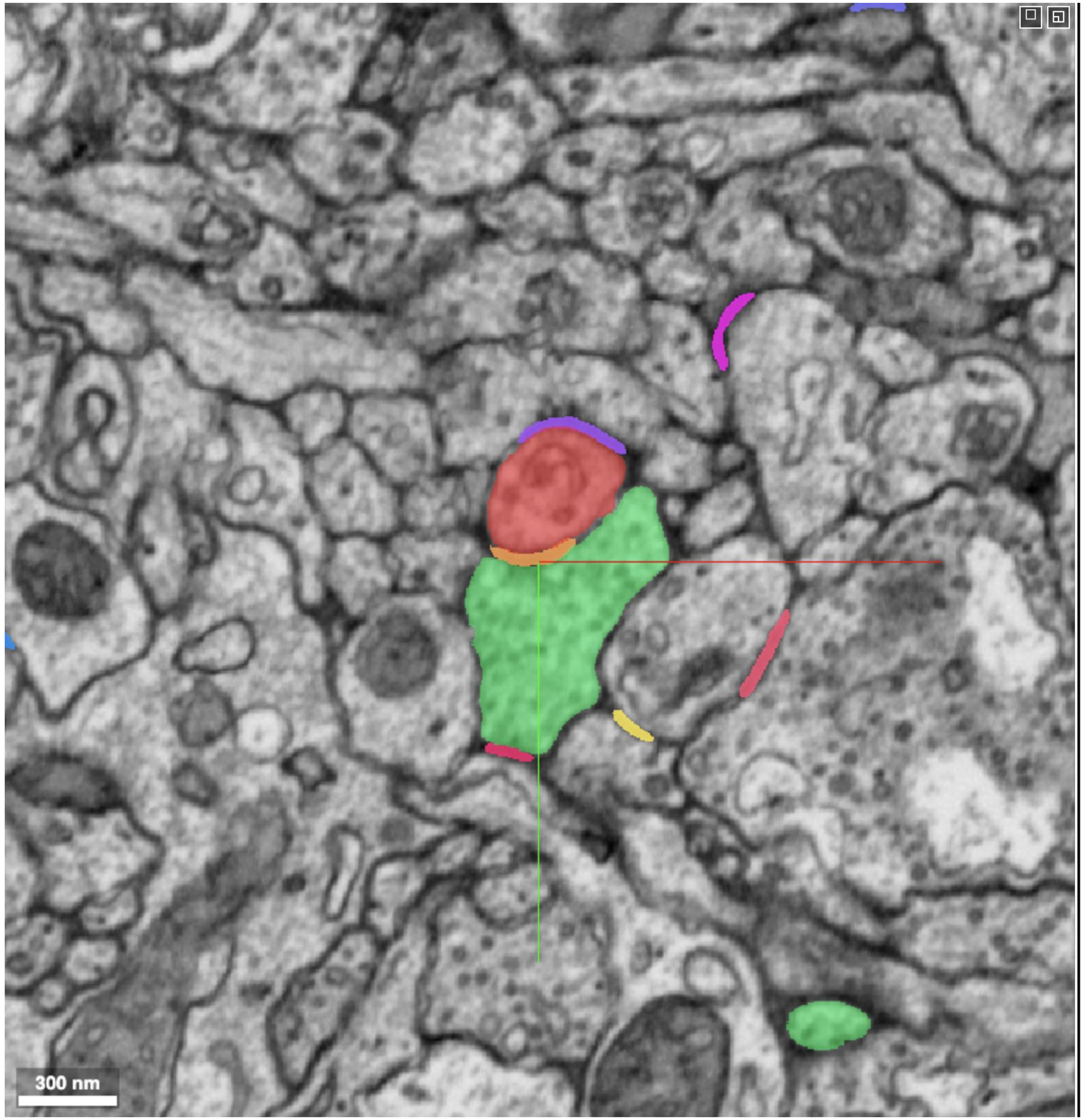

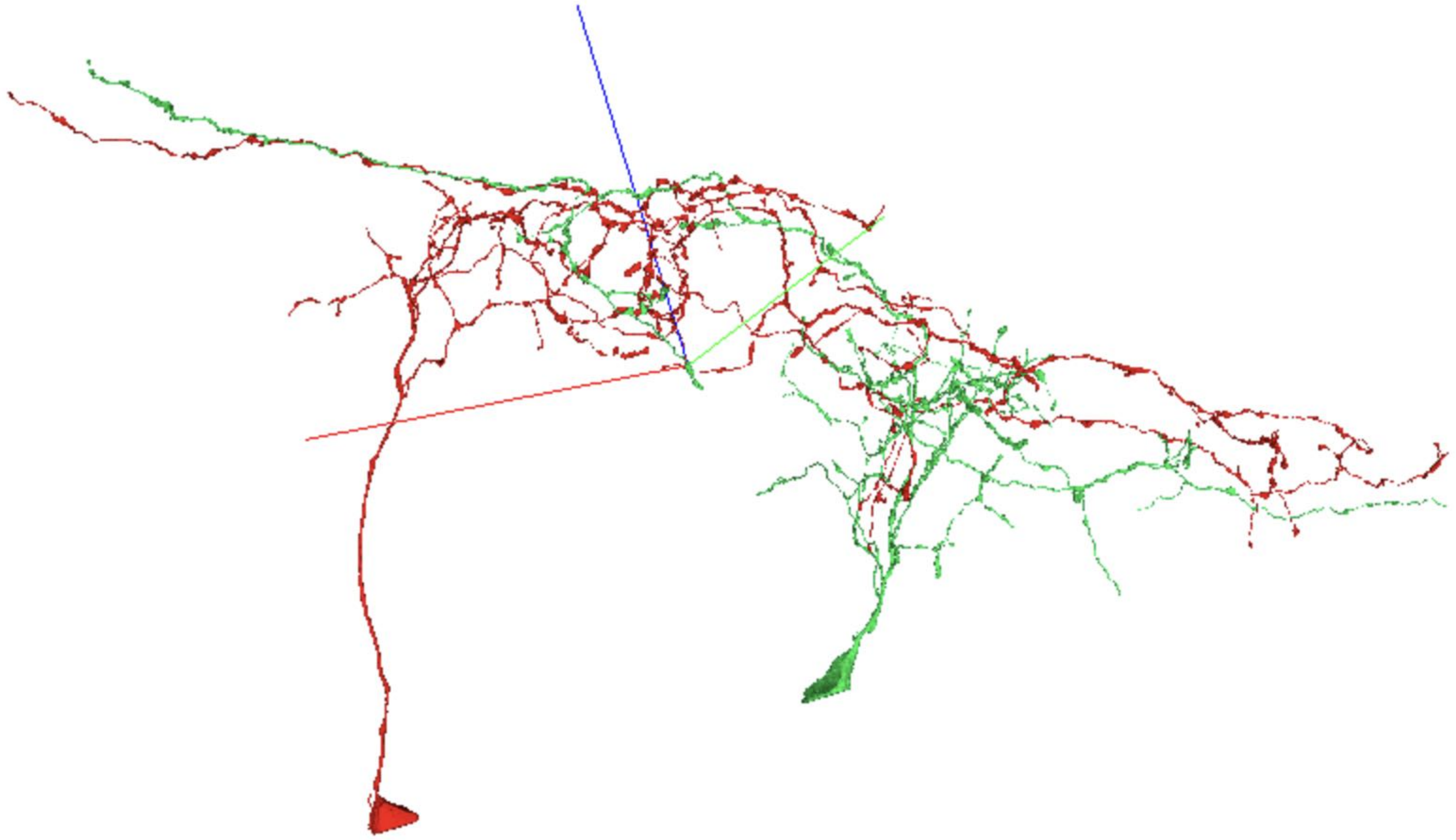

EM reconstruction of a larval zebrafish brainstem

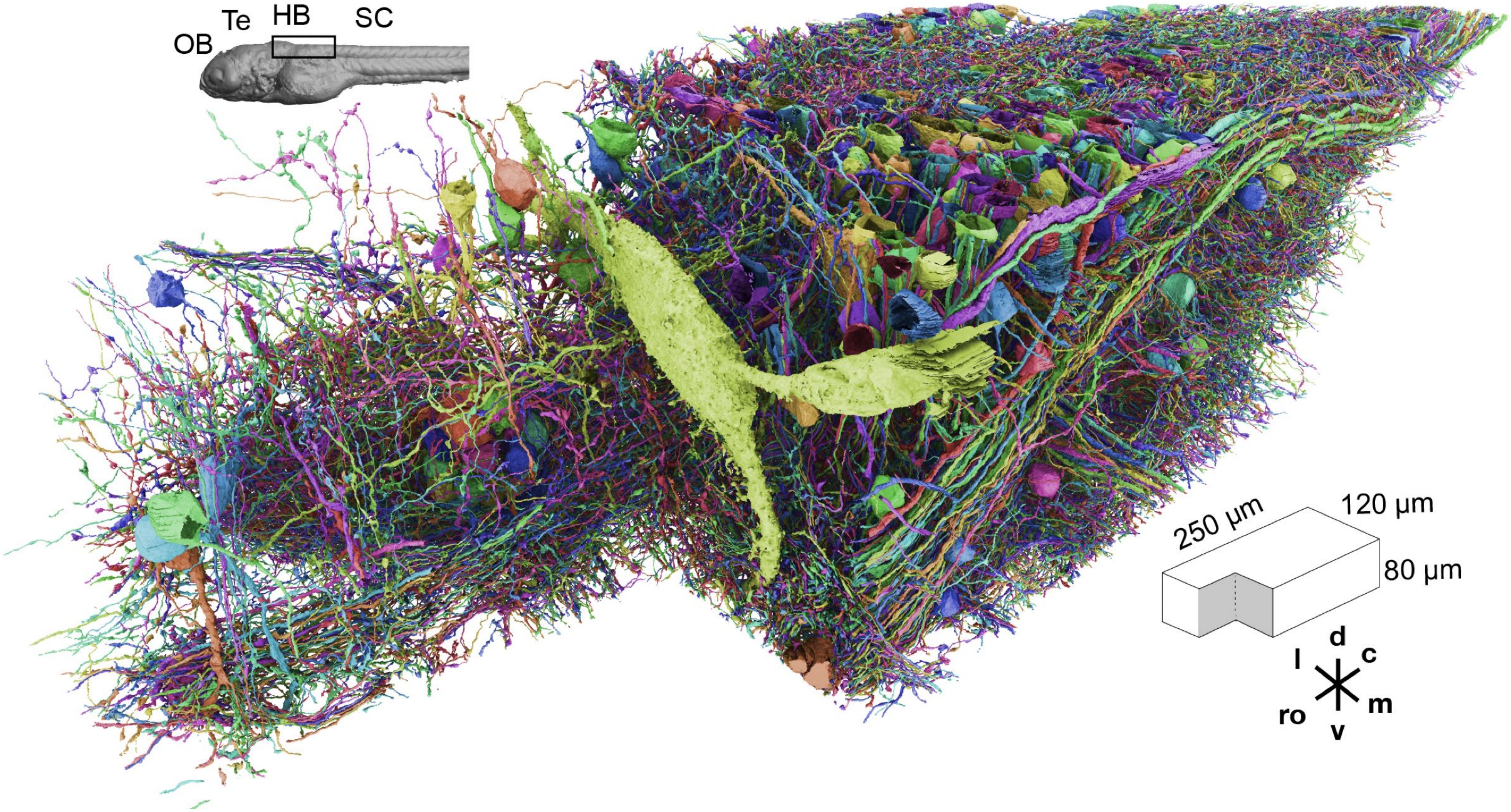

Rhobomeres 4 to 7/8

2,883 neurons

44,969 connections

75,195 synapses (within graph)

261,528 pre-synapses

248,826 post-synapses

Most neurons
are in the "periphery"
(~2344 in the previous paper)

The classic vestibule-ocular reflex (VOR) is feedforward

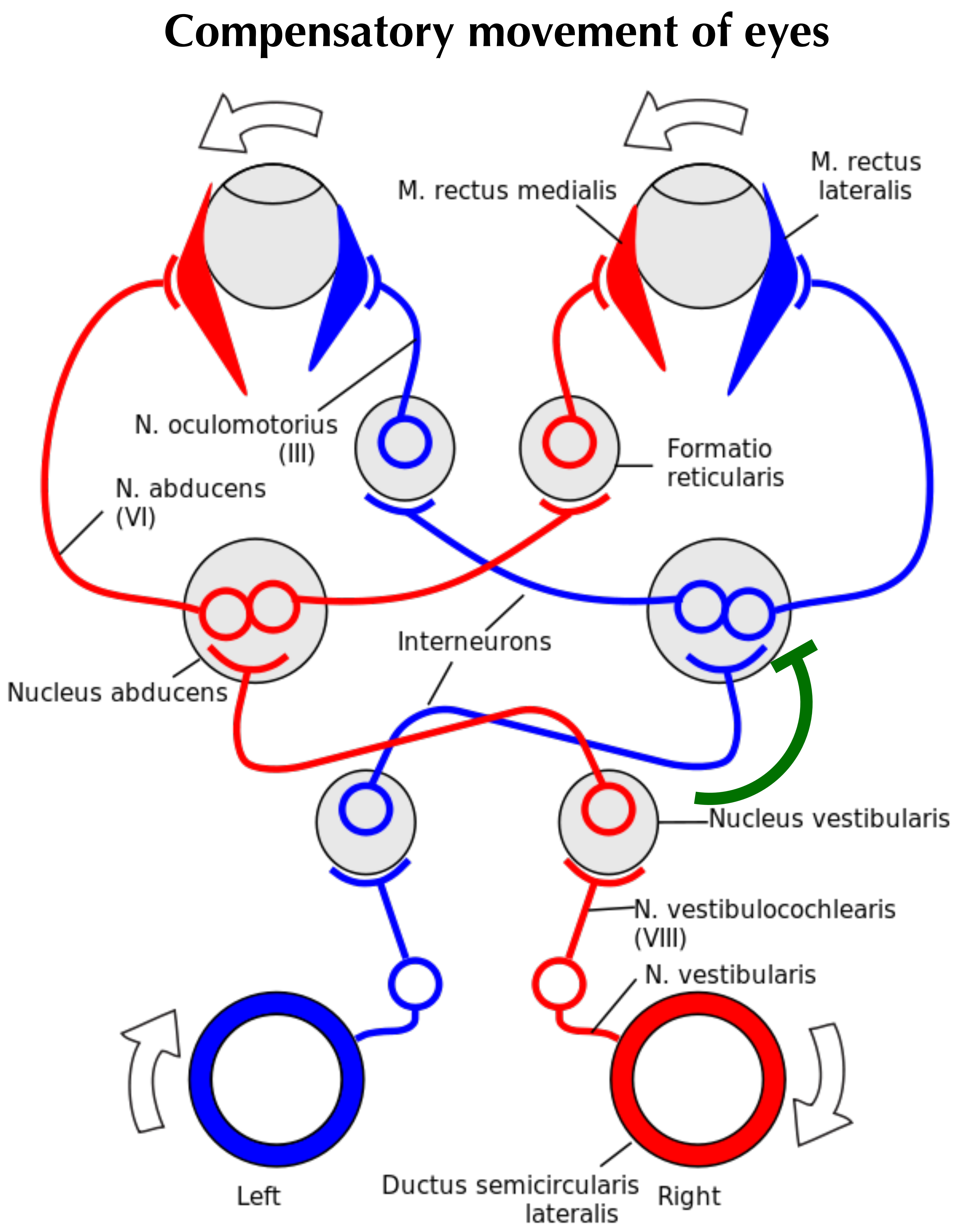

Registration to Z-Brain atlas help identify neurons

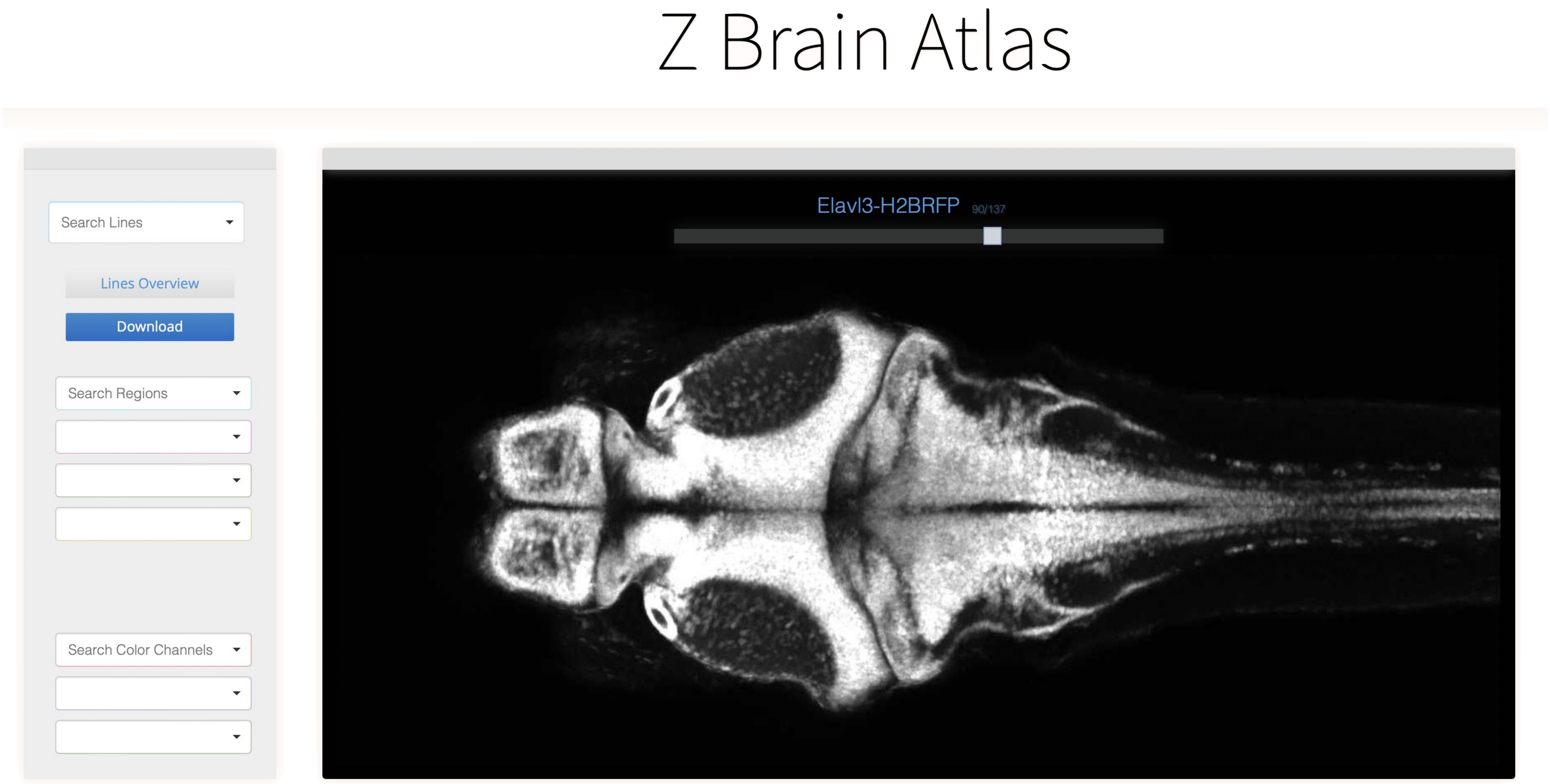

Randlett et al. 2015 from Engert Lab

Identifying descending octaval (DO) neurons by originating from vestibulocochlear nerve

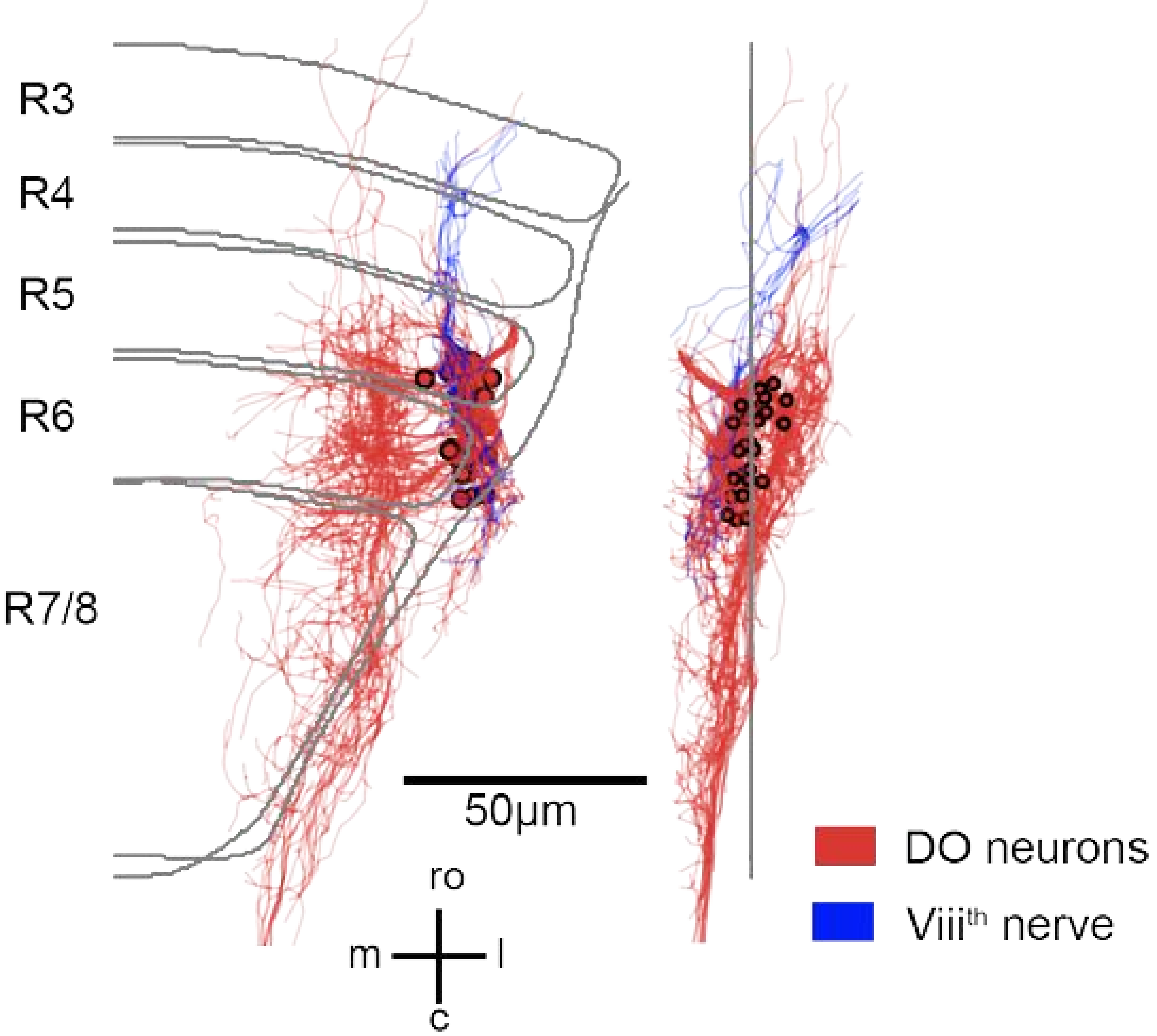

Vestibulocochlear nerve

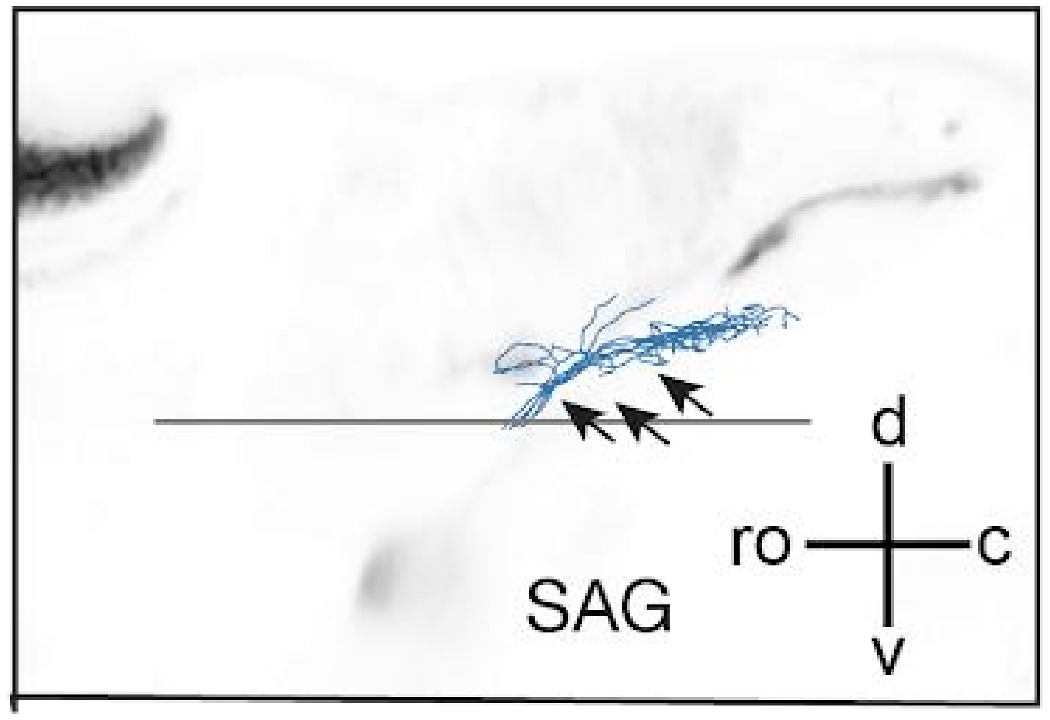

Maximum intensity projection

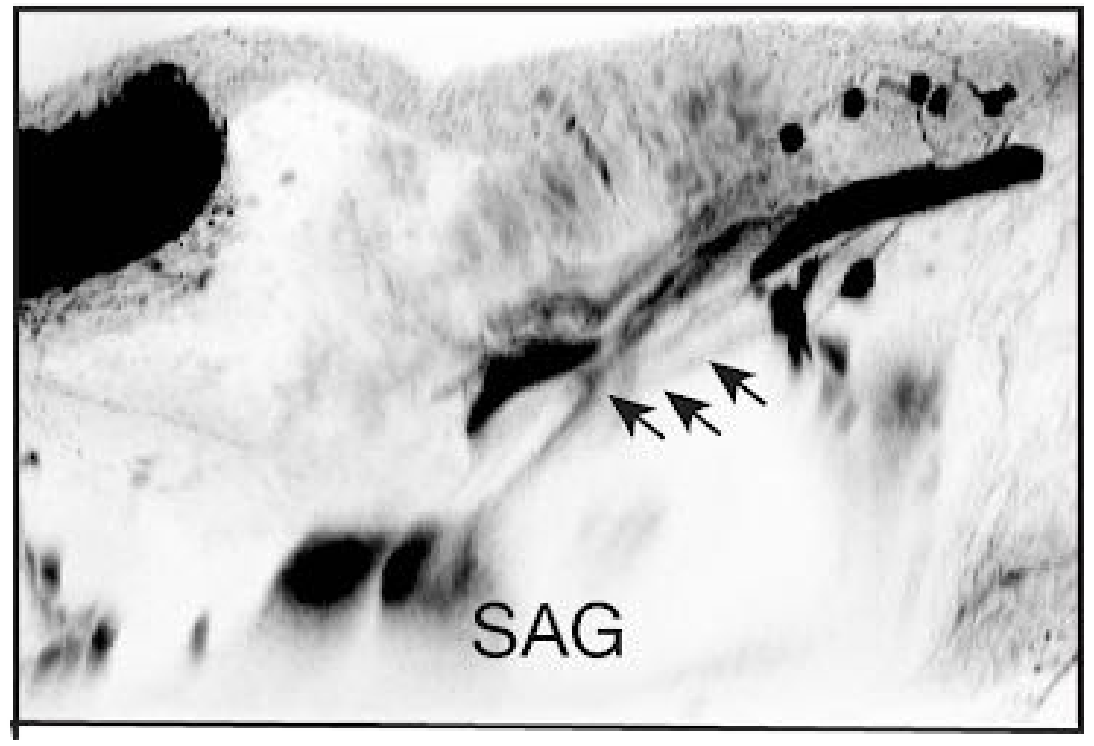

ZBB-isl2-GFP

Zbb-gad1b-GFP

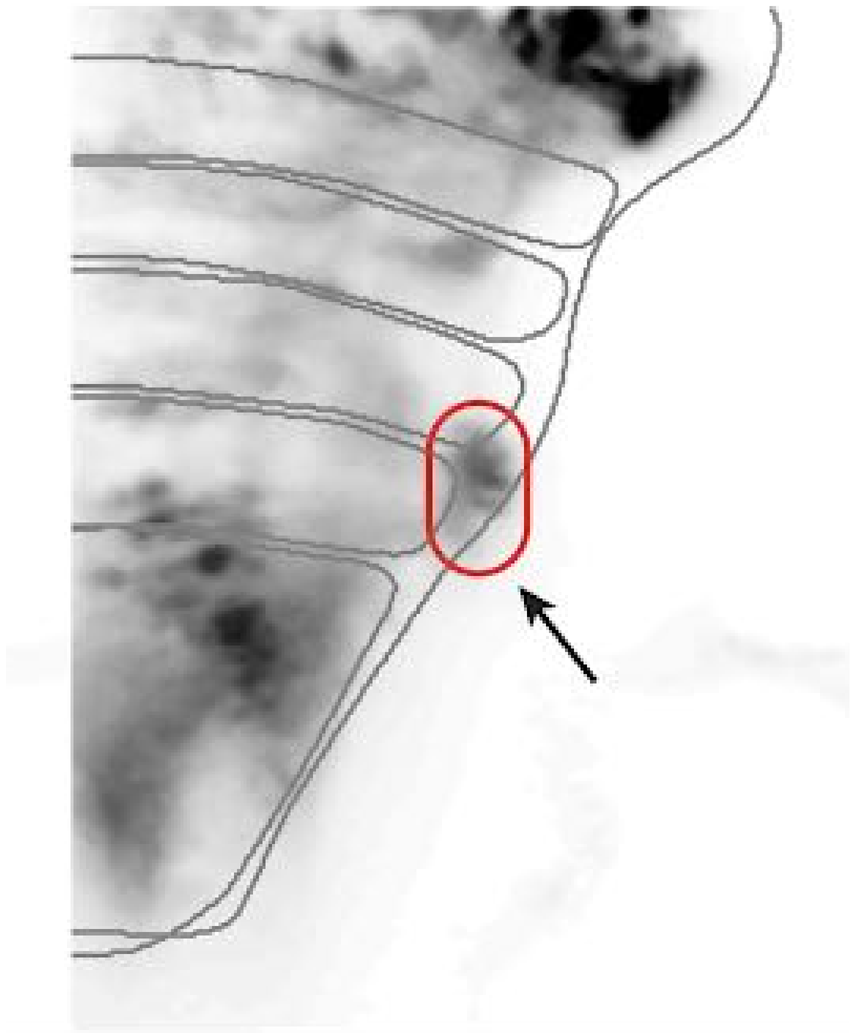

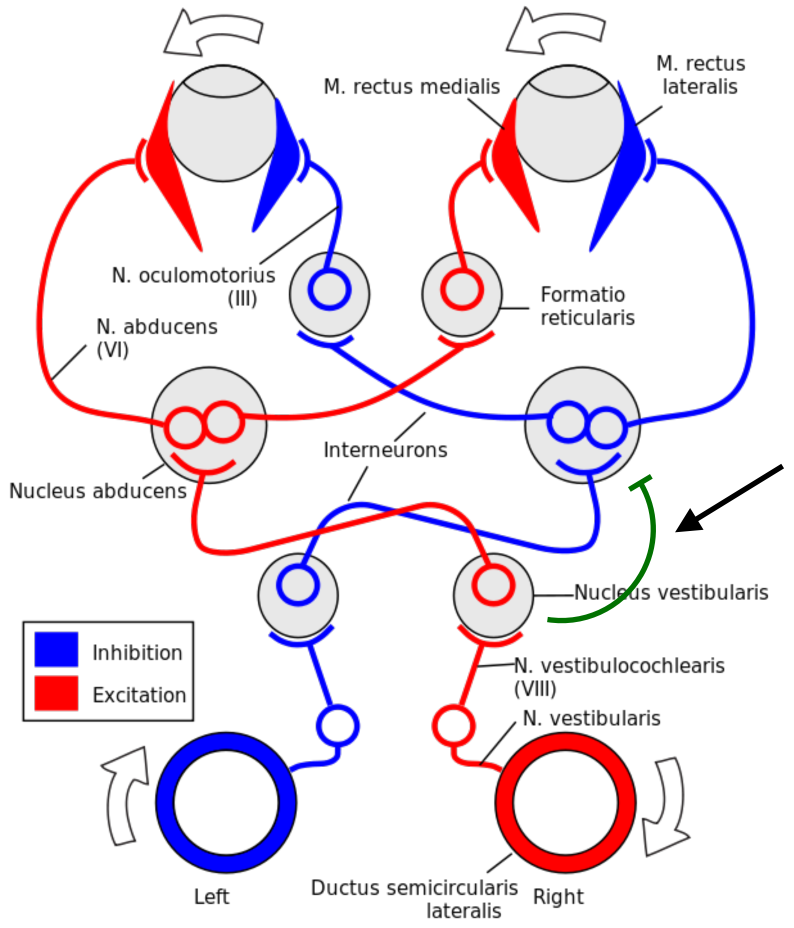

DO neurons

Identifying abducens (ABD) neurons by overlapping with transgenic lines

32 abducens motor neurons (ABD_M)

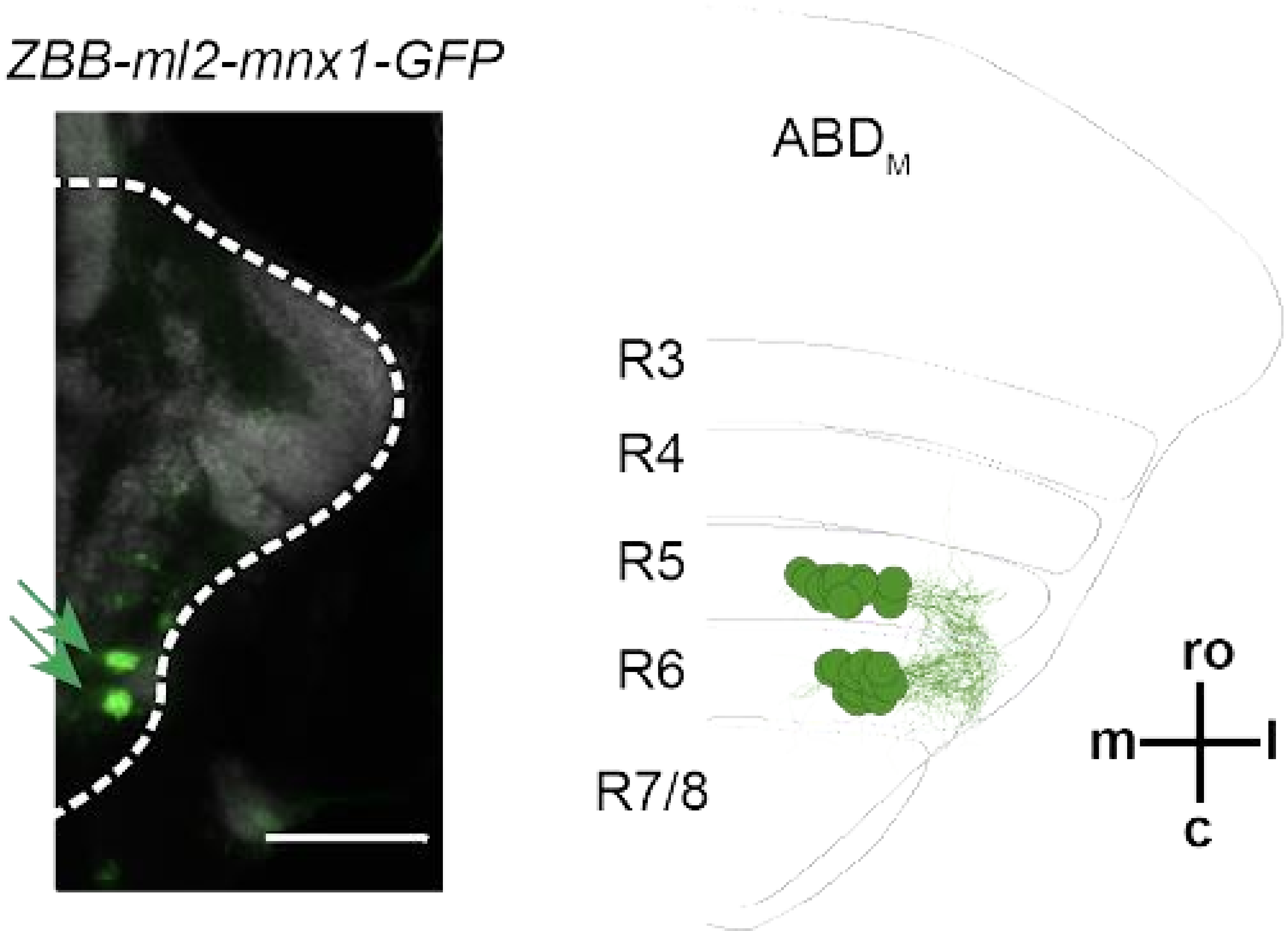

22 abducens internuclear neurons (ABD_I)

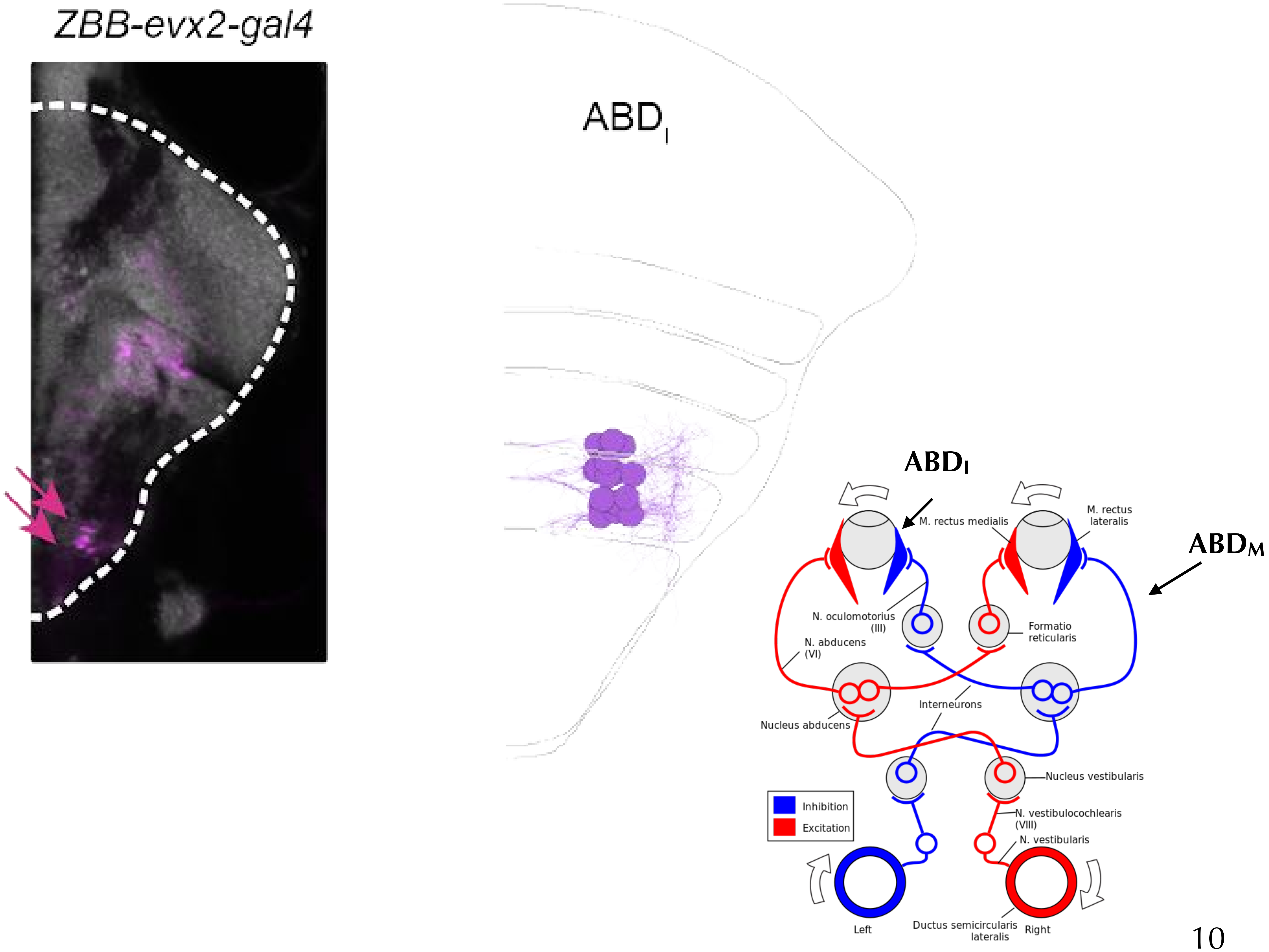

Identifying of reticulospinal (RS) neurons by overlapping with spinal backfills

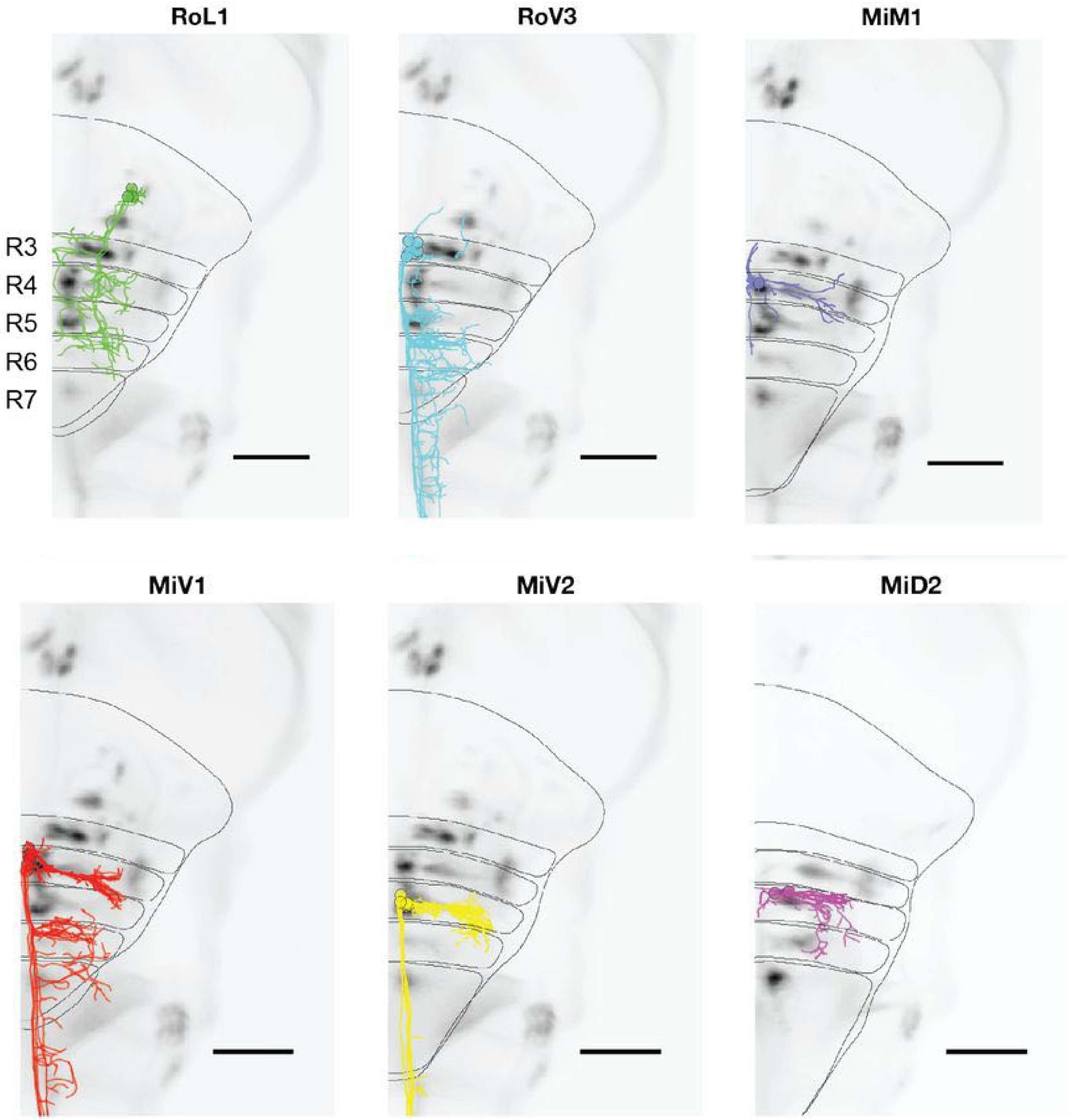

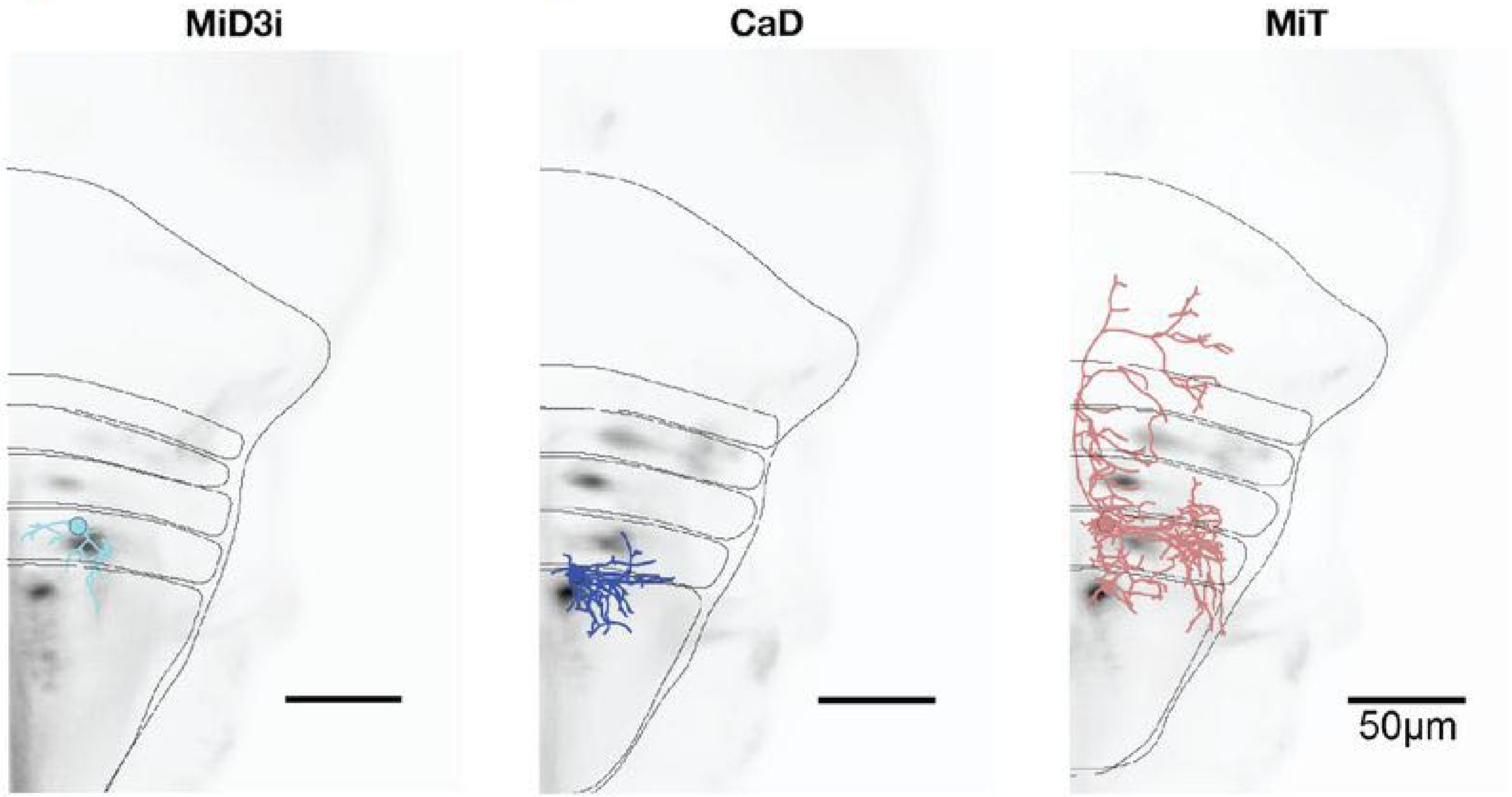

\

Alleviate truncation effect by restricting to “center” subgraph neurons

neurons with
 # presynpases > threshold

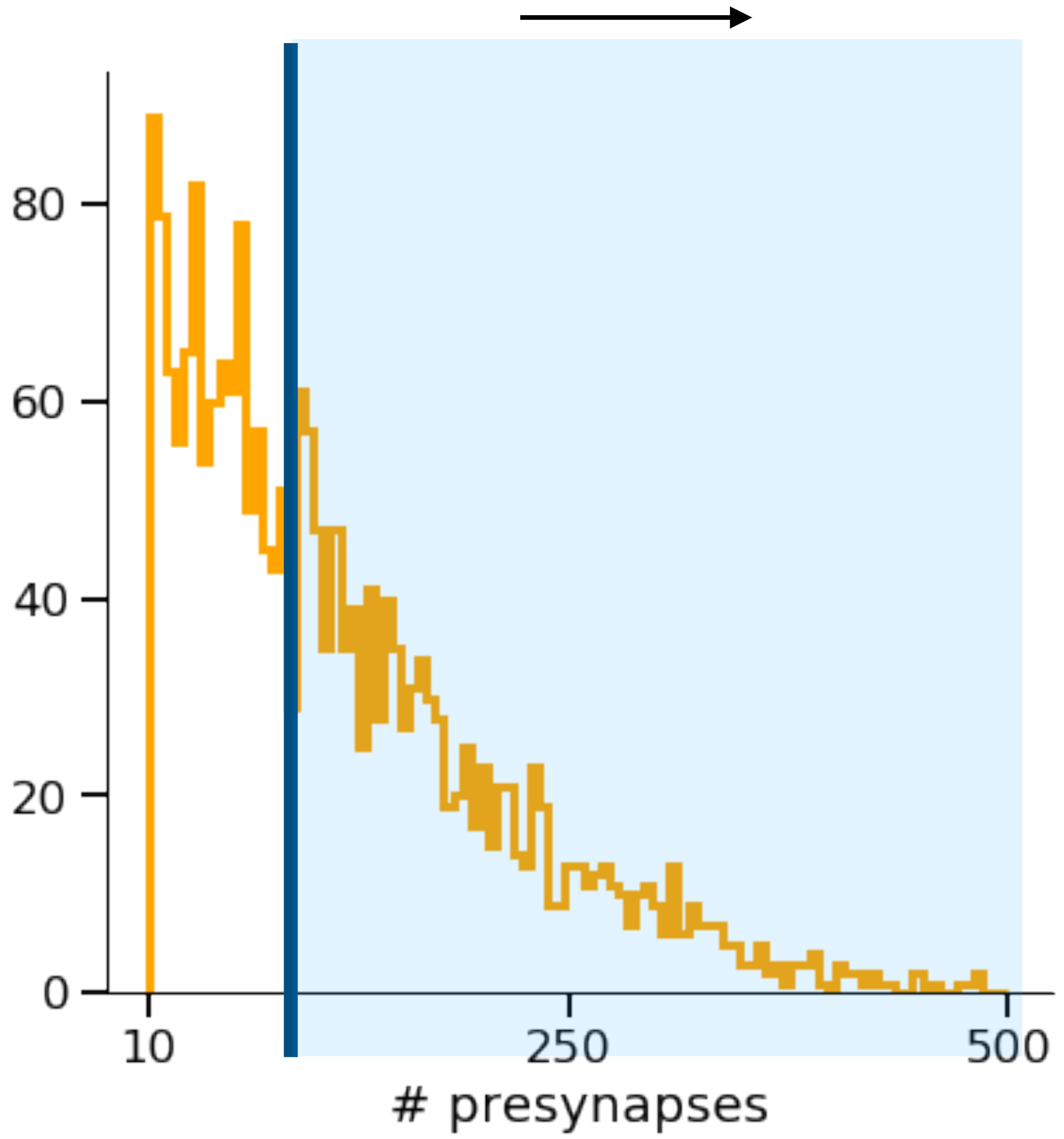

(relatively complete axons)

Alleviate truncation effect by restricting to “center” subgraph neurons

neurons with
 # presynpases > threshold ∩ **neurons with**
 # postynpases > threshold

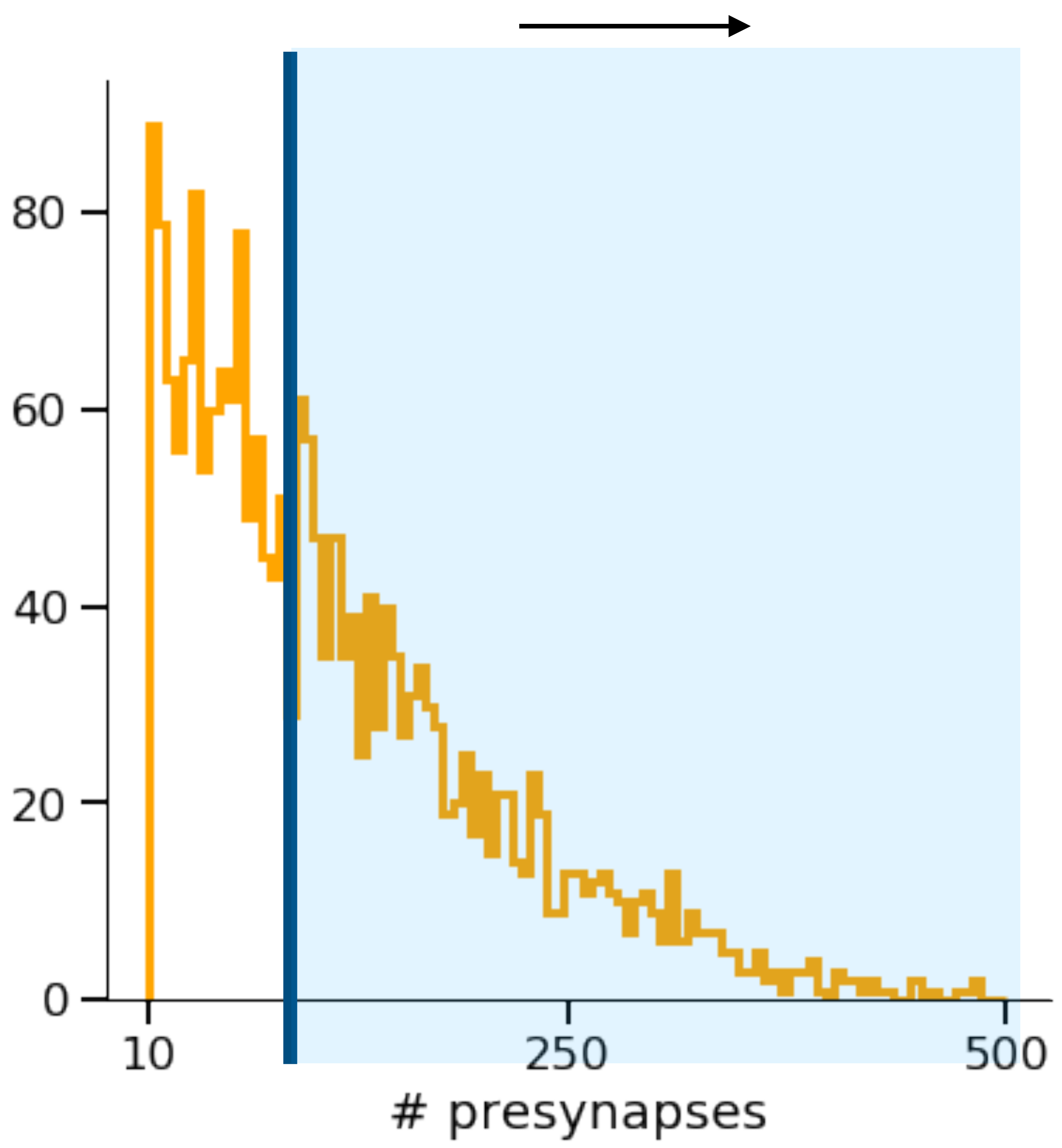

(relatively complete axons)

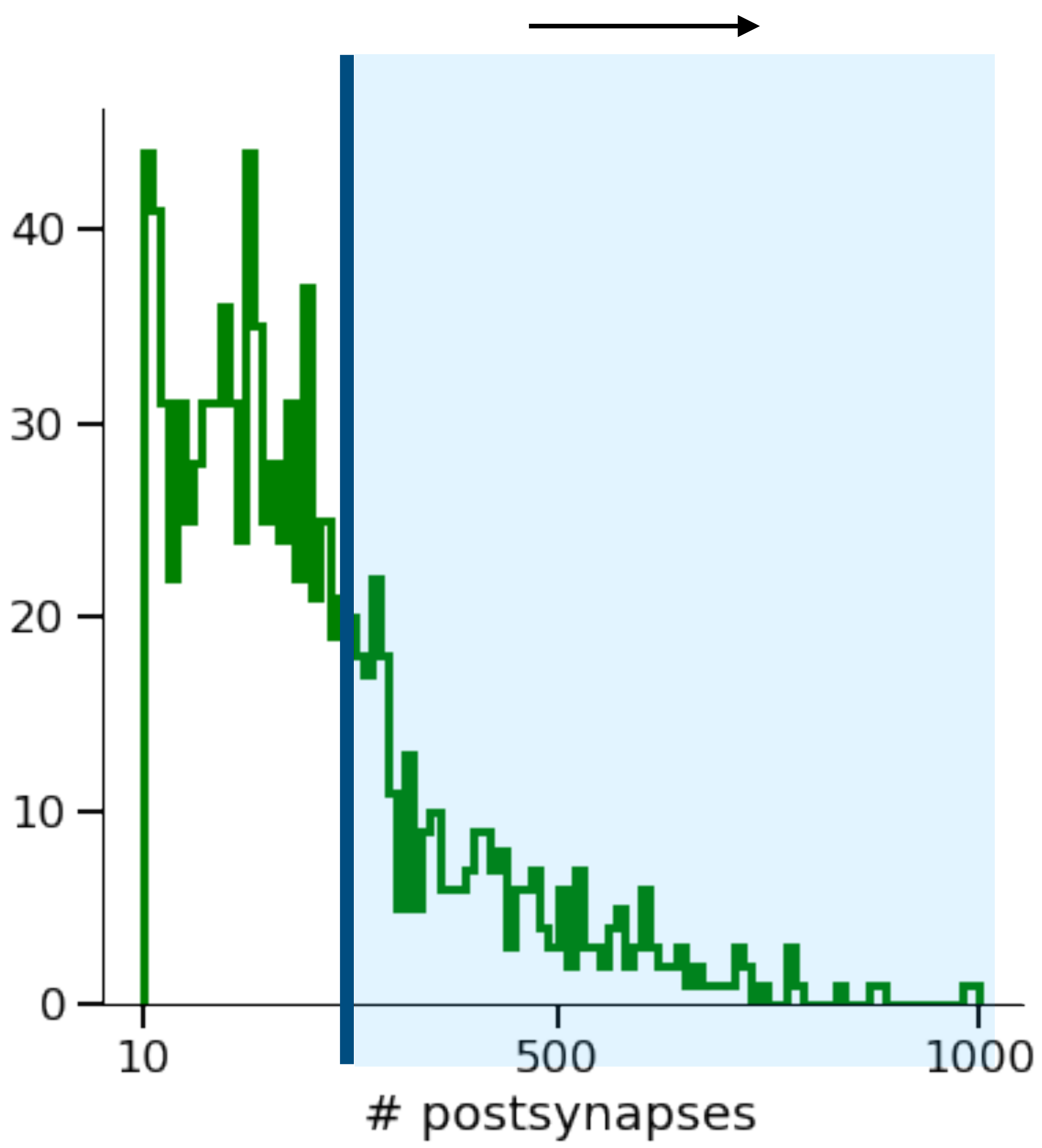

(relatively complete dendrites)

Alleviate truncation effect by restricting to “center” subgraph neurons

neurons with
 # presynpases > threshold

∩

neurons with
 # postynpases > threshold

=

neurons in
a less truncated center subgraph

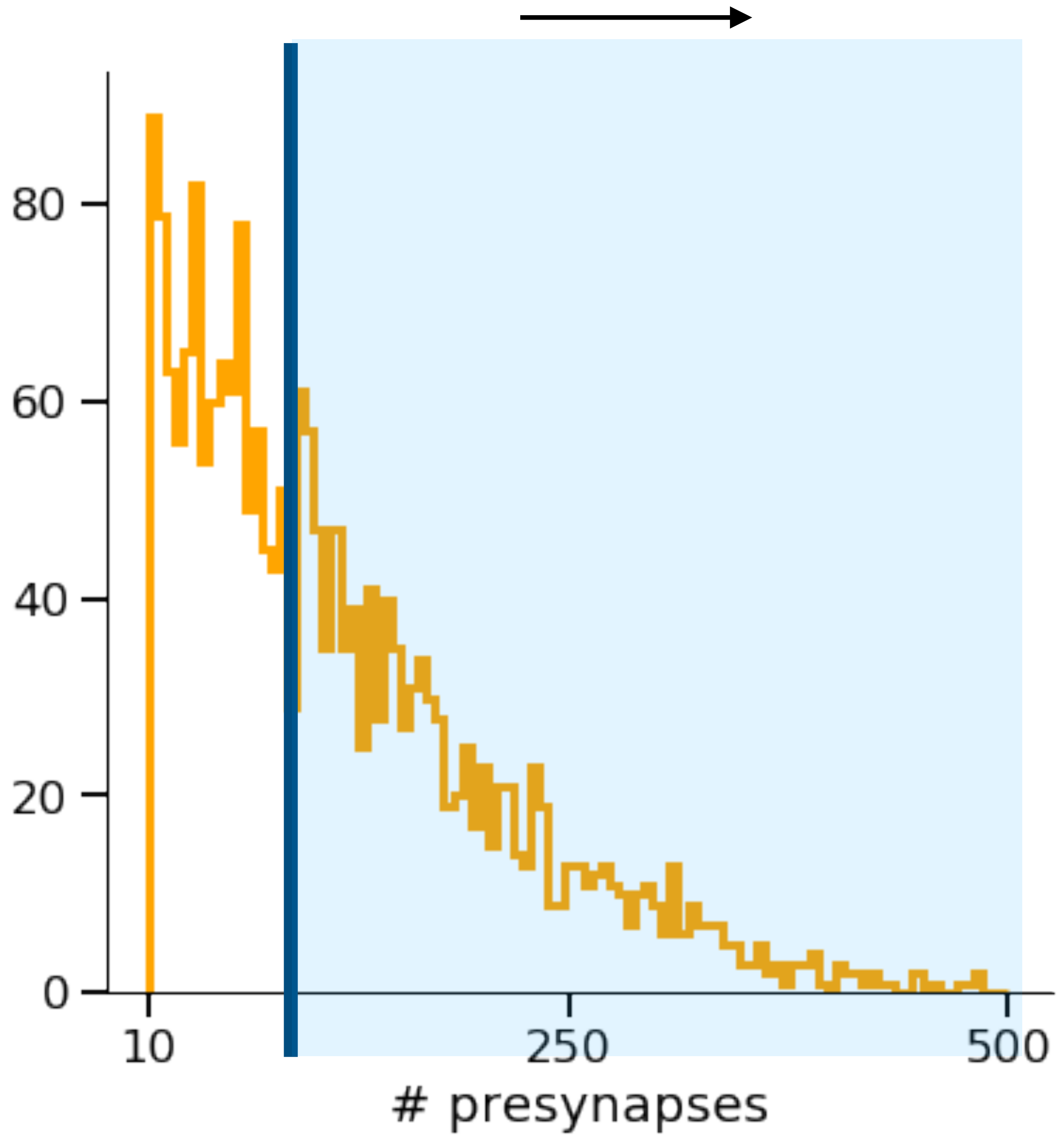

(relatively complete axons)

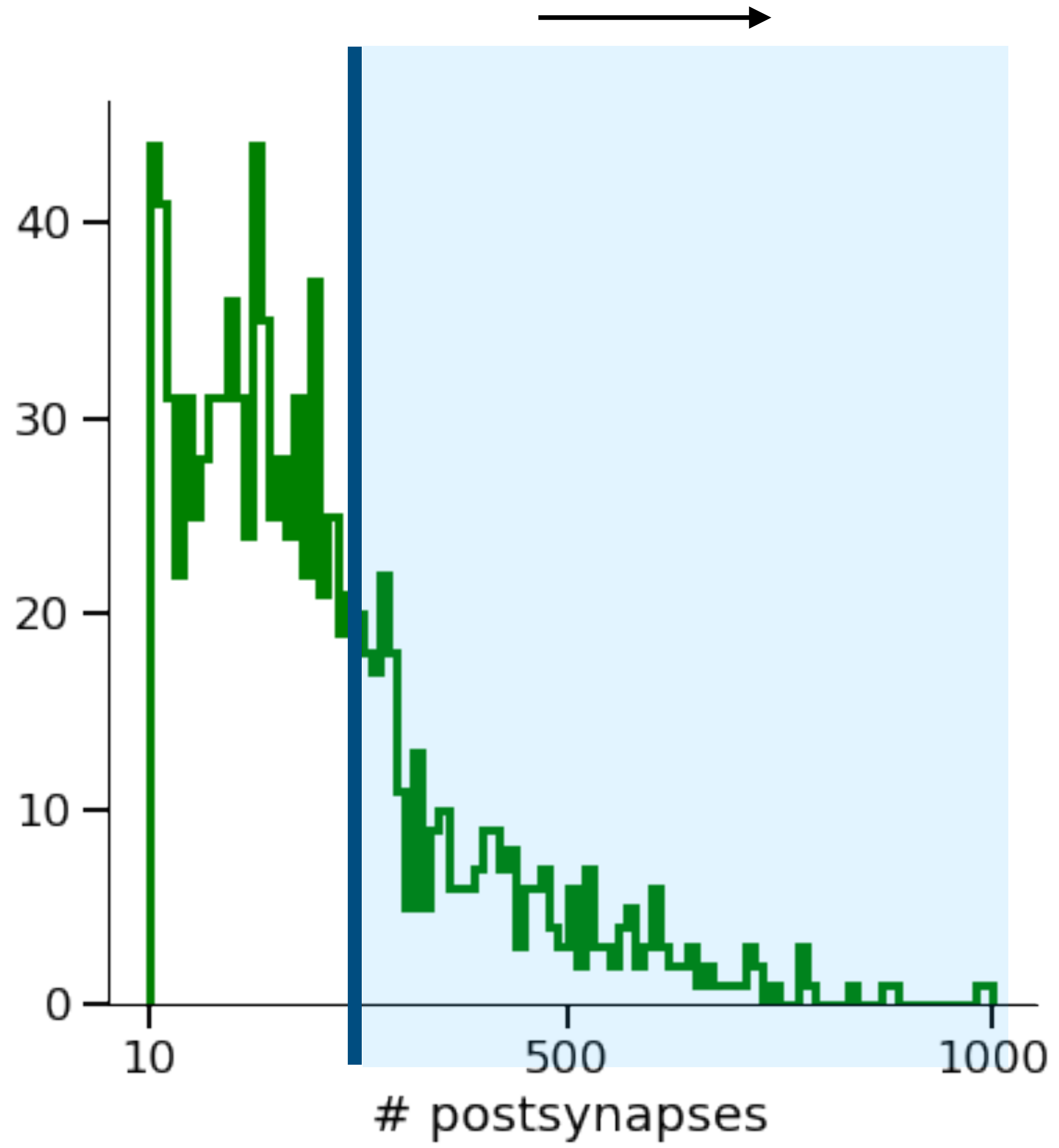

(relatively complete dendrites)

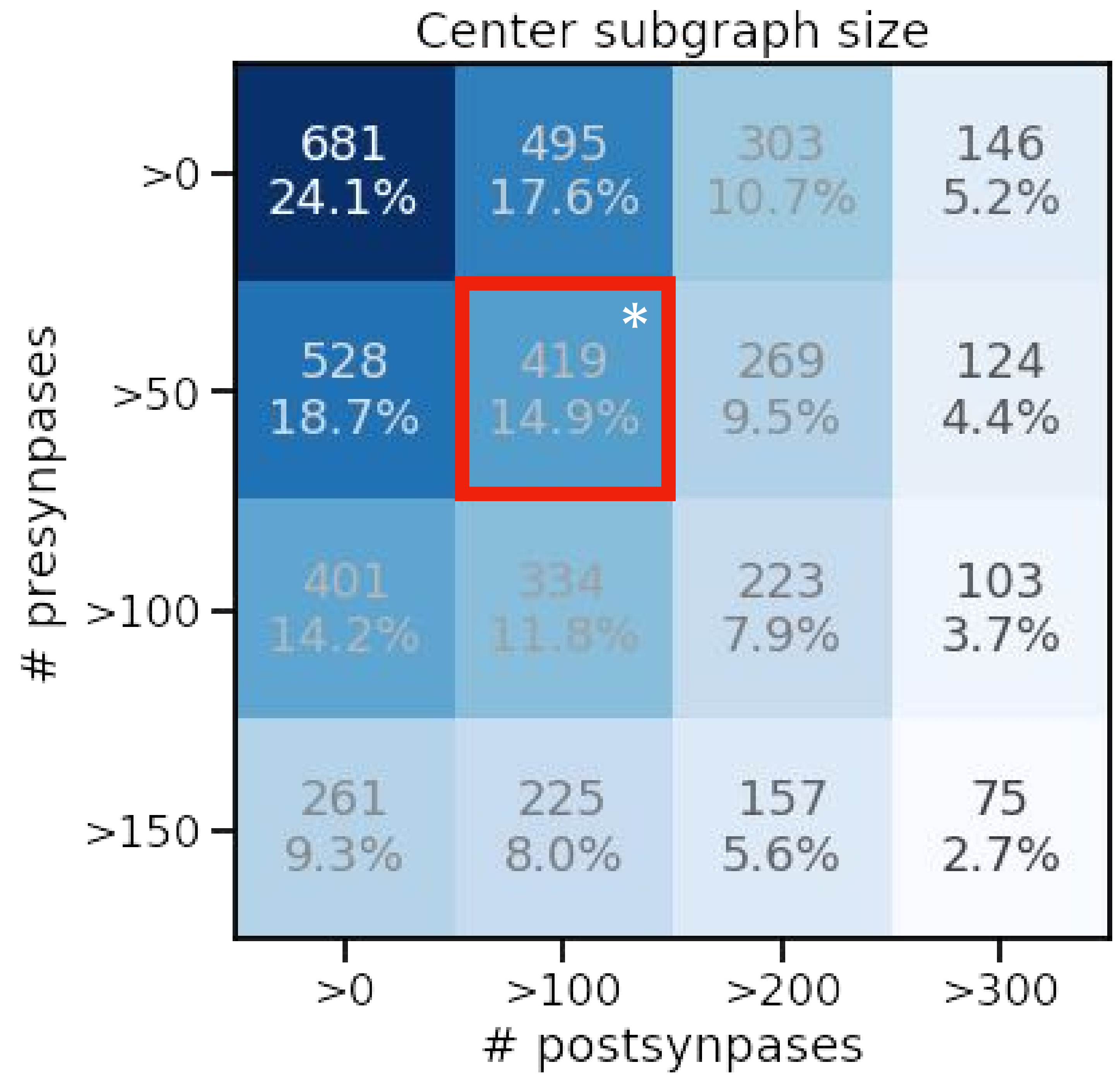

Center subgraph size

# presynpases \ # postsynpases	>0	>100	>200	>300
>0	681 24.1%	495 17.6%	303 10.7%	146 5.2%
>50	528 18.7%	419 14.9% *	269 9.5%	124 4.4%
>100	401 14.2%	334 11.8%	223 7.9%	103 3.7%
>150	261 9.3%	225 8.0%	157 5.6%	75 2.7%

*** 5,605 connections**

I. Two-Module Structure: Oculomotor and Axial

Degree-Corrected Stochastic Block Modeling (DC-SBM, Karrer and Newman 2011)

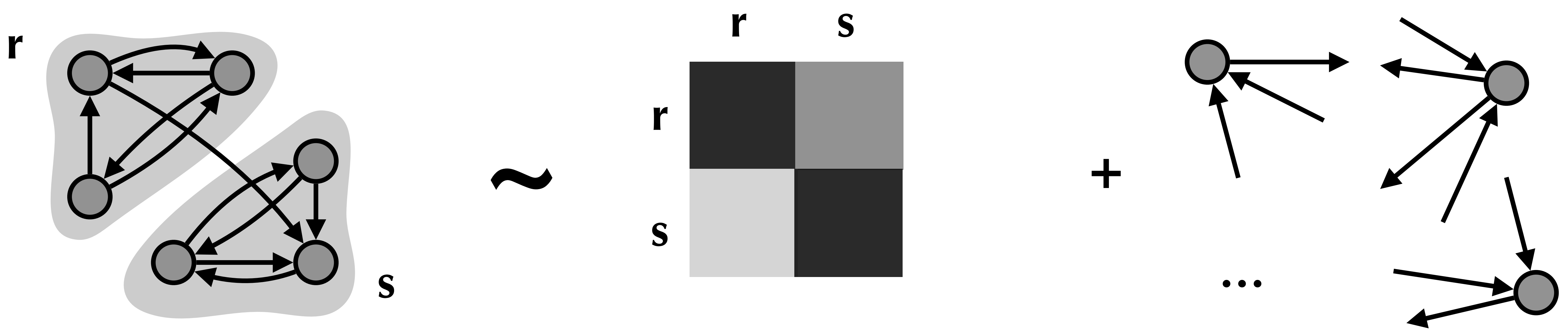

Observed graph G

Connection probability p_{rs}

Degree sequence $\{k_i^+\}, \{k_i^-\}$

Minimizing microcanonical entropy (Bianconi 2009):

$$S \simeq -M - \sum_i \ln(k_i^+!) - \sum_i \ln(k_i^-!) - \sum_{rs} e_{rs} \ln\left(\frac{e_{rs}}{\sum_s e_{rs} \sum_r e_{rs}}\right)$$

DC-SBM reveals a “modular” structure of the center subgraph

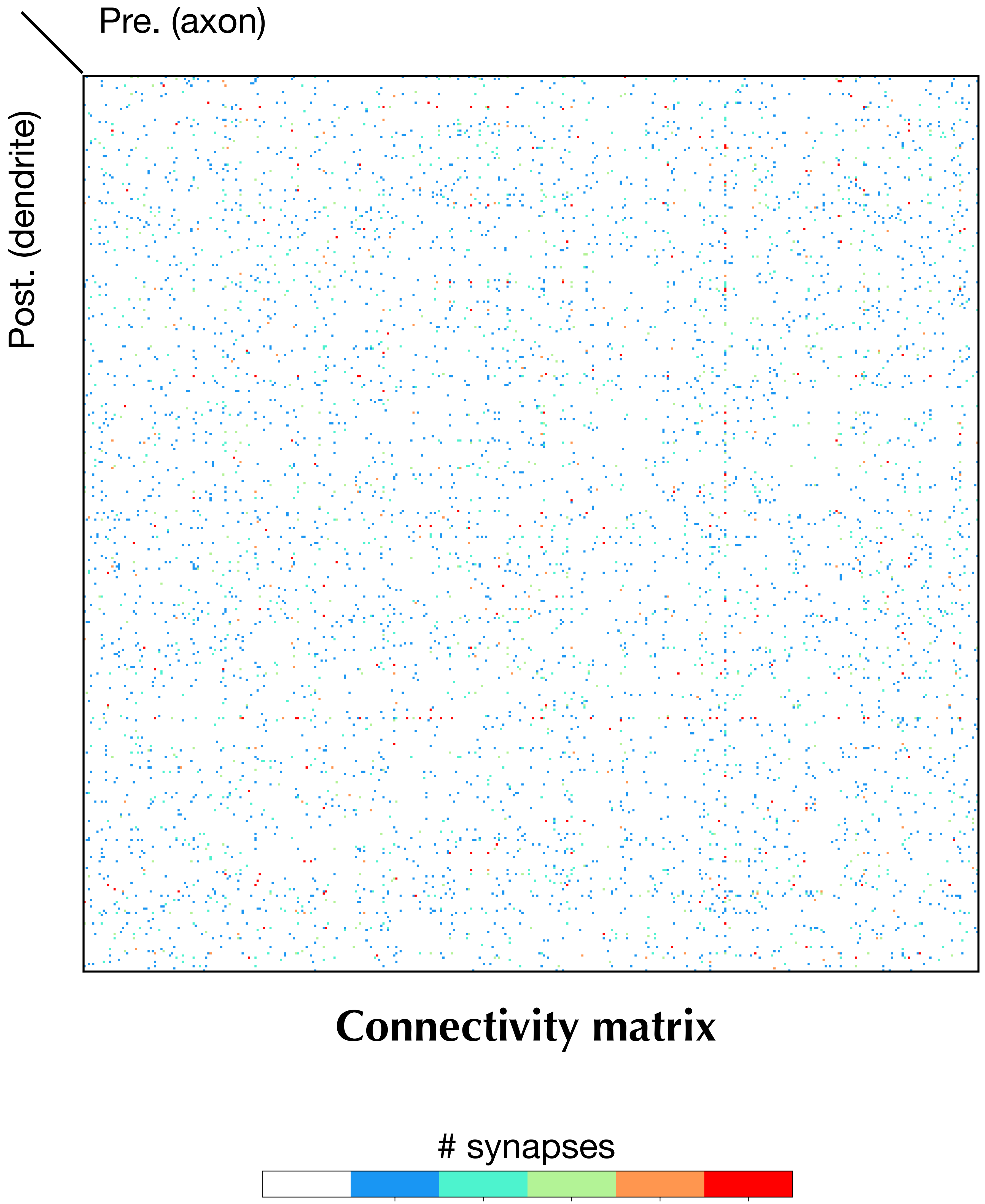

Connectivity matrix

DC-SBM reveals a “modular” structure of the center subgraph

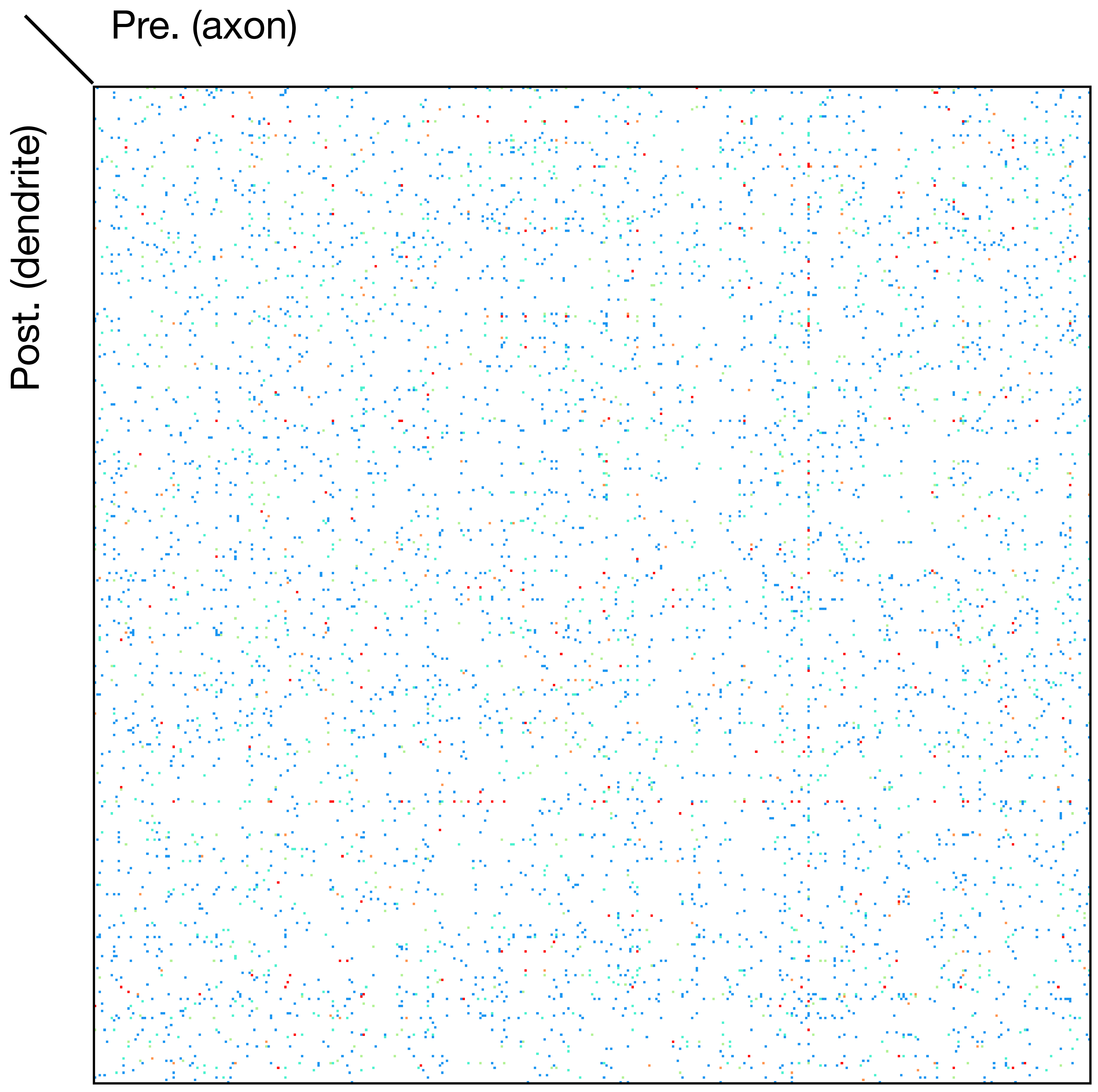

Connectivity matrix

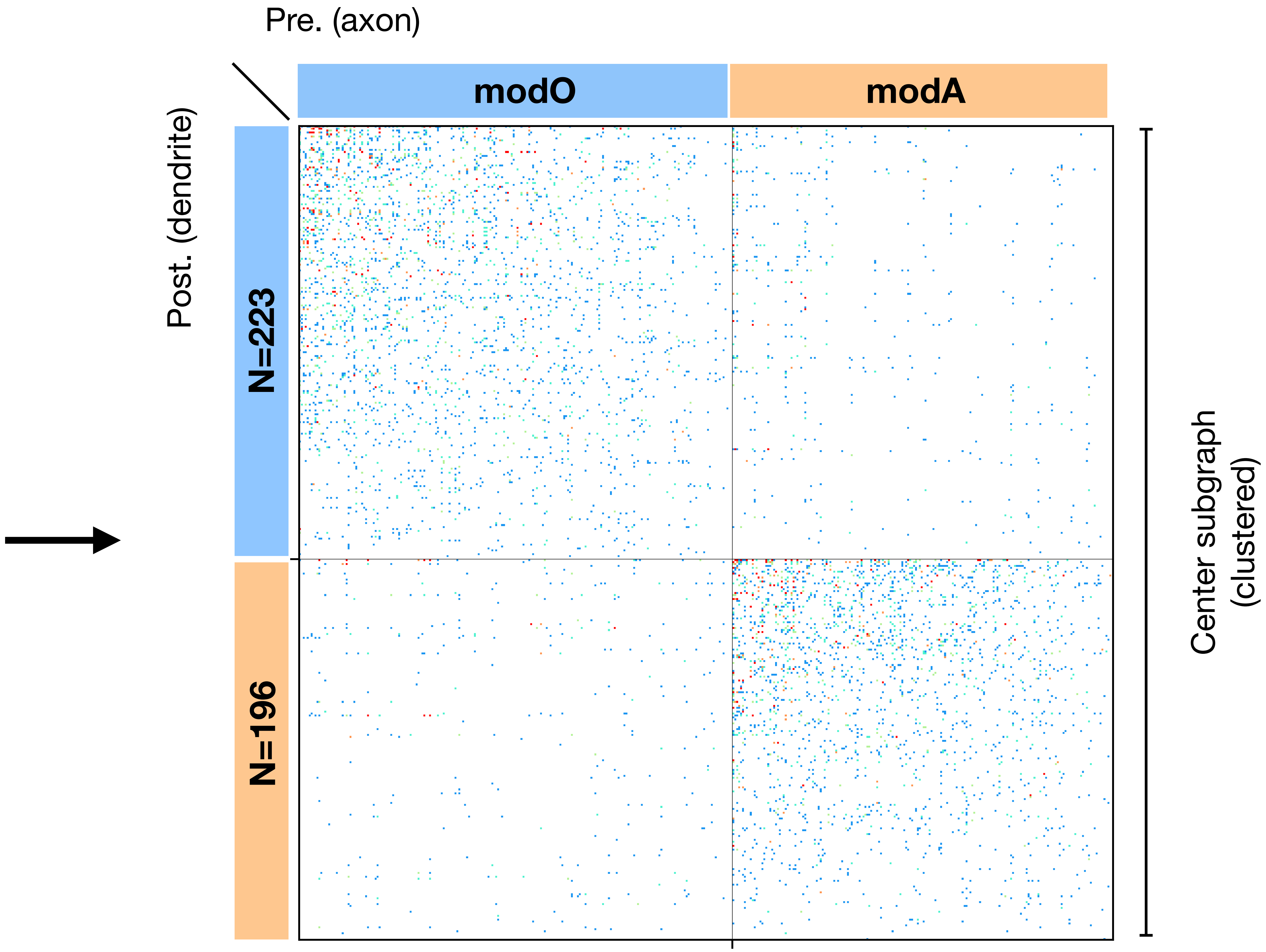

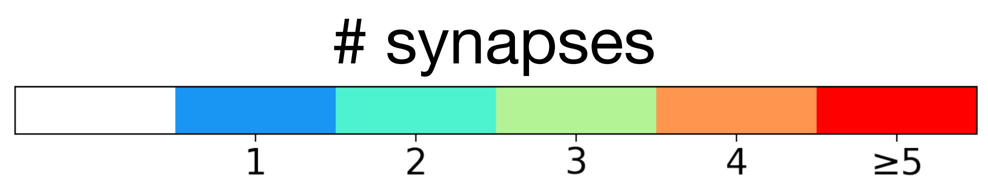

Biological validation of the 2-module structure

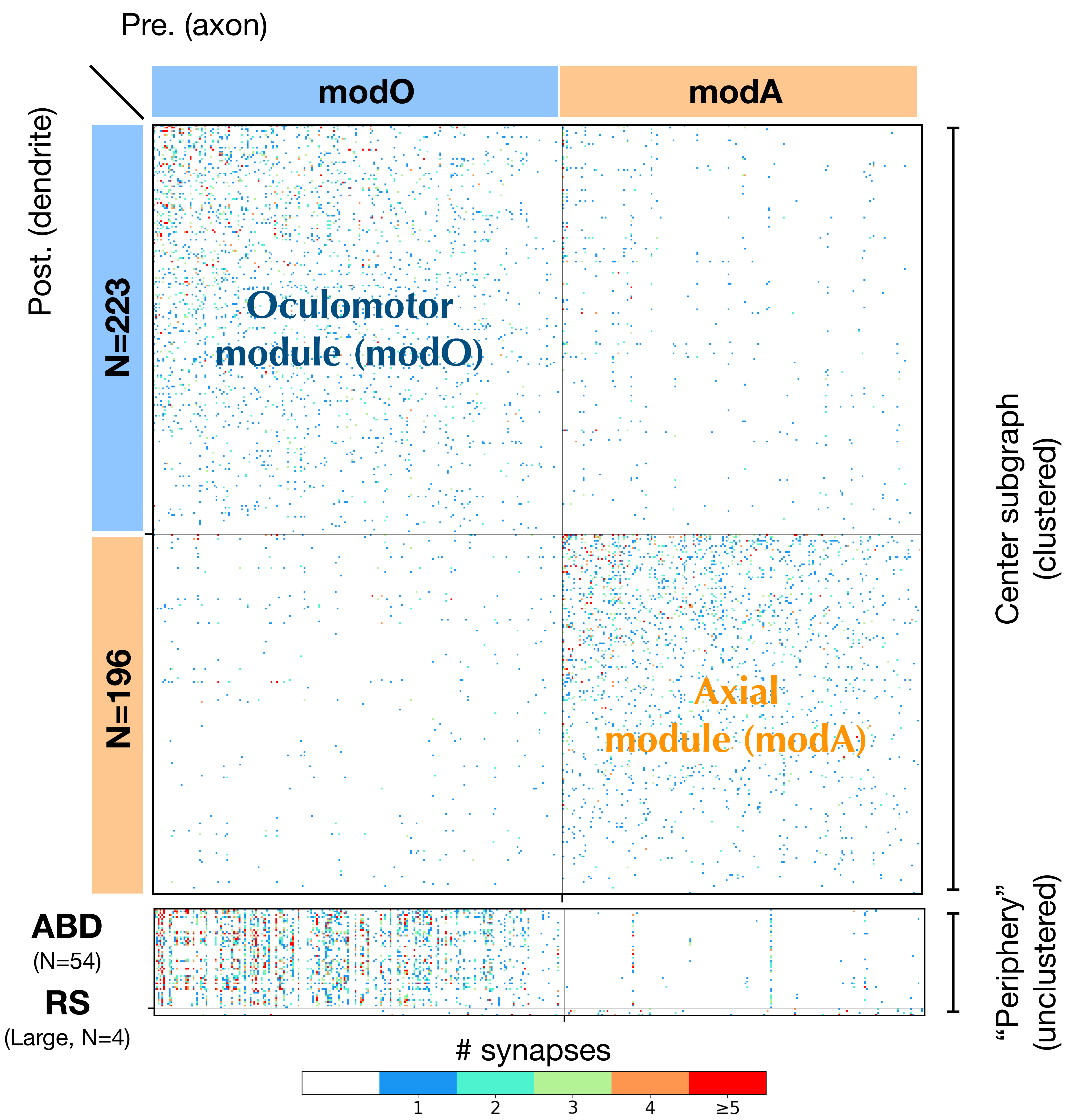

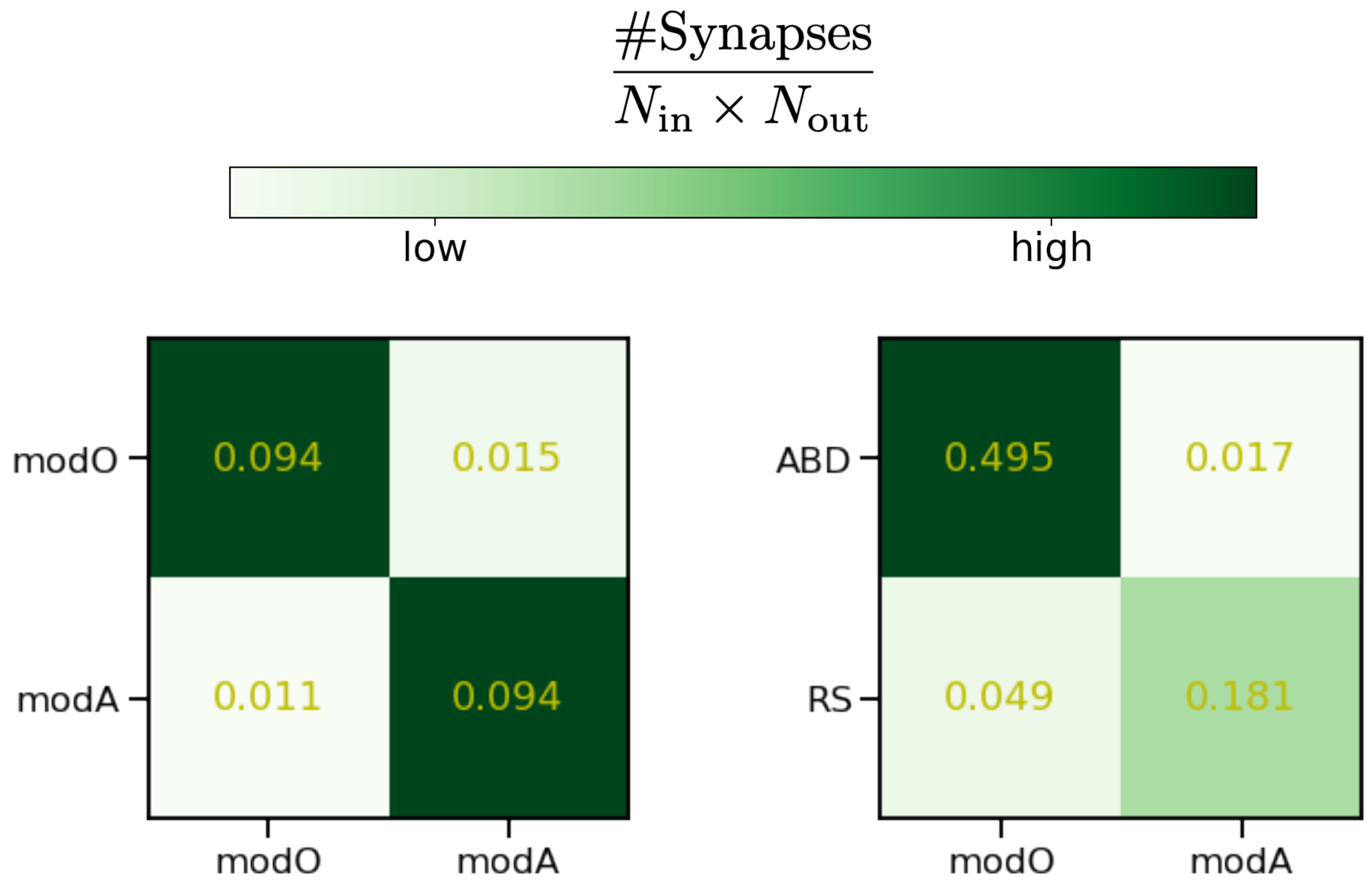

Intermingled and distributed: modO and modA are not brain "nuclei"

Soma position

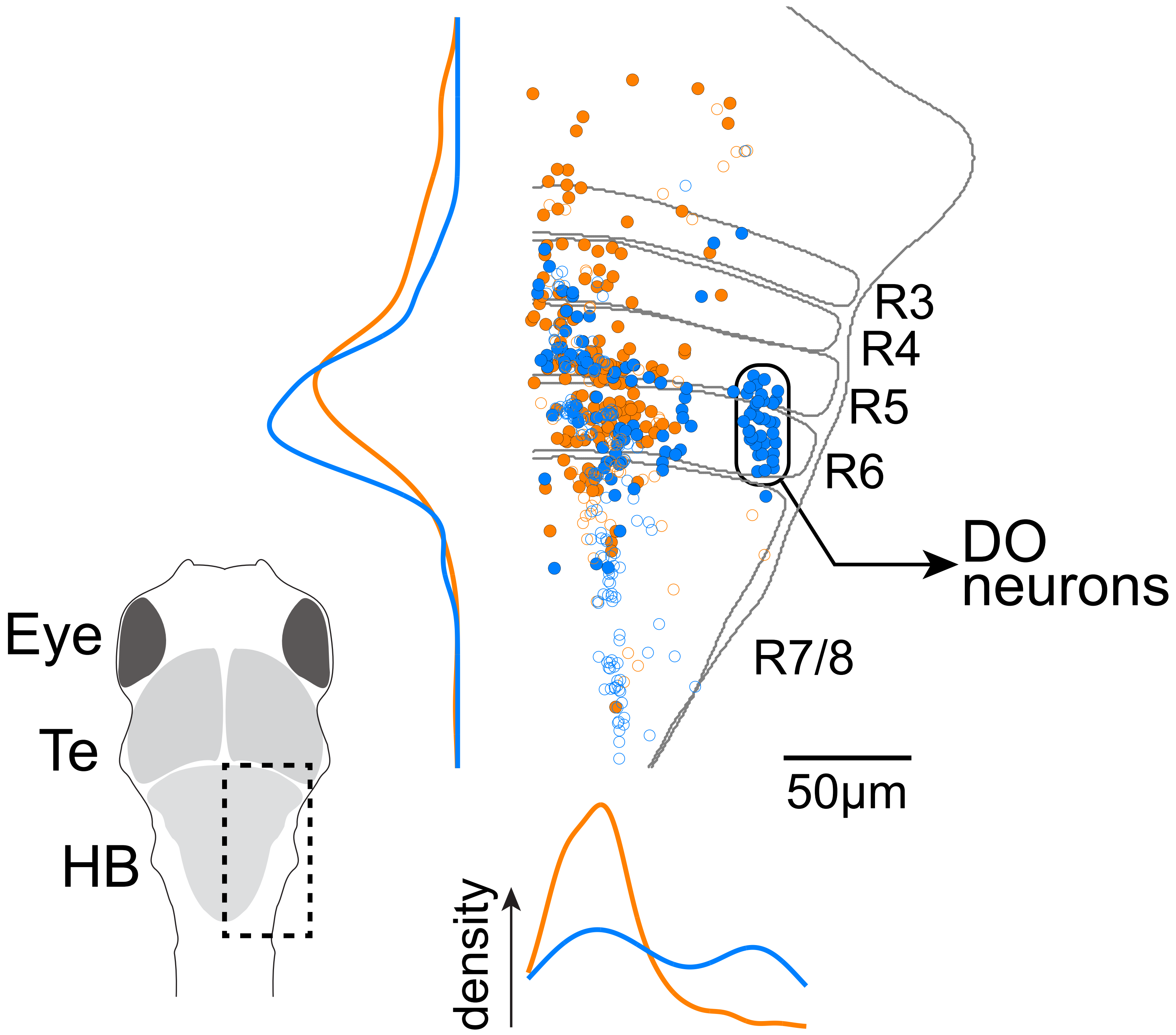

Intermingled and distributed: modO and modA are not brain “nuclei”

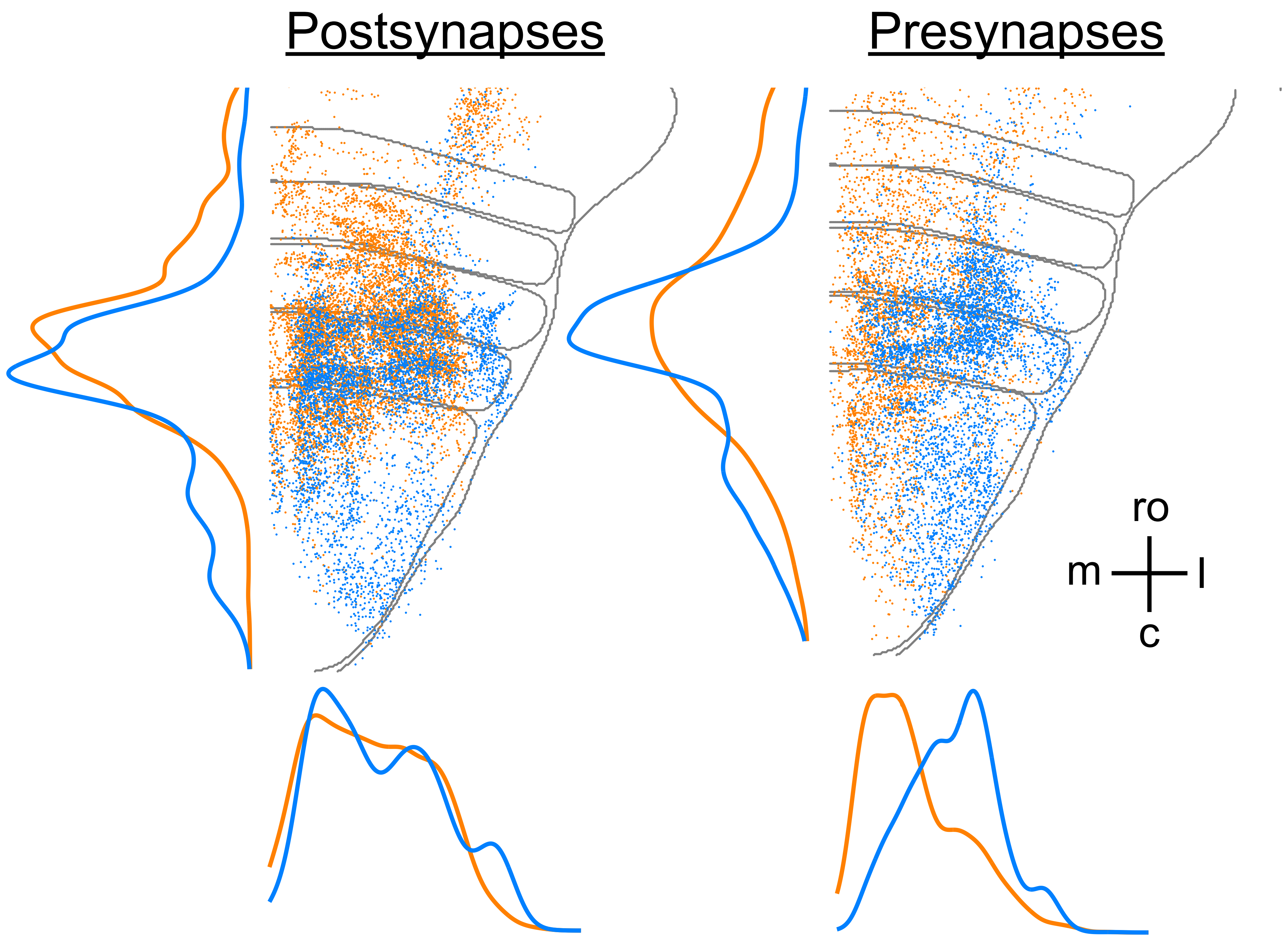

Peters′ rule can only partially explain the modularity of the center subgraph

Potential synapses

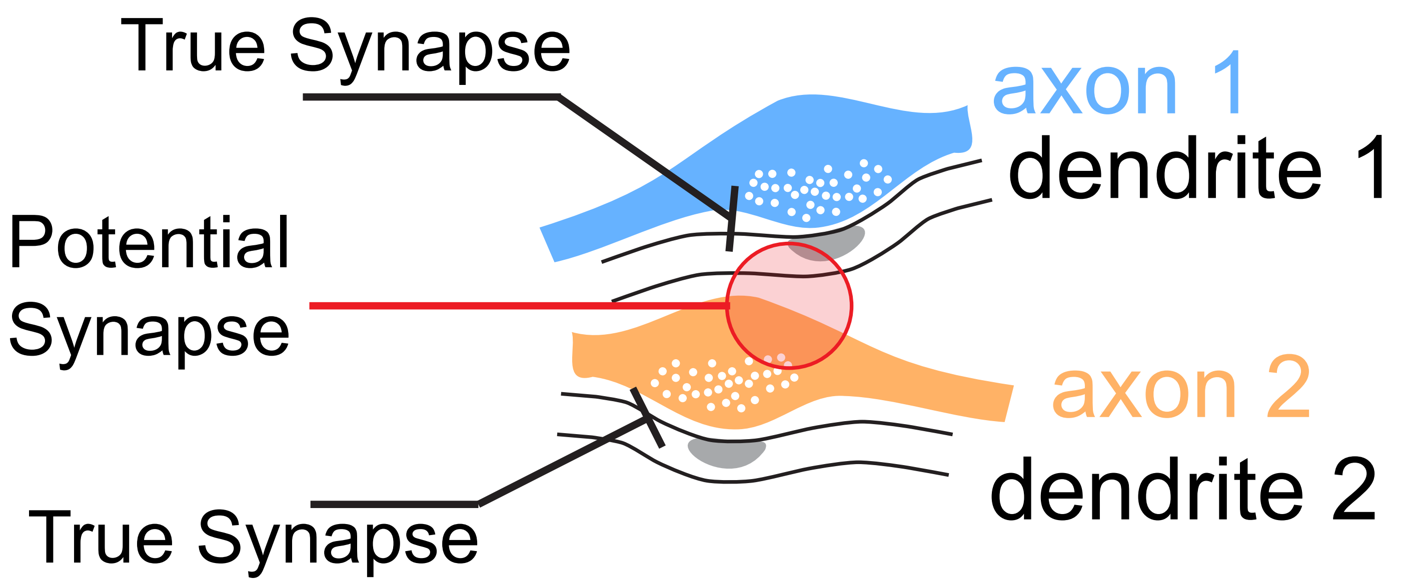

Peters′ rule: neural connectivity can be explained by overlaps between axons and dendrites

Peters' rule can only partially explain the modularity of the center subgraph

Potential synapses

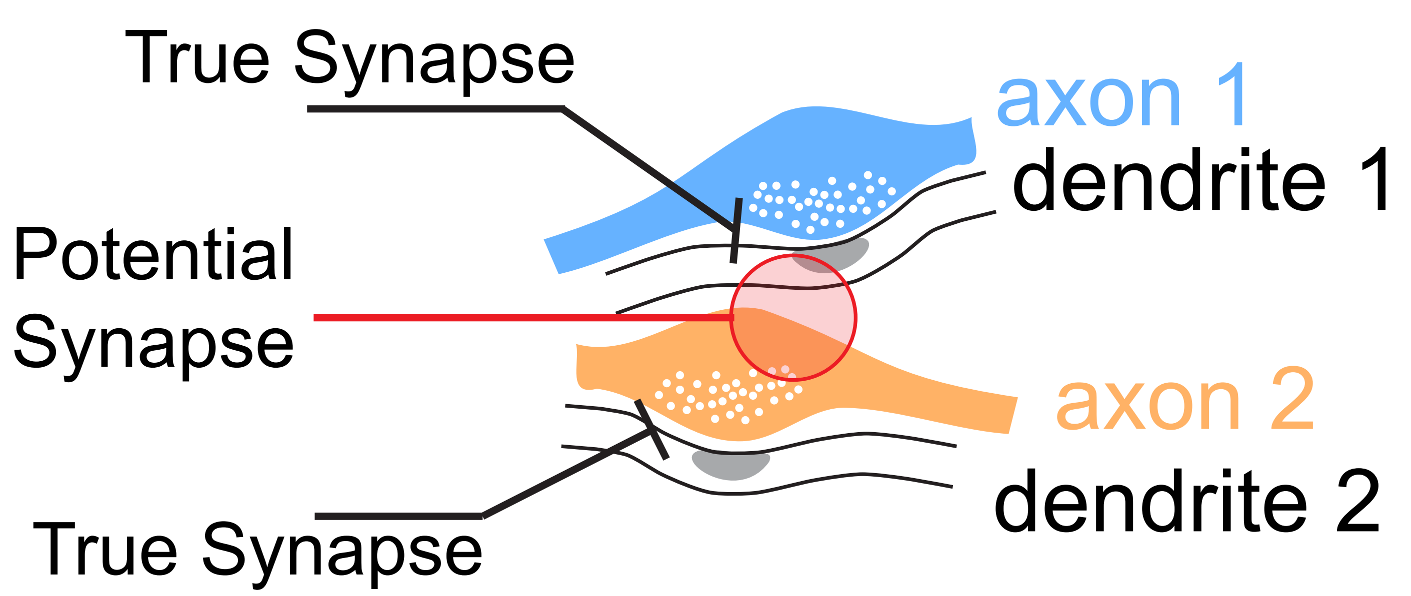

Modularity decreases as we include more distant potential synapses

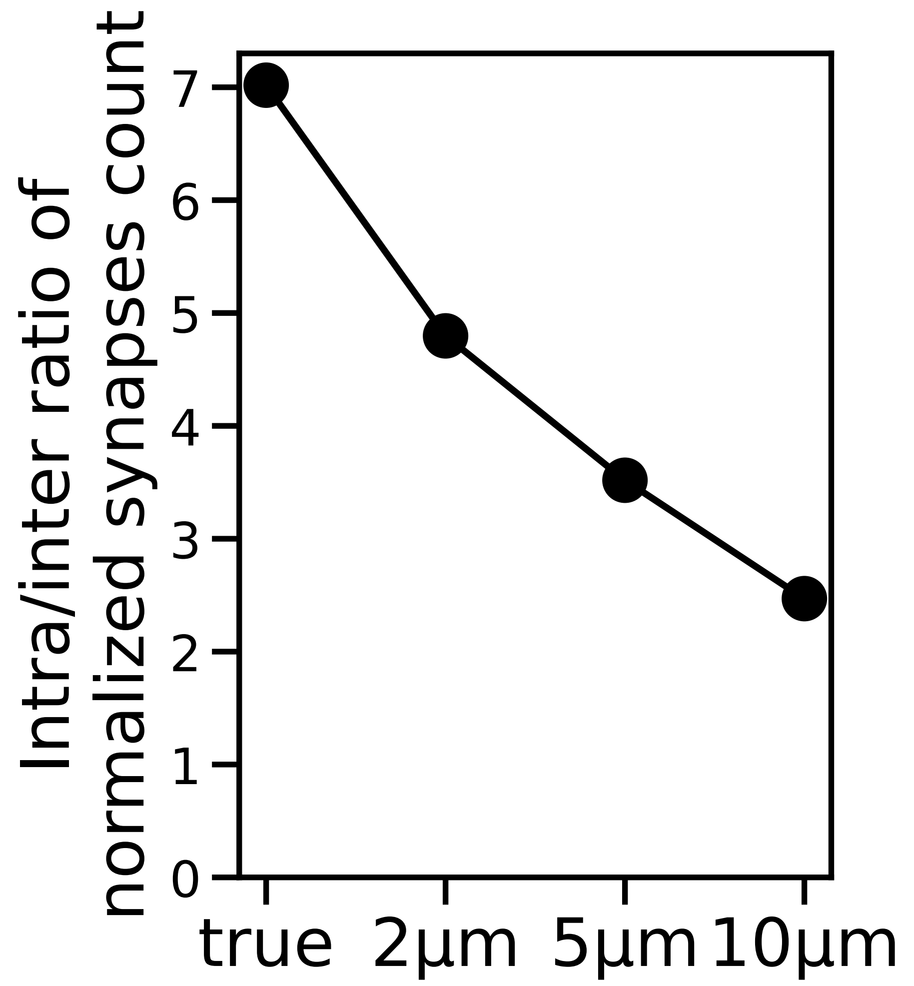

II. Functional Significance of Weak Connections

Massive presence of weak connections in connectomes

One connection, many synapses (stronger)

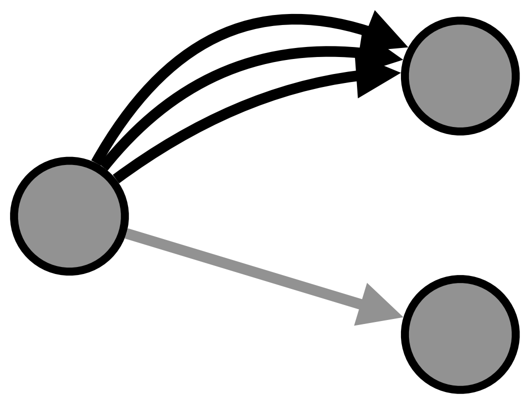

One connection, few synapses (weaker)

Massive presence of weak connections in connectomes

One connection, many synapses (stronger)

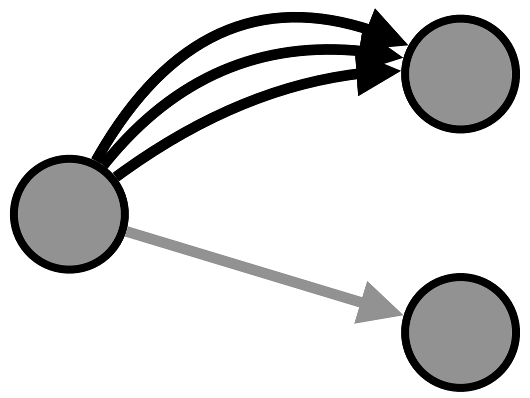

One connection, few synapses (weaker)

adult *C. elegans*

42% weak connections (Cook et al. 2019)

adult *Drosophila*

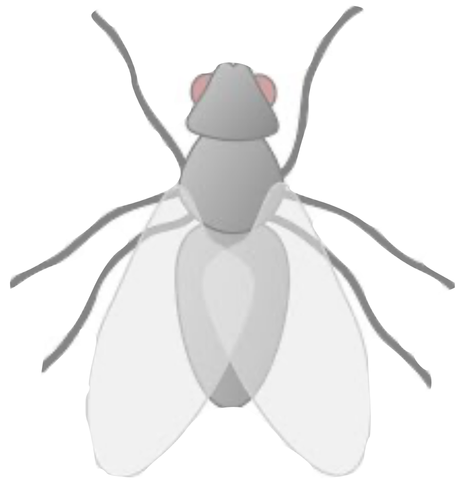

45% weak connections (Scheffer et al. 2019)

Massive presence of weak connections in connectomes

One connection, many synapses (stronger)

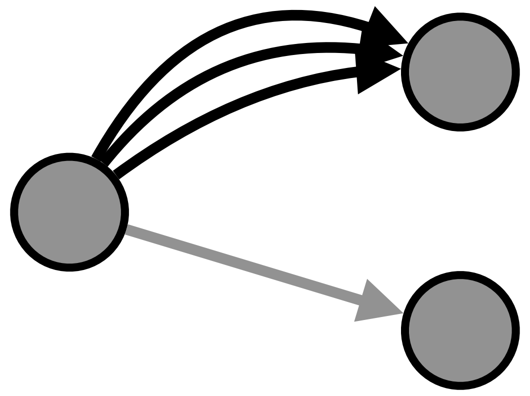

One connection, few synapses (weaker)

adult *C*. elegans

42% weak connections (Cook et al. 2019)

adult *Drosophila*

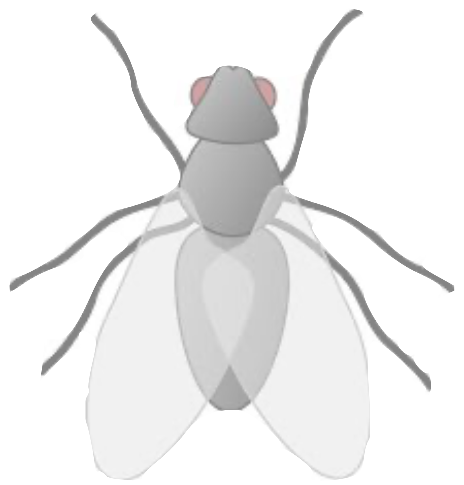

45% weak connections (Scheffer et al. 2019)

P36 mouse visual cortex

89% weak connections (Dorkenwald et al. 2019)

Massive presence of weak connections in connectomes

One connection, many synapses (stronger)

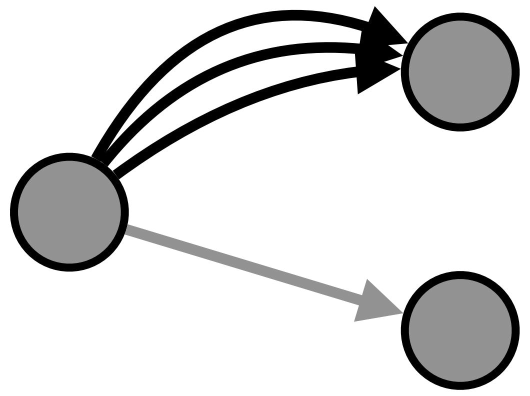

One connection, few synapses (weaker)

adult *C. elegans*

42% weak connections (Cook et al. 2019)

adult *Drosophila*

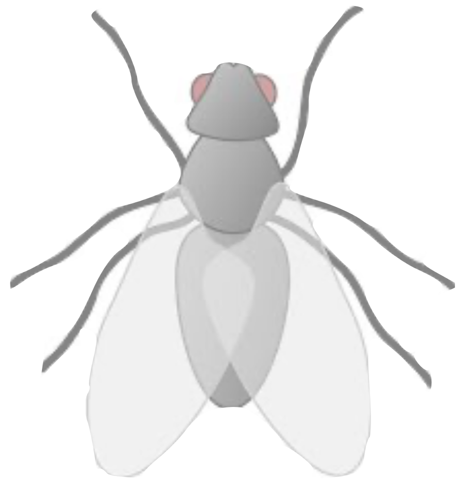

45% weak connections (Scheffer et al. 2019)

larval zebrafish

~65% weak connections

P36 mouse visual cortex

89% weak connections (Dorkenwald et al. 2019)

More than 60% connections are weak in the zebrafish center subgraph

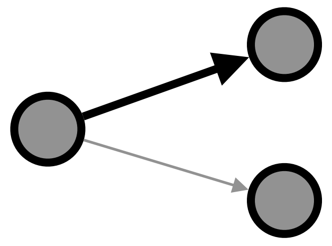

One connection, many synapses (stronger)

One connection, few synapses (weaker)

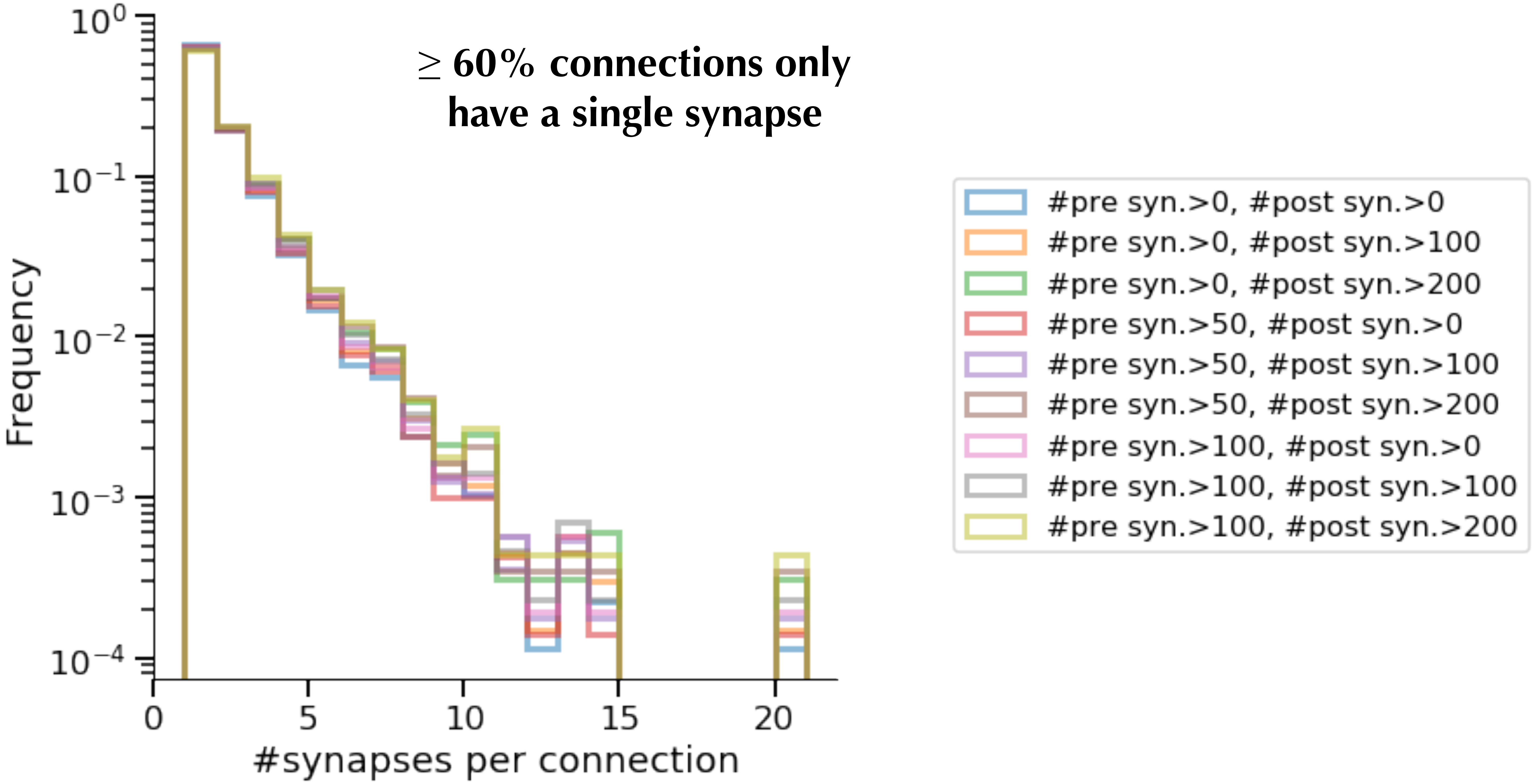

≥ 60% connections only have a single synapse

1st evidence:
DC-SBM finds similar modular structure in the weak and strong subgraphs

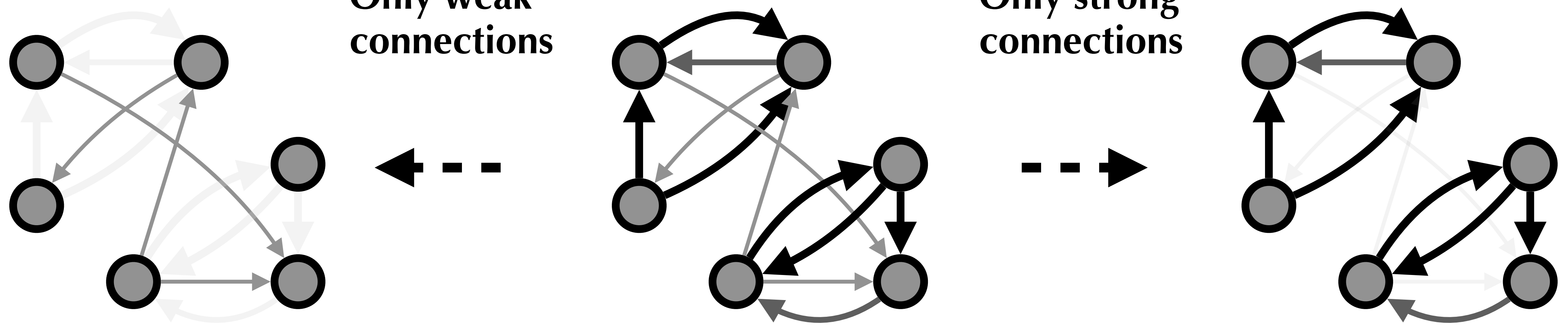

64.3% of total connections

Only weak connections

Only strong connections

35.7% of total connections

weak subgraph
single synapse

full subgraph
all connections

strong subgraph
# of synapses ≥ 2

1st evidence:
DC-SBM finds similar modular structure in the weak and strong subgraphs

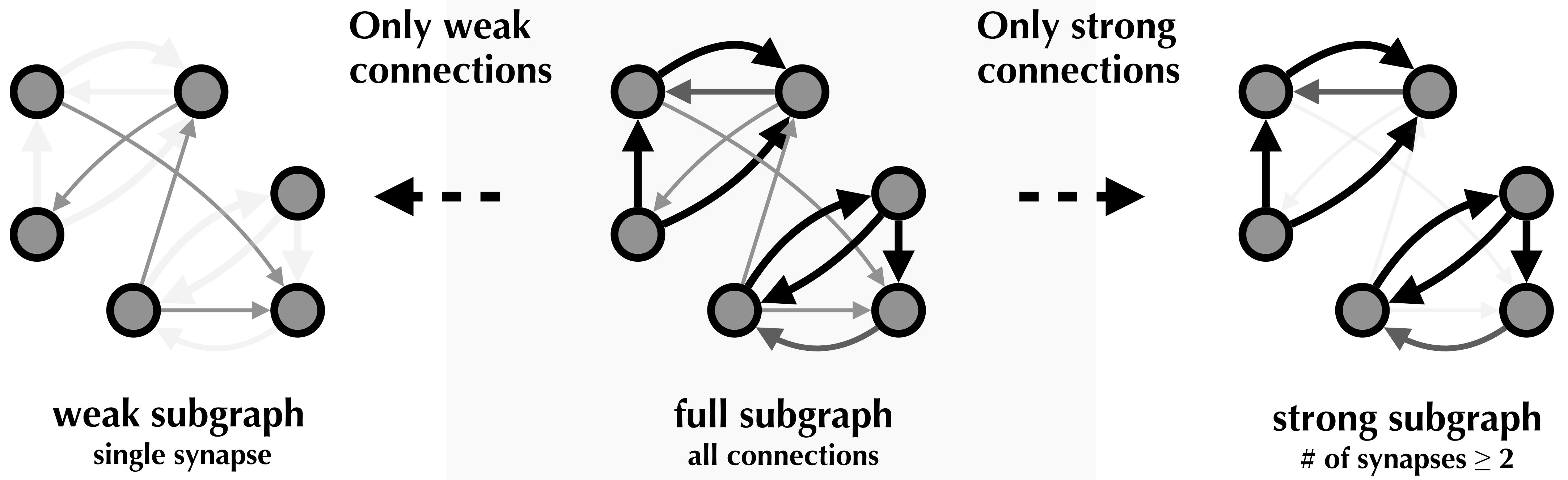

Only weak connections

Only strong connections

weak subgraph
single synapse

full subgraph
all connections

strong subgraph
# of synapses ≥ 2

Rand index = 0.997

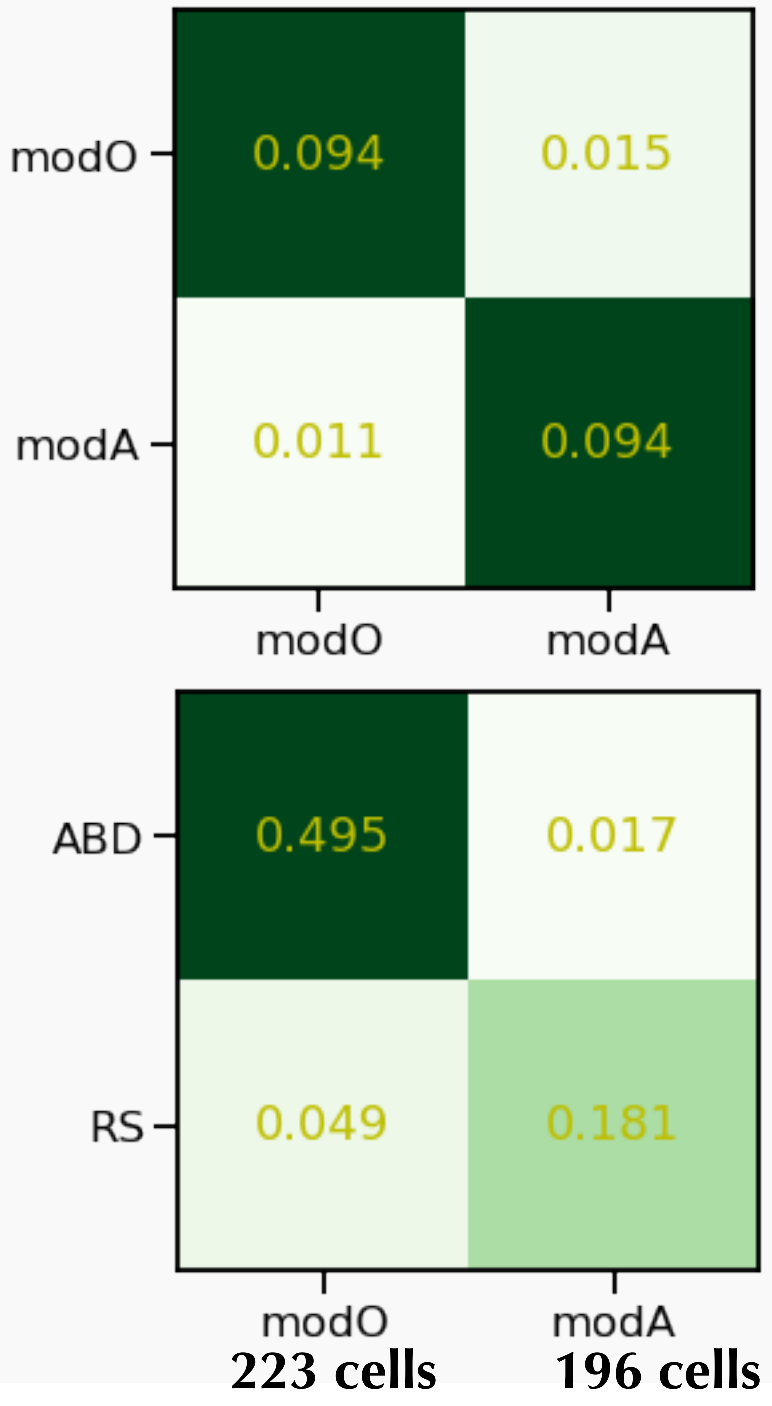

	modO	modA
modO	0.094	0.015
modA	0.011	0.094

	modO	modA
ABD	0.495	0.017
RS	0.049	0.181

223 cells **196 cells**

$$\frac{\#\text{Synapses}}{N_{\text{in}} \times N_{\text{out}}}$$

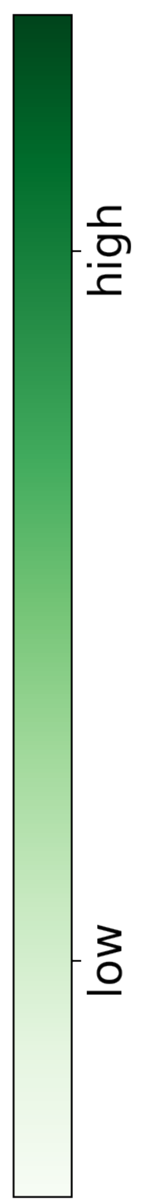

1st evidence:
DC-SBM finds similar modular structure in the weak and strong subgraphs

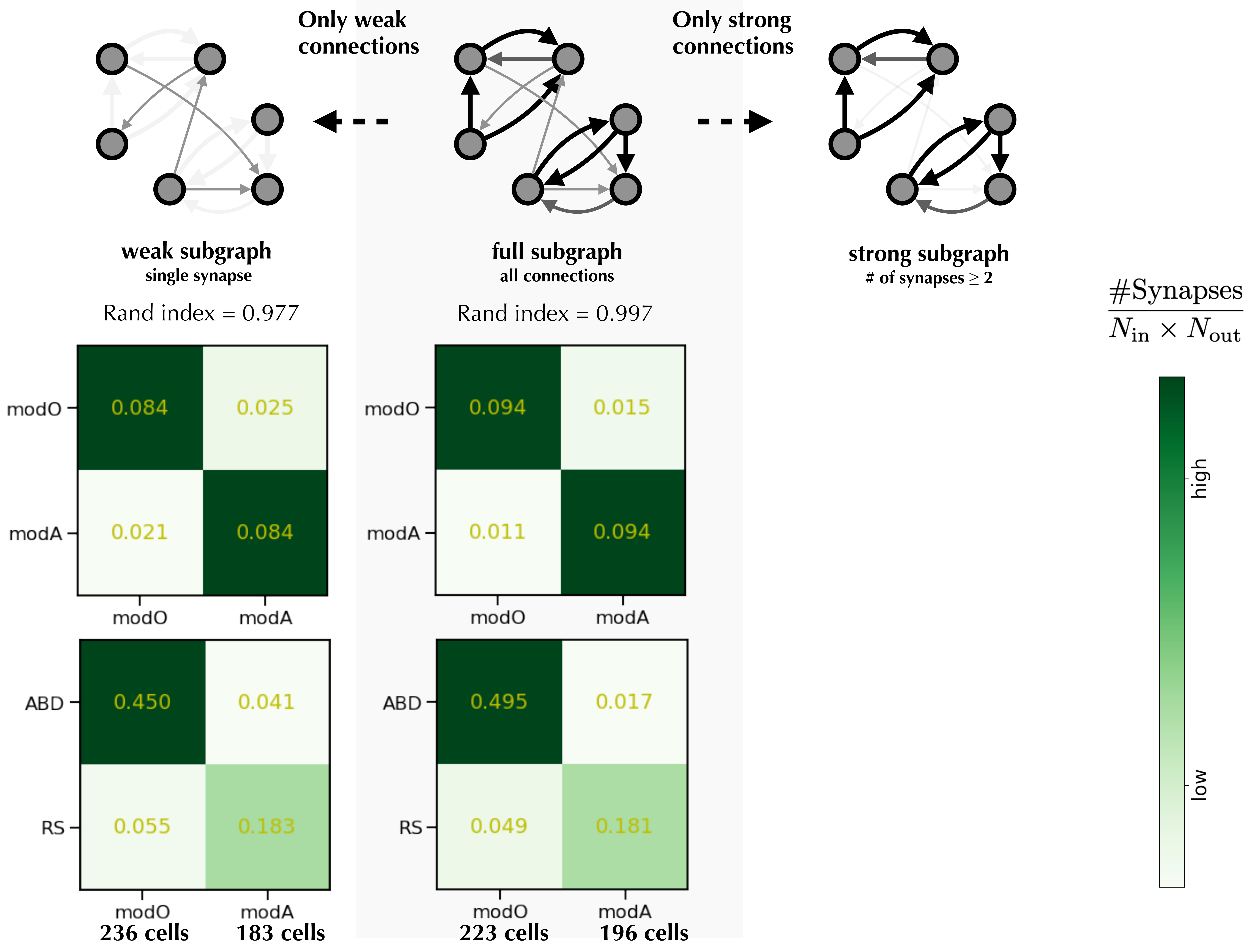

Only weak connections

Only strong connections

weak subgraph
single synapse

Rand index = 0.977

	modO	modA
modO	0.084	0.025
modA	0.021	0.084

	modO	modA
ABD	0.450	0.041
RS	0.055	0.183
	236 cells	183 cells

full subgraph
all connections

Rand index = 0.997

	modO	modA
modO	0.094	0.015
modA	0.011	0.094

	modO	modA
ABD	0.495	0.017
RS	0.049	0.181
	223 cells	196 cells

strong subgraph
# of synapses ≥ 2

$$\frac{\#\text{Synapses}}{N_{\text{in}} \times N_{\text{out}}}$$

1st evidence:
DC-SBM finds similar modular structure in the weak and strong subgraphs

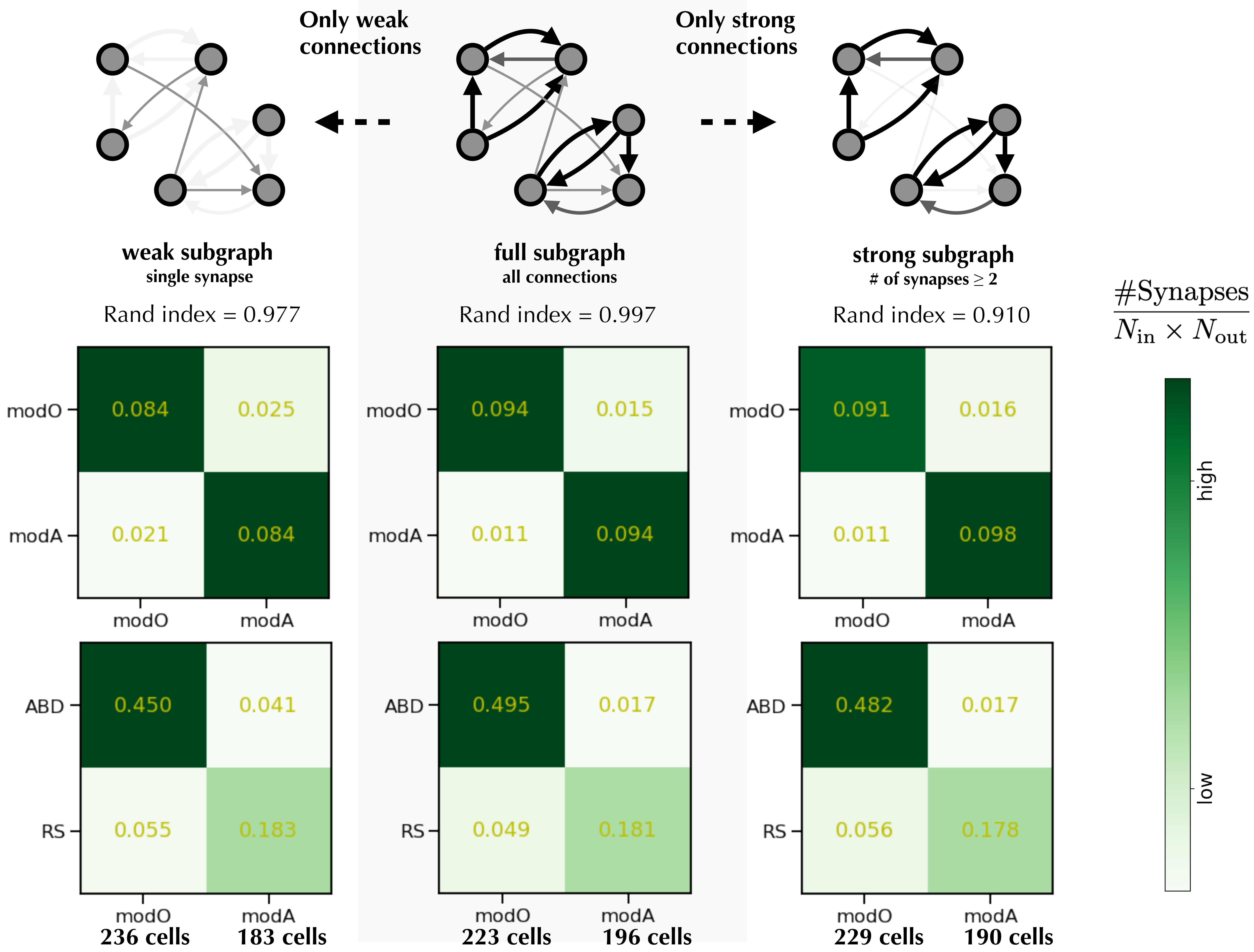

$$\frac{\#\text{Synapses}}{N_{\text{in}} \times N_{\text{out}}}$$

weak subgraph
single synapse

Rand index = 0.977

	modO	modA
modO	0.084	0.025
modA	0.021	0.084

	modO 236 cells	modA 183 cells
ABD	0.450	0.041
RS	0.055	0.183

full subgraph
all connections

Rand index = 0.997

	modO	modA
modO	0.094	0.015
modA	0.011	0.094

	modO 223 cells	modA 196 cells
ABD	0.495	0.017
RS	0.049	0.181

strong subgraph
# of synapses ≥ 2

Rand index = 0.910

	modO	modA
modO	0.091	0.016
modA	0.011	0.098

	modO 229 cells	modA 190 cells
ABD	0.482	0.017
RS	0.056	0.178

1st evidence:
DC-SBM finds similar modular structure in the weak and strong subgraphs

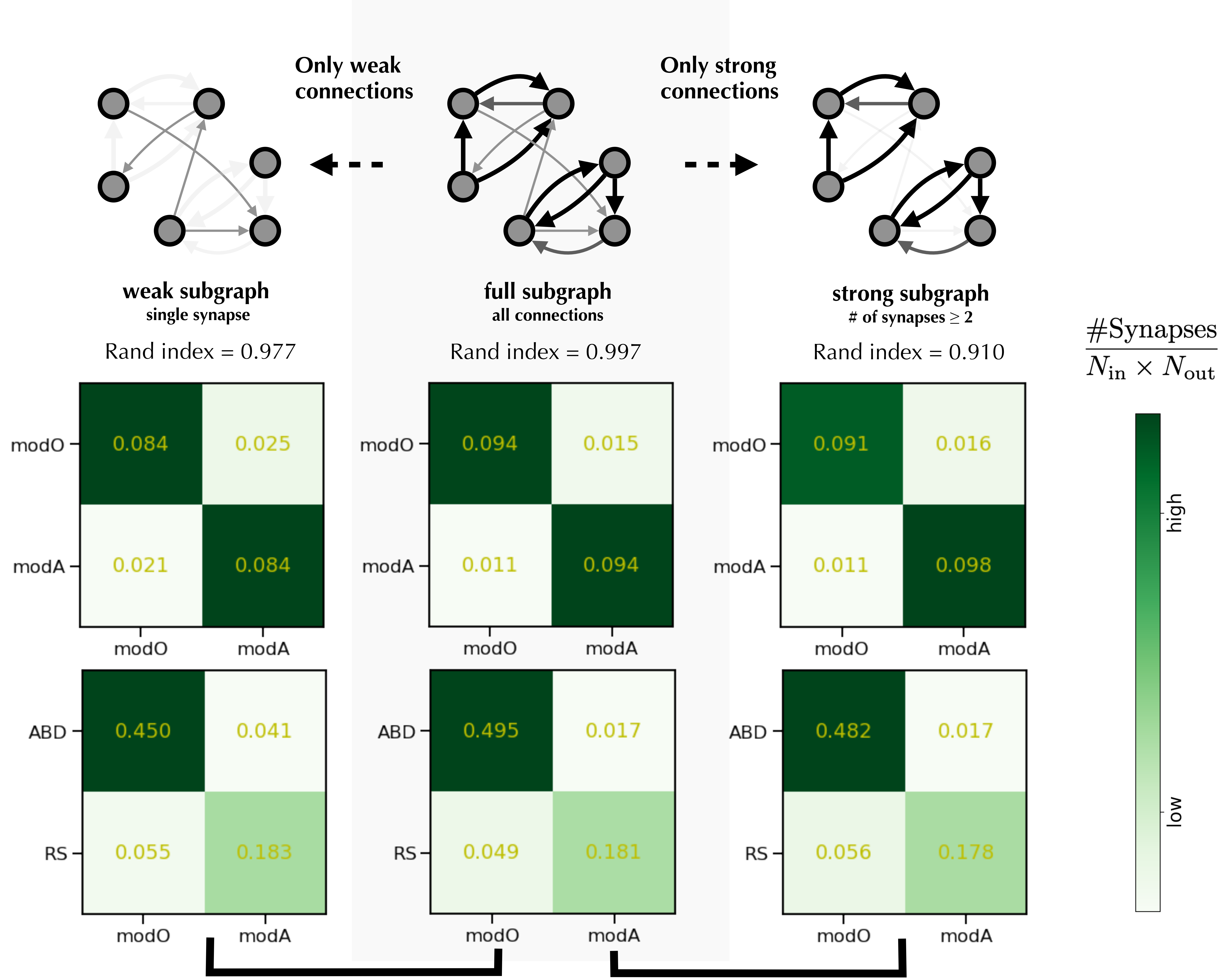

$$\frac{\#\text{Synapses}}{N_{\text{in}} \times N_{\text{out}}}$$

weak subgraph
single synapse

Rand index = 0.977

	modO	modA
modO	0.084	0.025
modA	0.021	0.084

	modO	modA
ABD	0.450	0.041
RS	0.055	0.183

full subgraph
all connections

Rand index = 0.997

	modO	modA
modO	0.094	0.015
modA	0.011	0.094

	modO	modA
ABD	0.495	0.017
RS	0.049	0.181

strong subgraph
# of synapses ≥ 2

Rand index = 0.910

	modO	modA
modO	0.091	0.016
modA	0.011	0.098

	modO	modA
ABD	0.482	0.017
RS	0.056	0.178

Rand index = 0.793

Rand index = 0.972

2nd evidence:
Measuring modularity of strong/weak subgraphs while keeping the block assignments

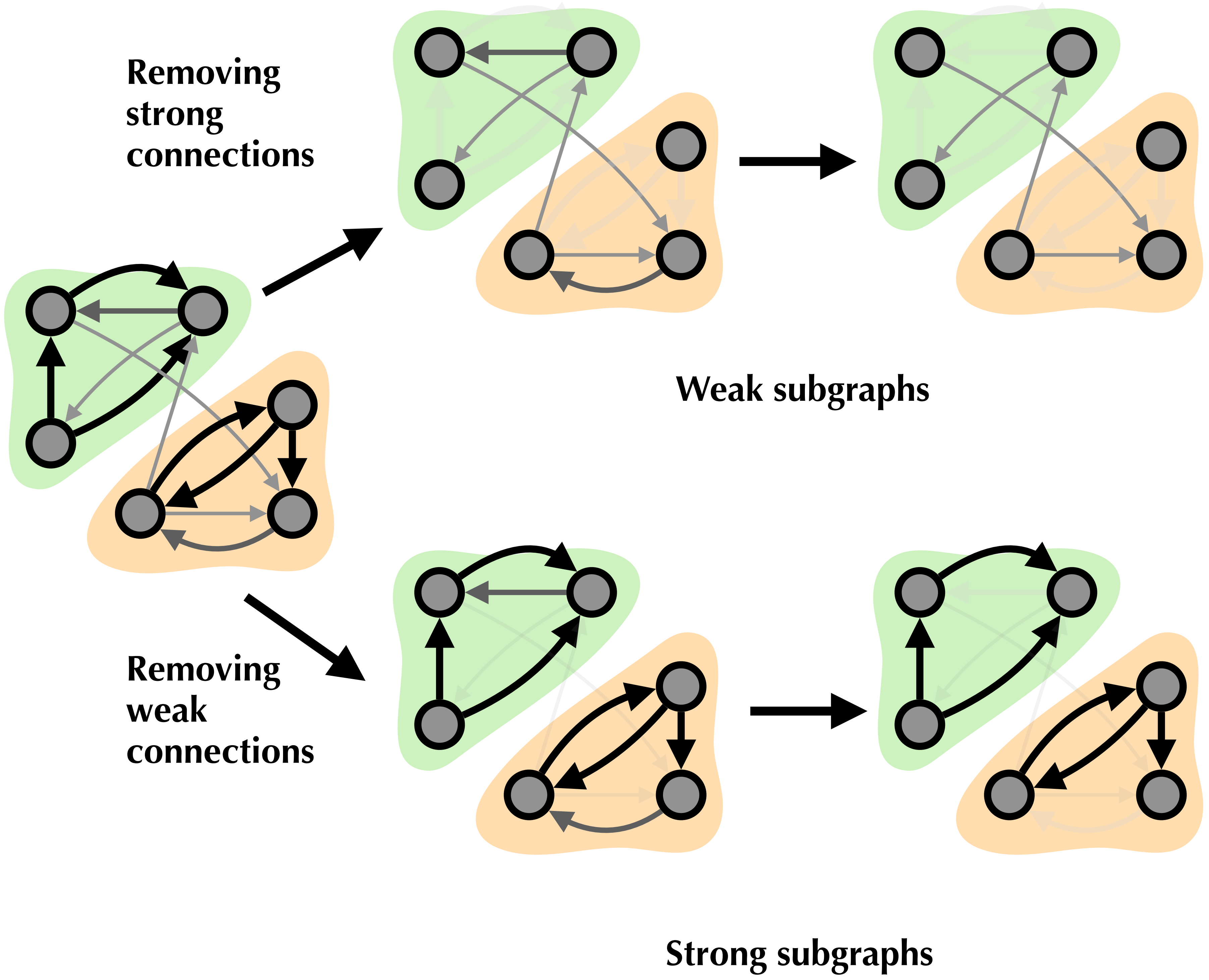

2nd evidence:
Measuring modularity of strong/weak subgraphs while keeping the block assignments

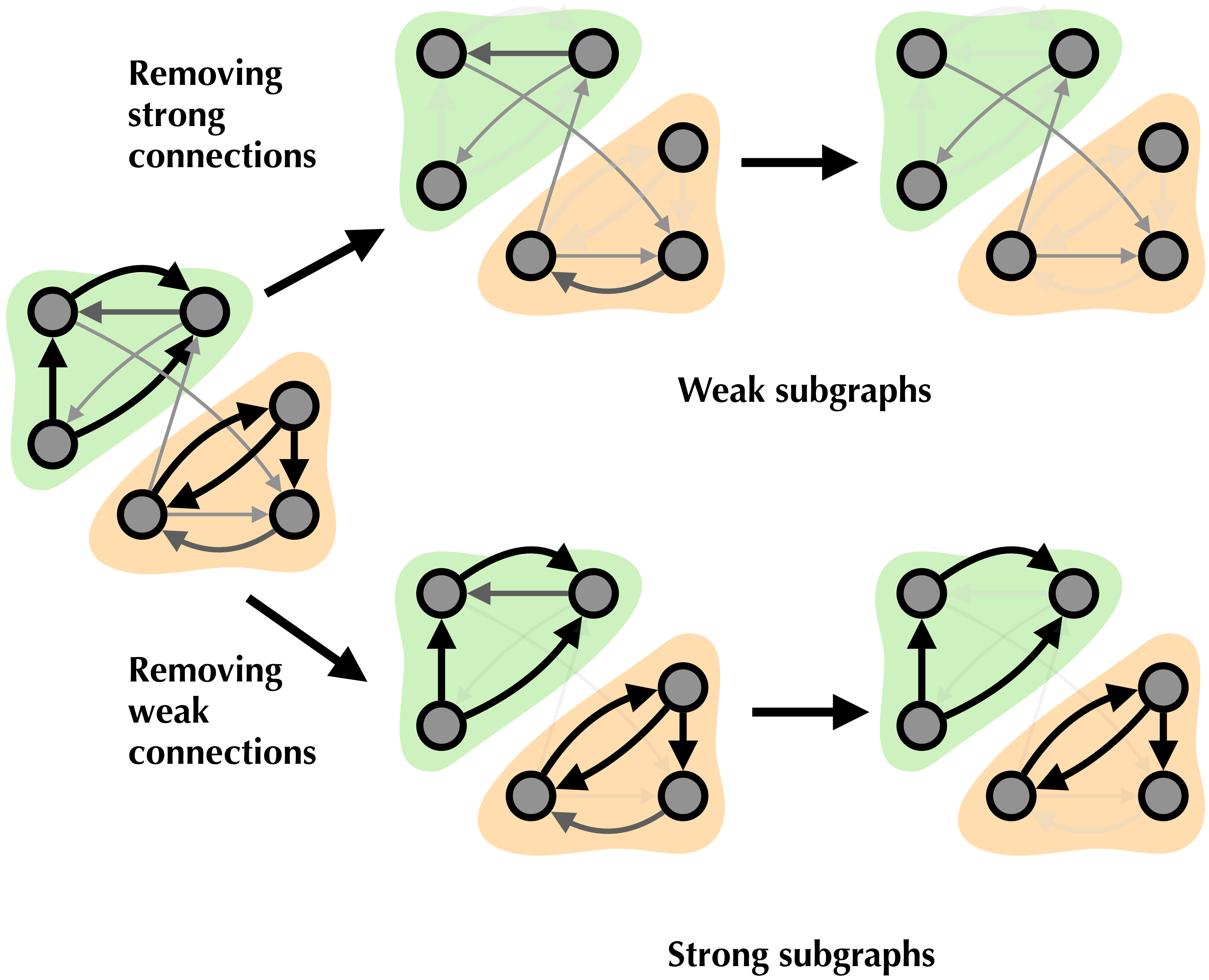

1. **Modularity Q (Newman, 2006)**

$$Q = \frac{1}{m}\sum_{ij}\left[A_{ij} - \frac{d_i^{+} d_j^{-}}{m}\right]\delta(c_i, c_j)$$

2nd evidence:
Measuring modularity of strong/weak subgraphs while keeping the block assignments

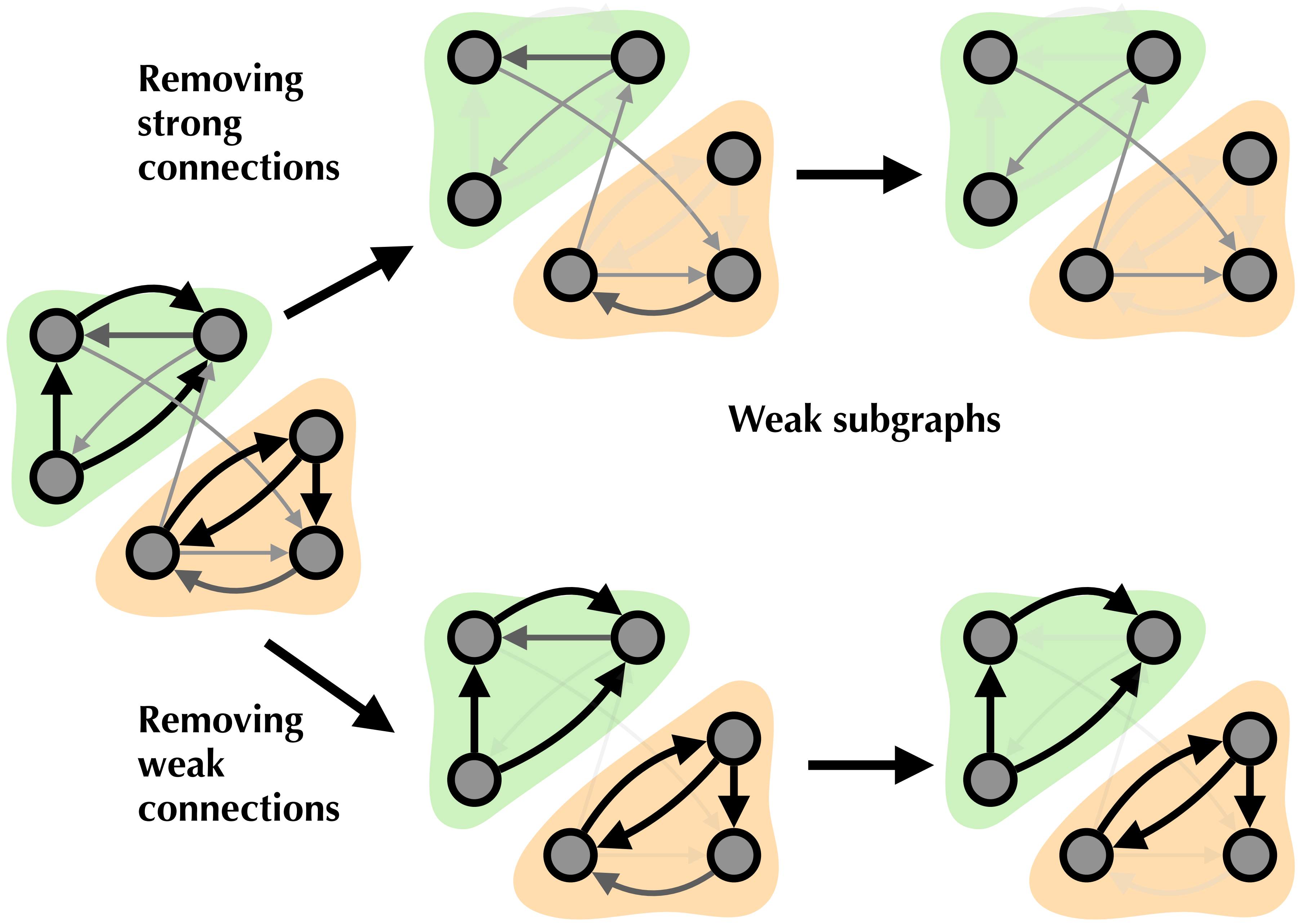

Removing strong connections

Weak subgraphs

Removing weak connections

Strong subgraphs

1. Modularity Q (Newman, 2006)

$$Q = \frac{1}{m} \sum_{ij} \left[A_{ij} - \frac{d_i^+ d_j^-}{m} \right] \delta(c_i, c_j)$$

2. Intra/inter Ratio

$$R = \sum_{ij} A_{ij} \delta(c_i, c_j) / \sum_{ij} A_{ij} (1 - \delta(c_i, c_j))$$

2nd evidence:
Measuring modularity of strong/weak subgraphs while keeping the block assignments

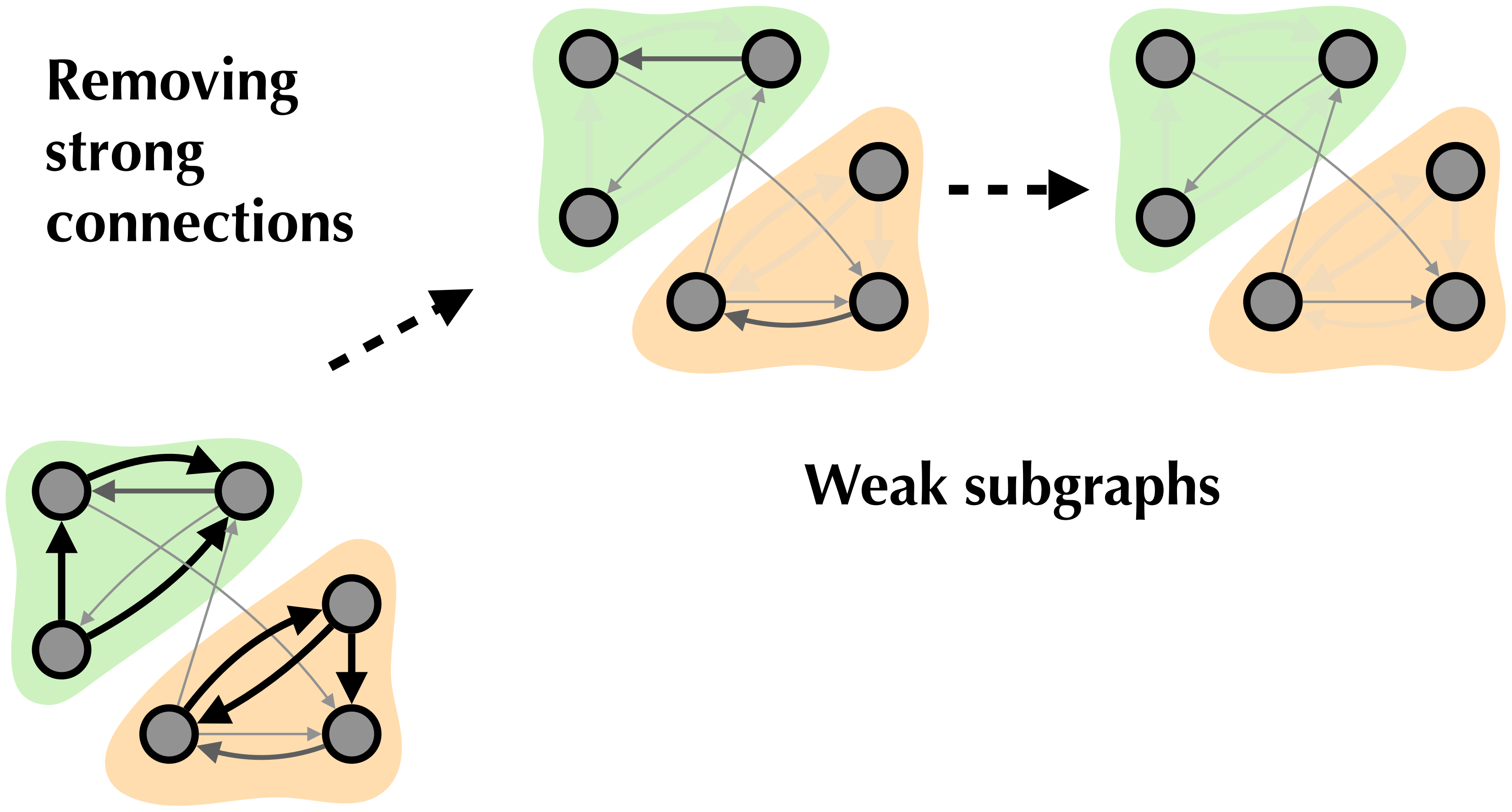

Removing strong connections

Weak subgraphs

2nd evidence:
Measuring modularity of strong/weak subgraphs while keeping the block assignments

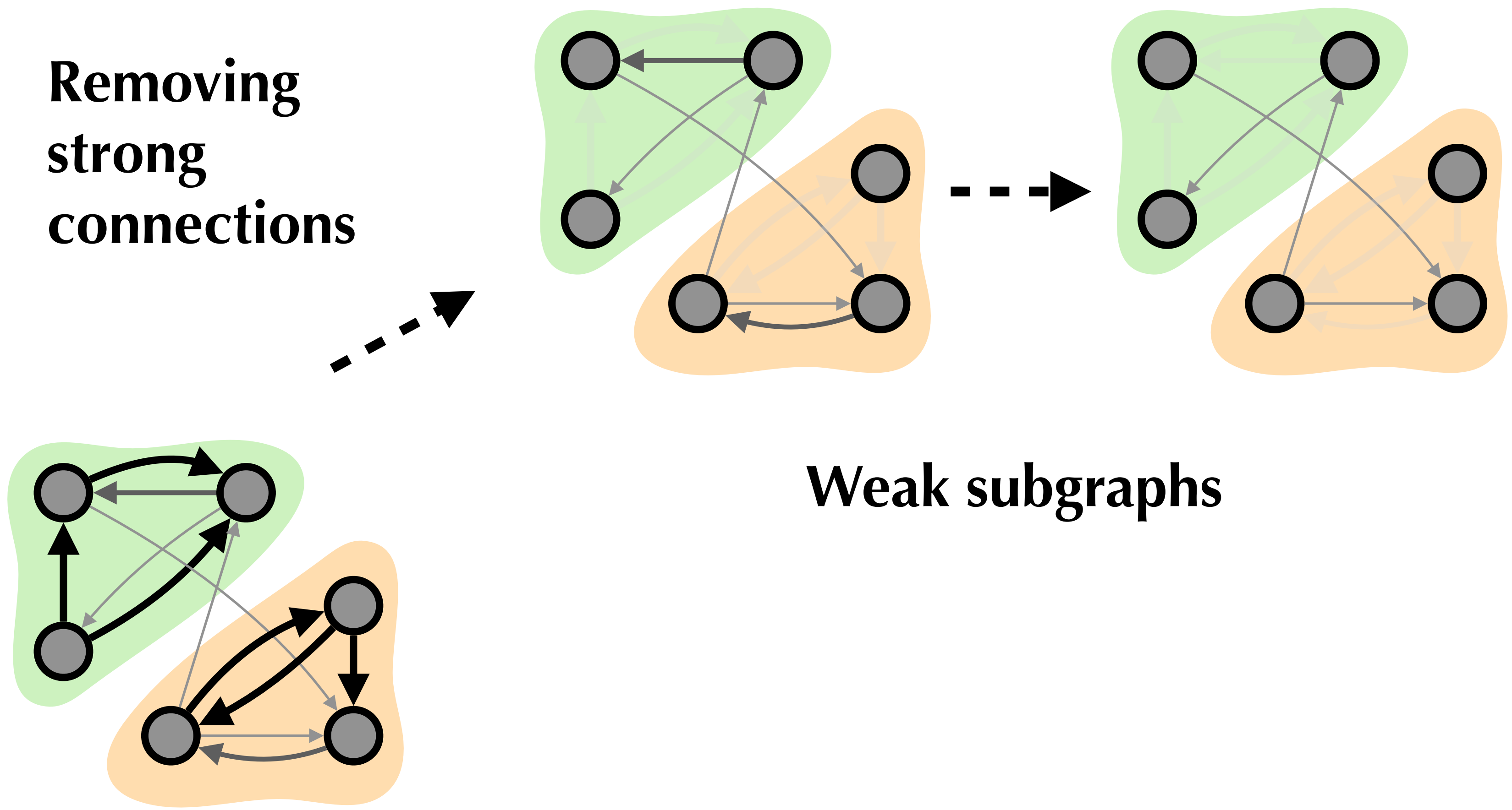

Removing strong connections

Weak subgraphs

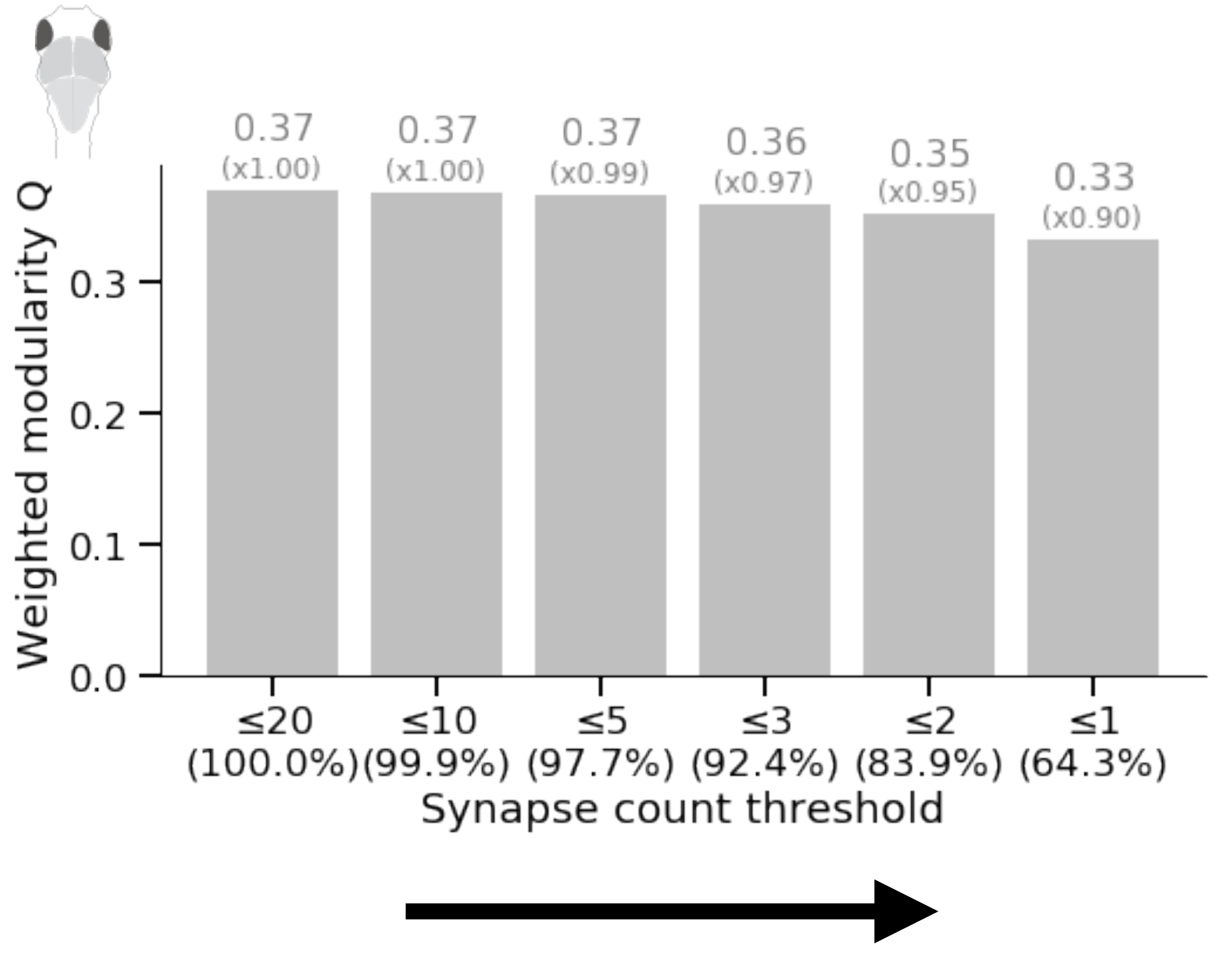

Remove strong connections

2nd evidence:
Measuring modularity of strong/weak subgraphs while keeping the block assignments

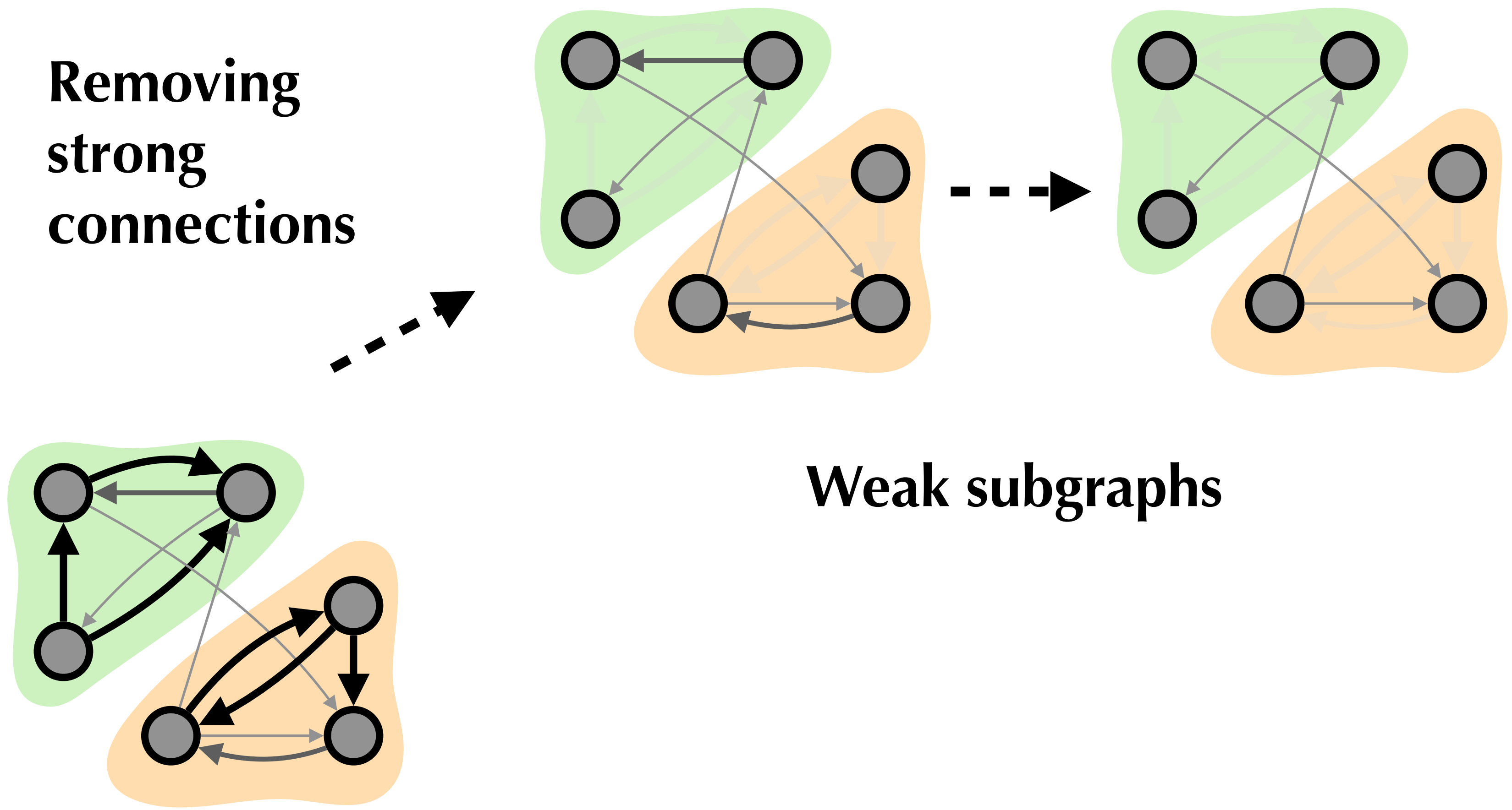

Removing strong connections

Weak subgraphs

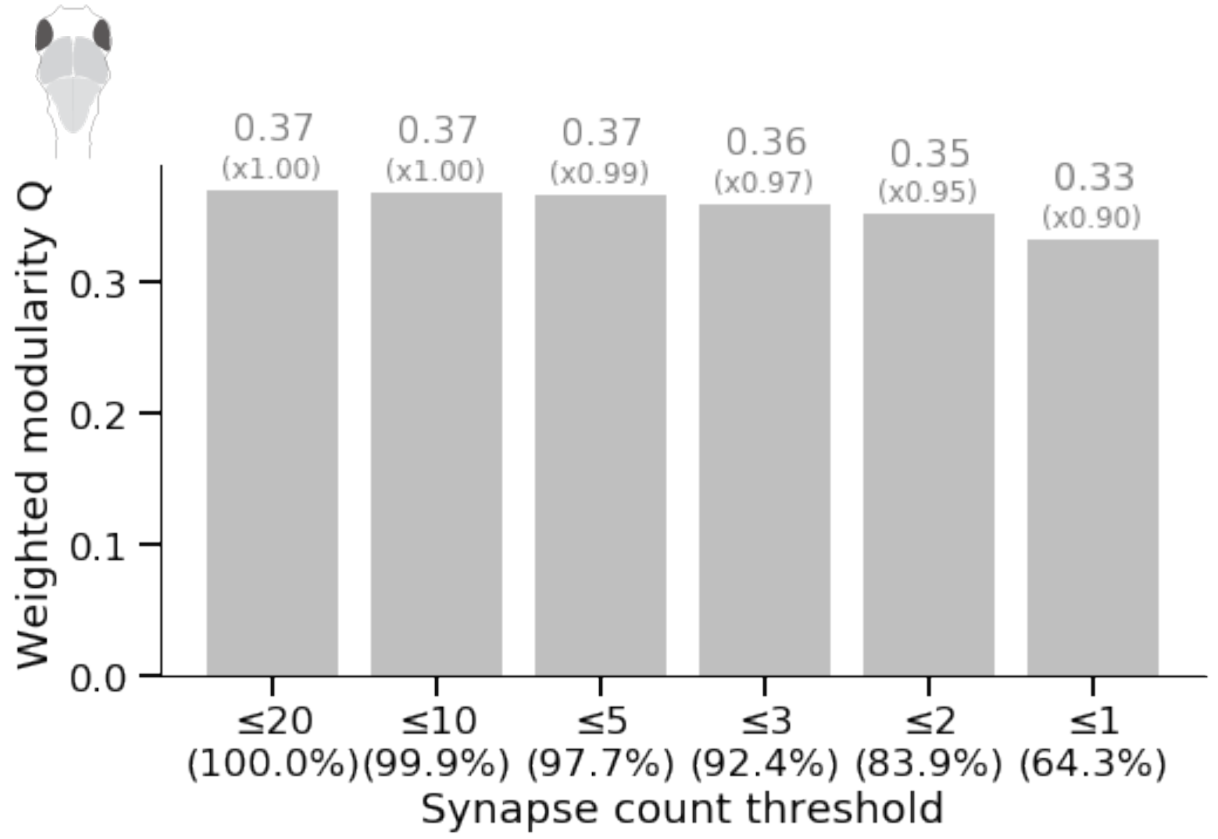

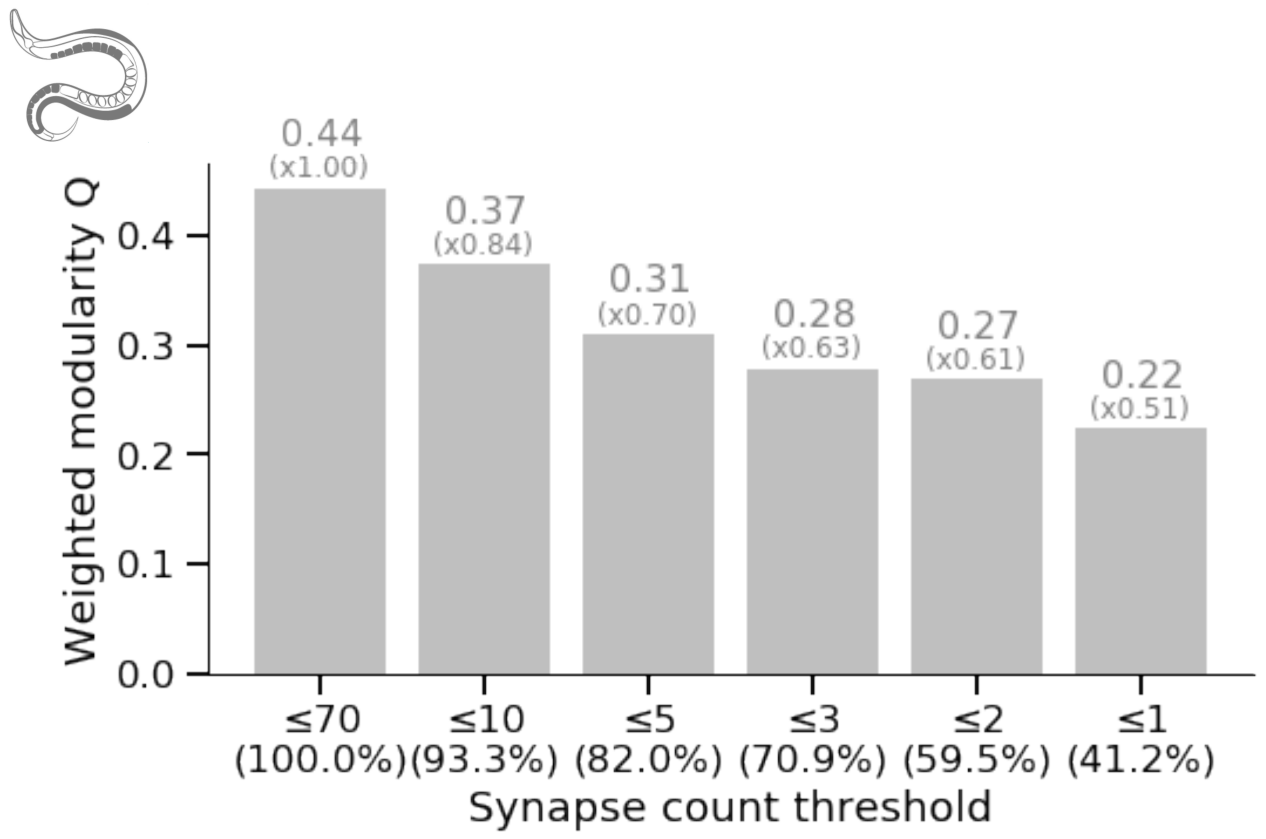

2nd evidence:
Measuring modularity of strong/weak subgraphs while keeping the block assignments

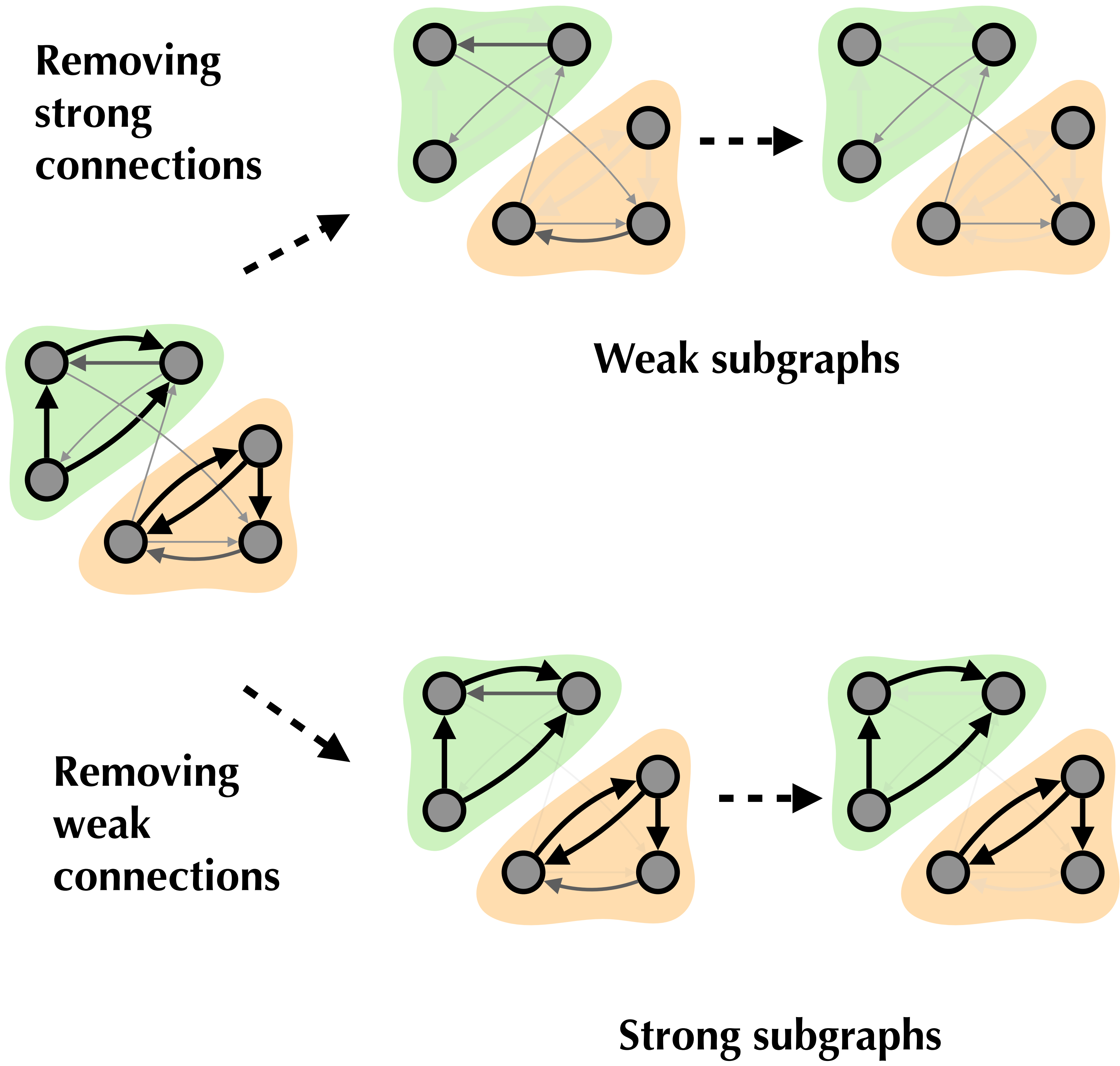

Removing strong connections

Weak subgraphs

Removing weak connections

Strong subgraphs

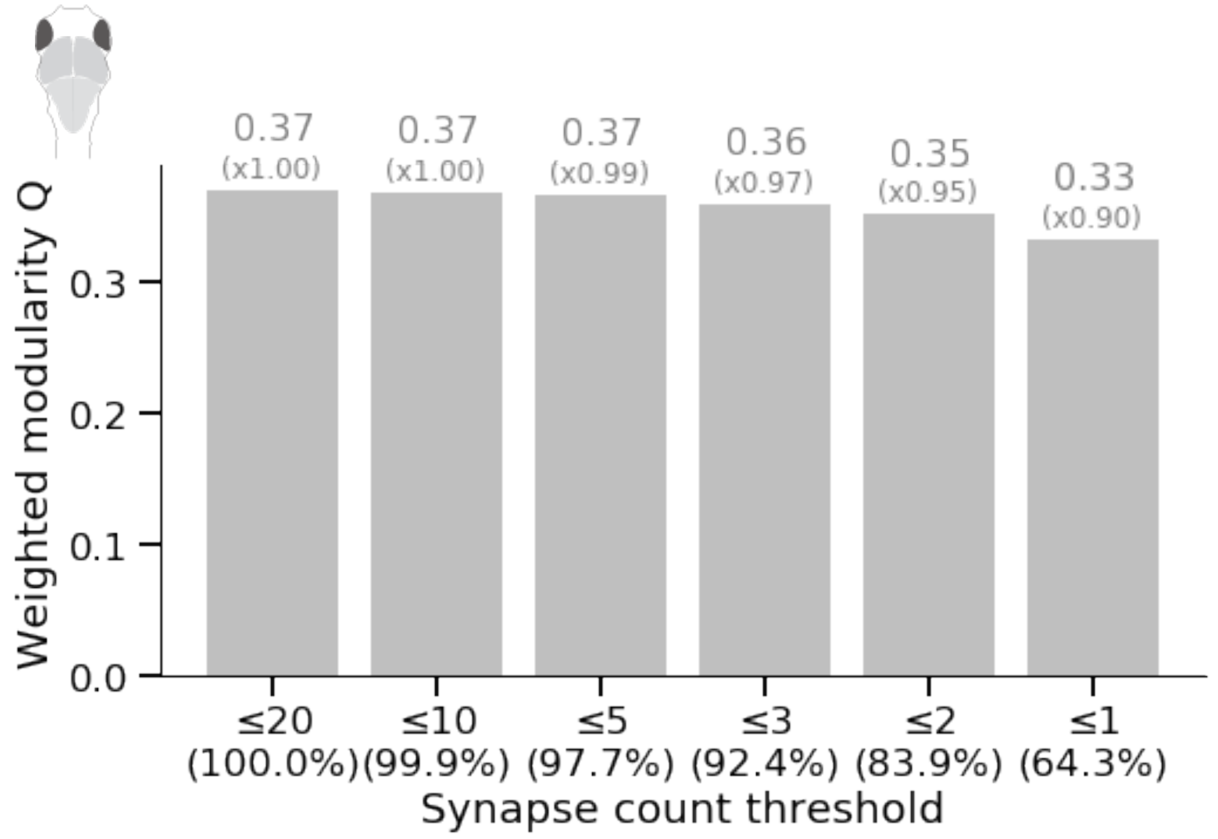

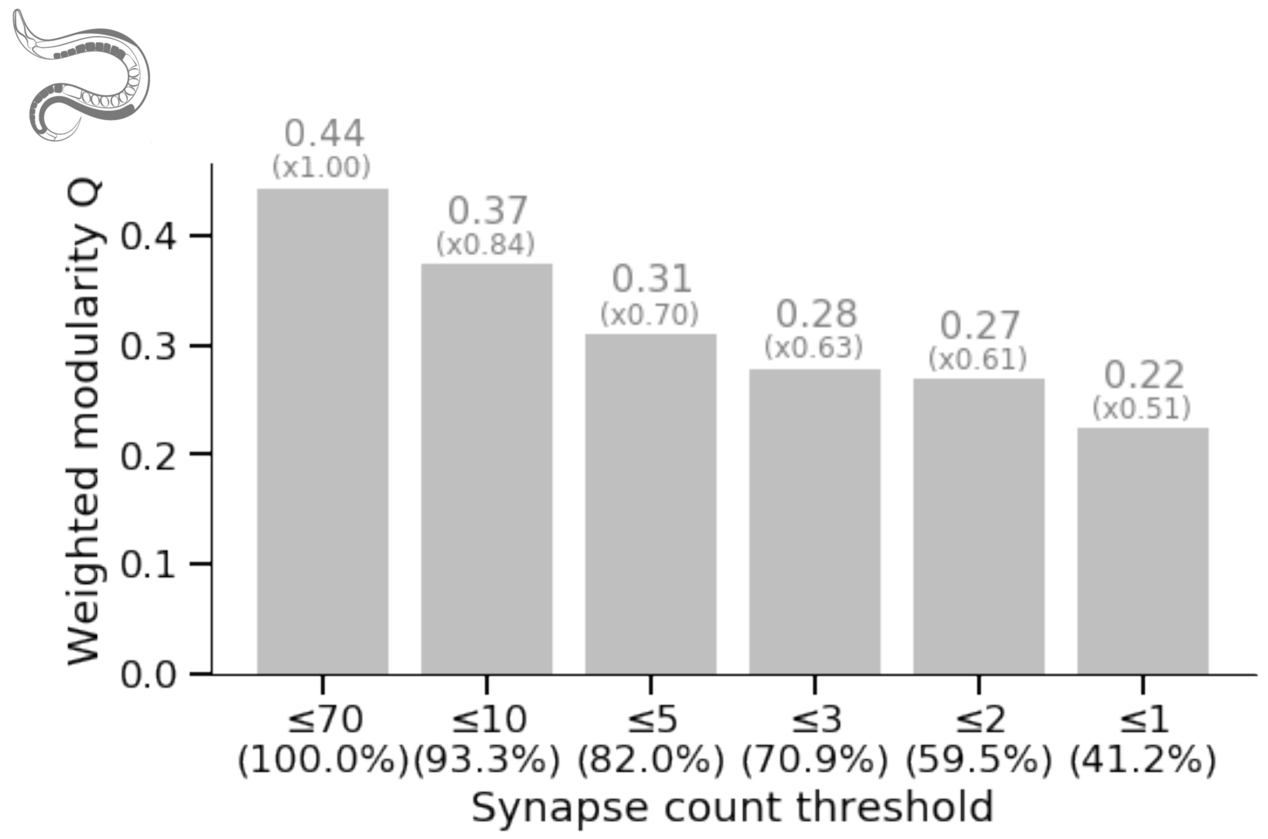

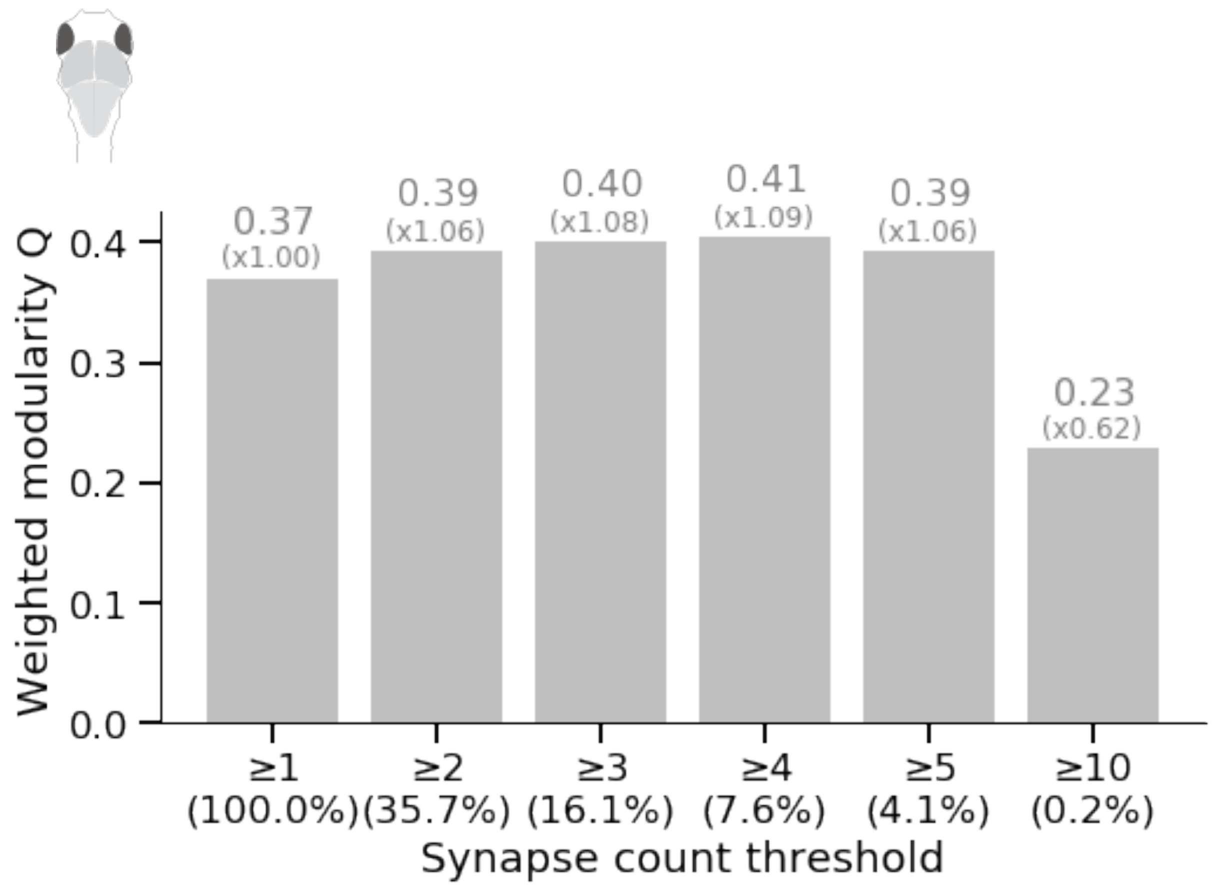

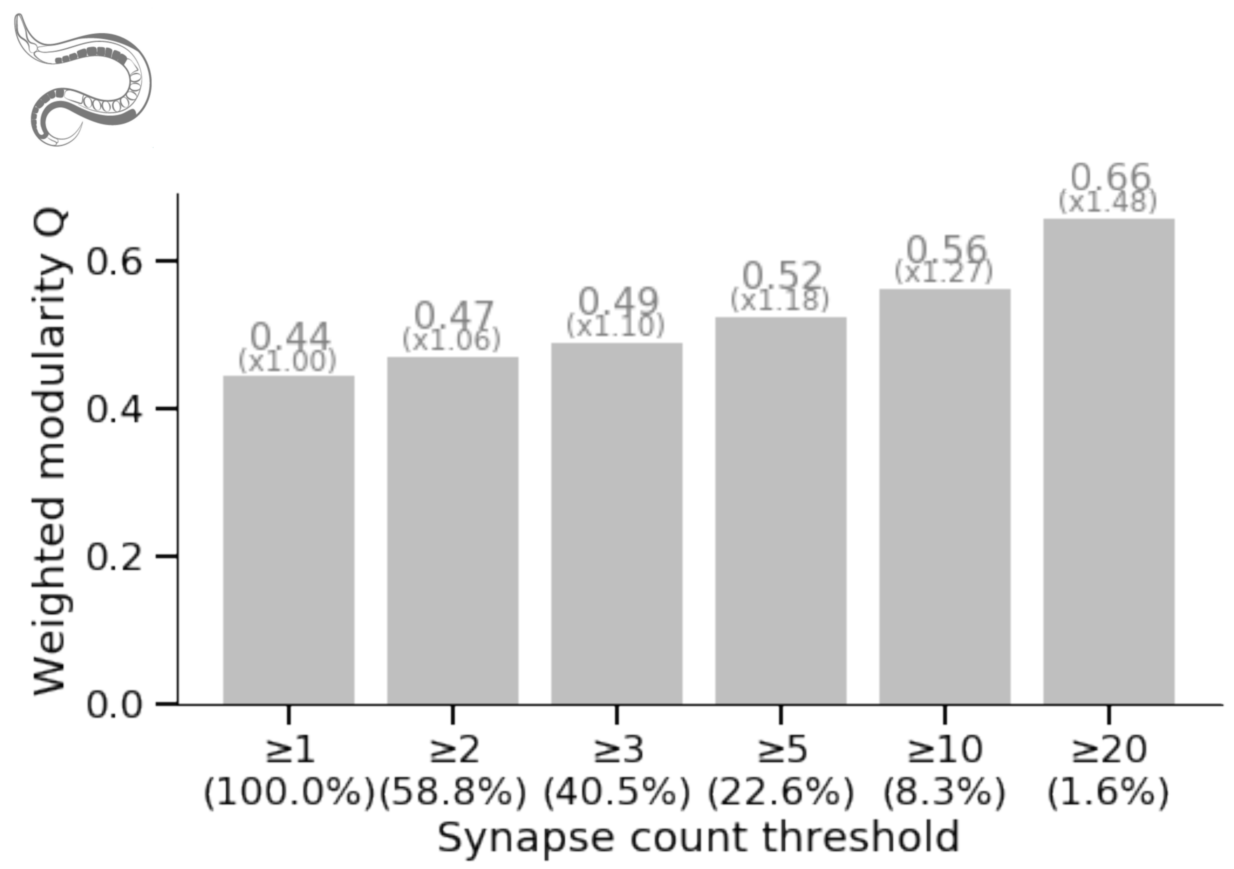

How to interpret this results?

- Weak connections involved in a lot of pathways (65% connections, 38% synapses)

How to interpret this results?

- Weak connections involved in a lot of pathways (65% connections, 38% synapses)
- Both zebrafish weak and strong connections are non-random, and have similar modular structures (while *C.* elegans weak connections are not modular)

How to interpret this results?

- Weak connections involved in a lot of pathways (65% connections, 38% synapses)

- Both zebrafish weak and strong connections are non-random, and have similar modular structures (while *C.* elegans weak connections are not modular)
  - Strong subgraph is slightly more modular than the entire graph
  - Weak subgraph is slightly less modular than the whole graph

How to interpret this results?

- Weak connections involved in a lot of pathways (65% connections, 38% synapses)
- Both zebrafish weak and strong connections are non-random, and have similar modular structures (while *C.* elegans weak connections are not modular)
  - Strong subgraph is slightly more modular than the entire graph
  - Weak subgraph is slightly less modular than the whole graph
- Could the strong vs weak connection modularity be explained by Peters' rule?

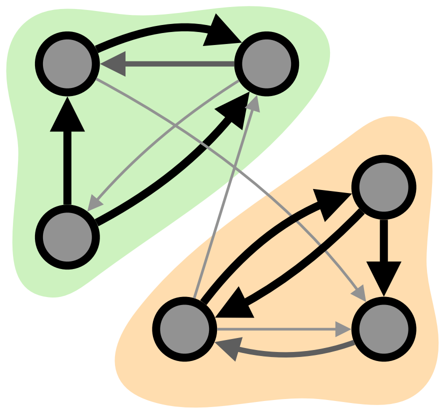

Suppose each axonal-dendritic contact will form a synapses with probability *p*

There're more contacts within modules and two modules are roughly equal sized.

=> More contacts between within-module neuronal pairs
=> weak connections are less likely

III. Cyclic Structure in the Oculomotor Module

C. elegans connectome is approximately feedforward (Varshney et al. 2011, Cook et al. 2019)

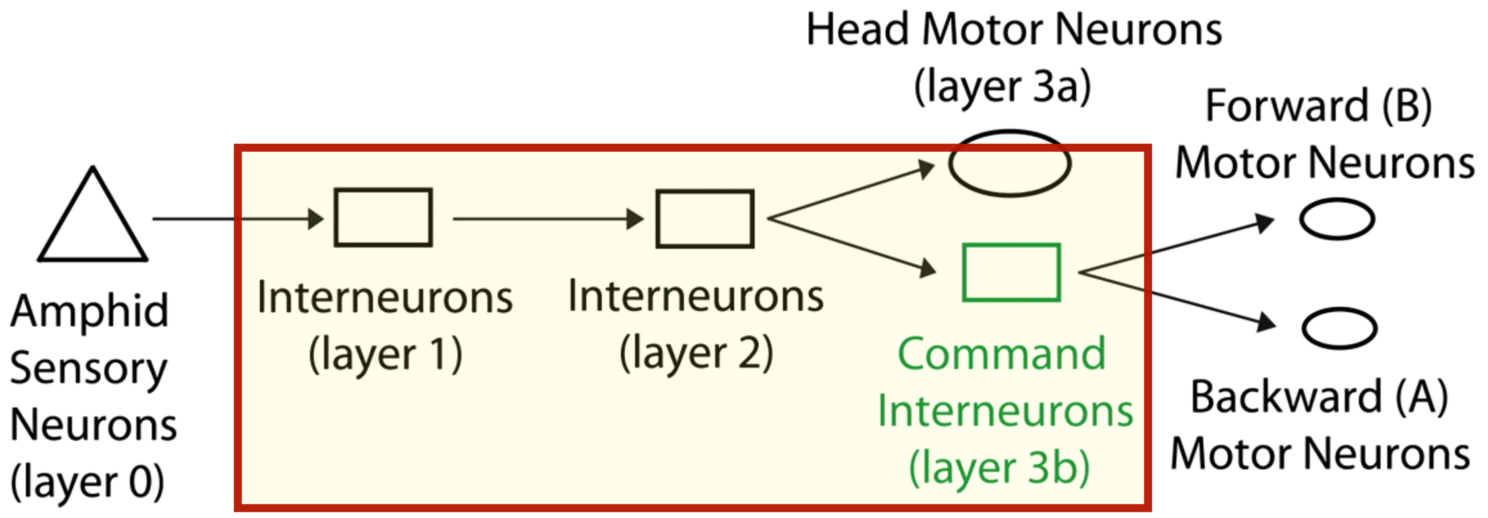

Gray et al. 2005

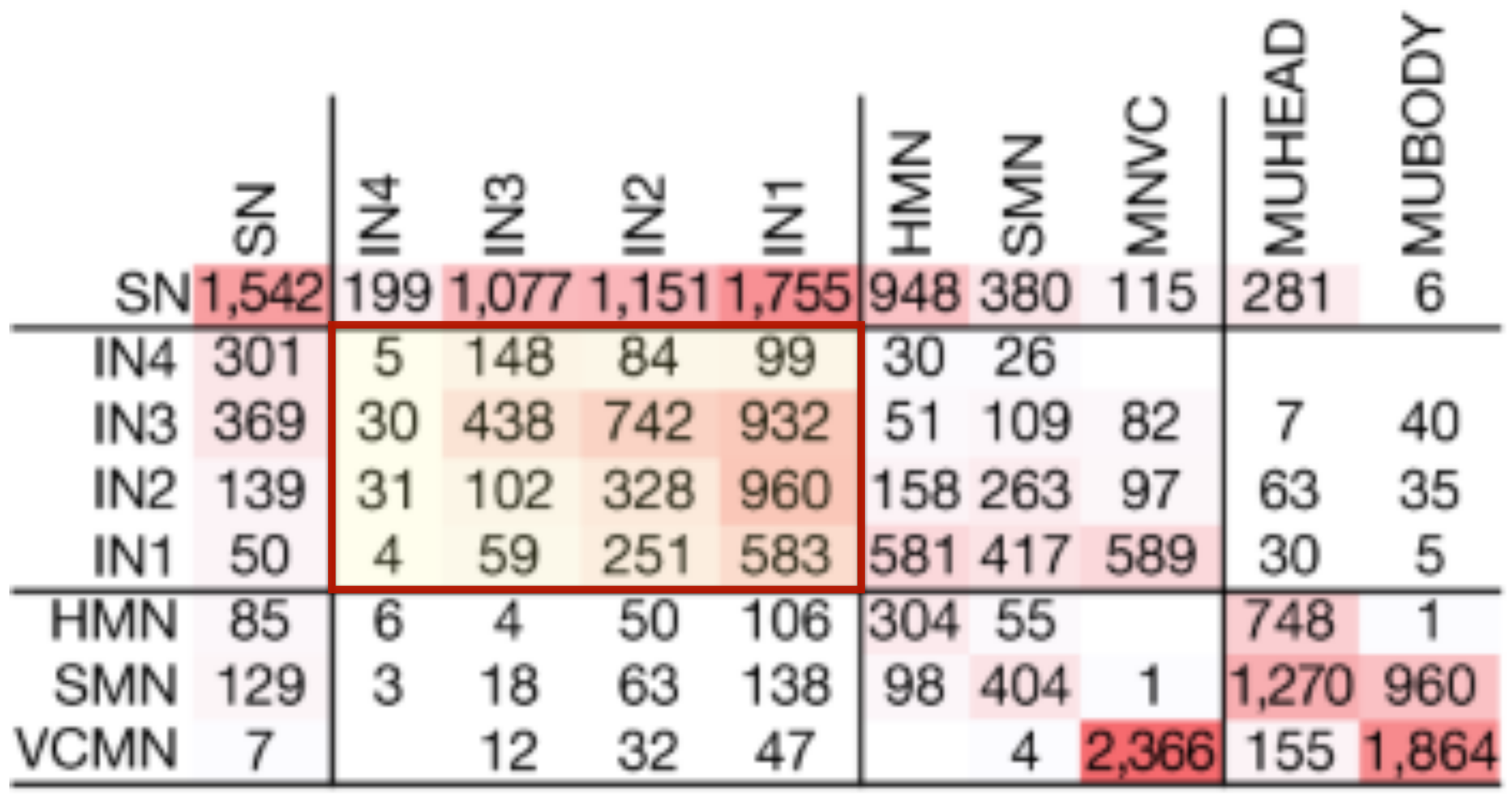

	SN	IN4	IN3	IN2	IN1	HMN	SMN	MNVC	MUHEAD	MUBODY
SN	1,542	199	1,077	1,151	1,755	948	380	115	281	6
IN4	301	5	148	84	99	30	26			
IN3	369	30	438	742	932	51	109	82	7	40
IN2	139	31	102	328	960	158	263	97	63	35
IN1	50	4	59	251	583	581	417	589	30	5
HMN	85	6	4	50	106	304	55		748	1
SMN	129	3	18	63	138	98	404	1	1,270	960
VCMN	7		12	32	47		4	2,366	155	1,864

Cook et al. 2019

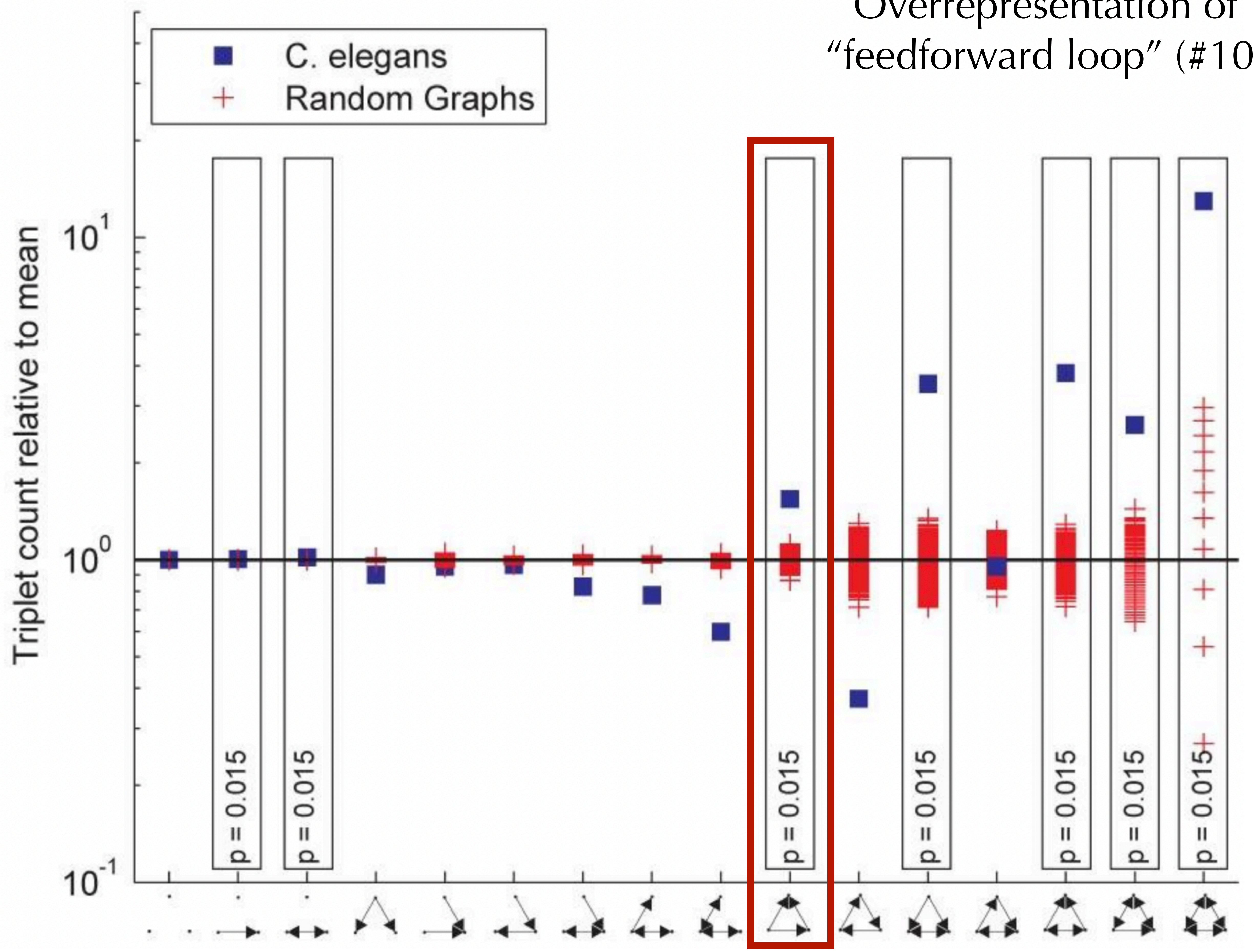

Overrepresentation of
“feedforward loop” (#10)

Varshney et al. 2011

Greater reciprocity than random networks

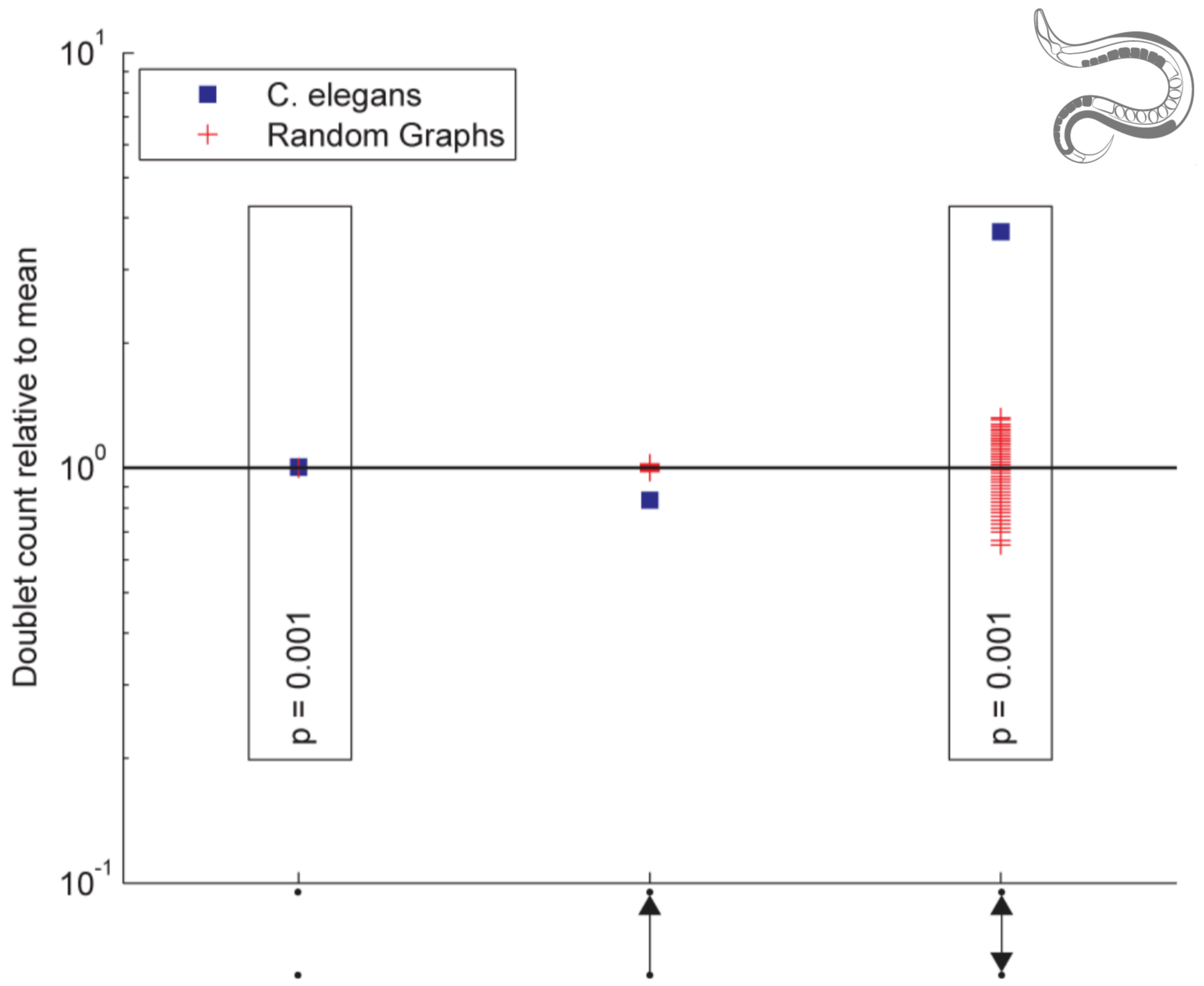

Varshney et al. 2011

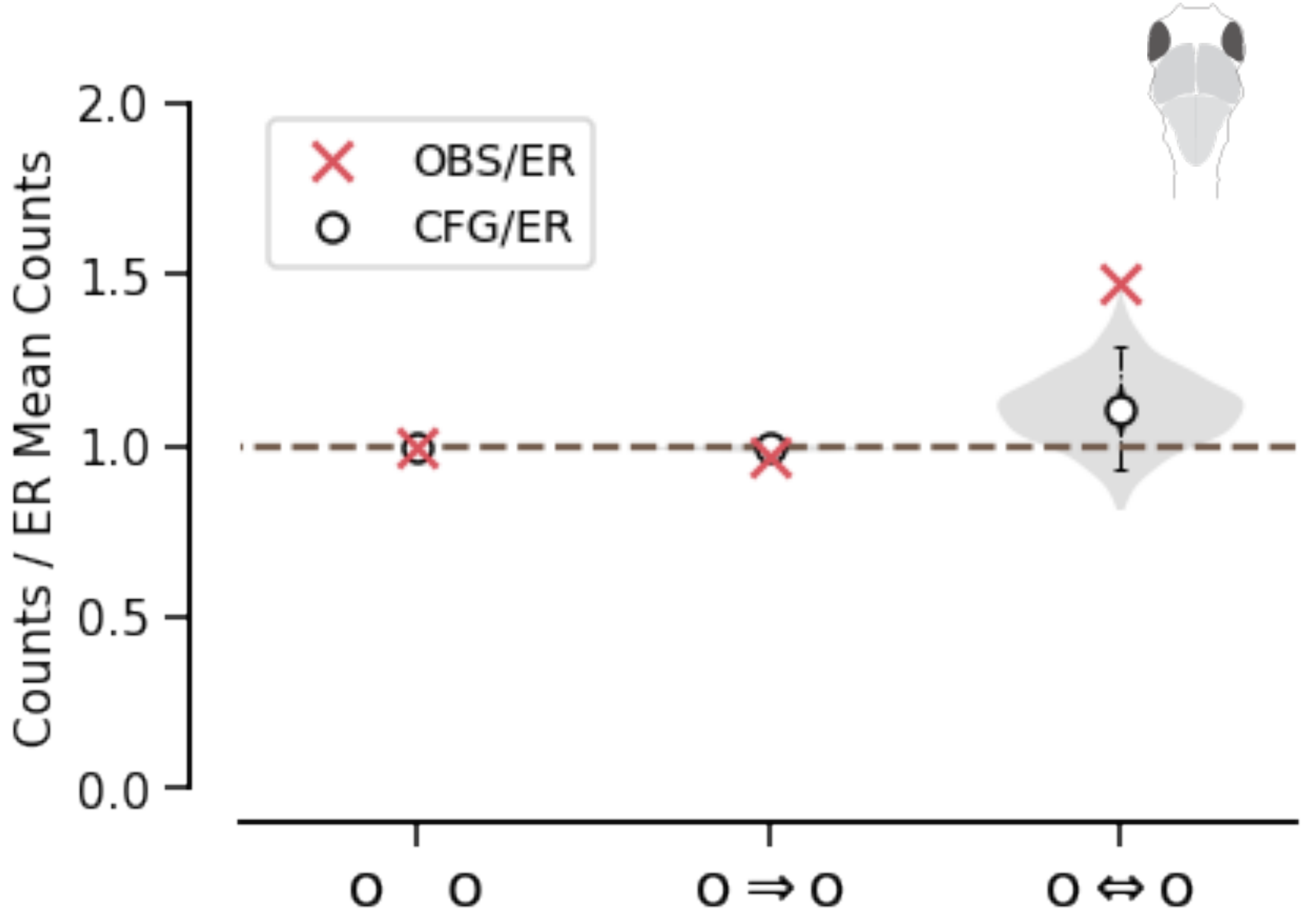

Zebrafish oculomotor module

Recurrent motifs are overrepresented in the zebrafish modO

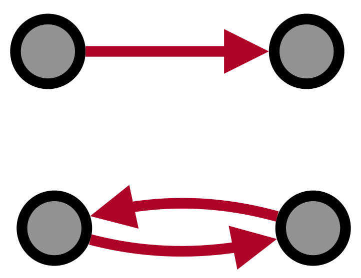

$$p_{uni} = \frac{\#\text{uni-edge}}{n(n-1)}$$

$$p_{bi} = \frac{\#\text{bi-edge}}{n(n-1)/2}$$

Generalized Erdős-Rényi model (gER)
preserving stats of 2-cell motifs

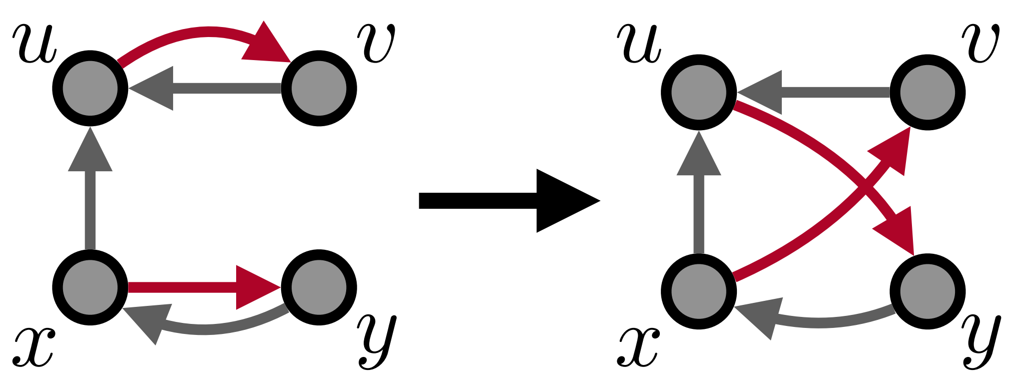

Configuration model (CFG)
degree-preserving rewiring

$$(u,v),(x,y) \rightsquigarrow (u,y),(x,v)$$

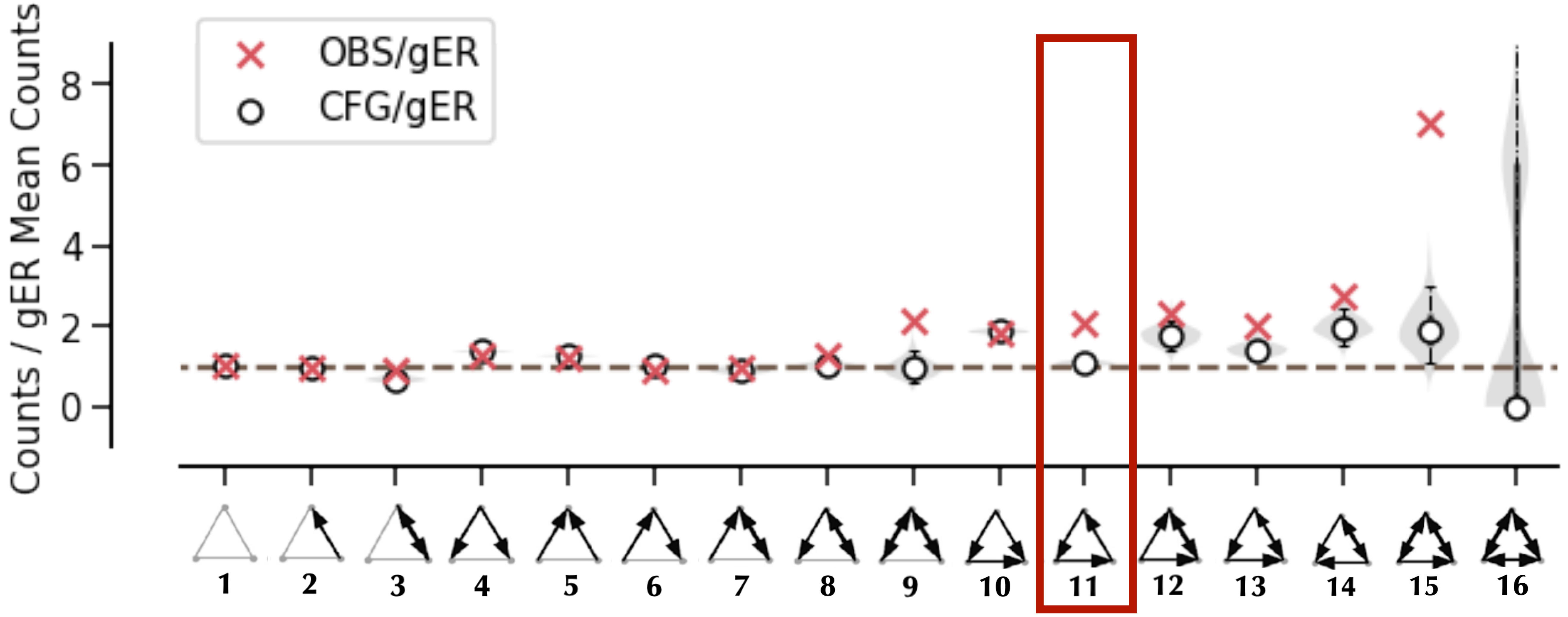

Recurrent motifs are overrepresented in the zebrafish modO

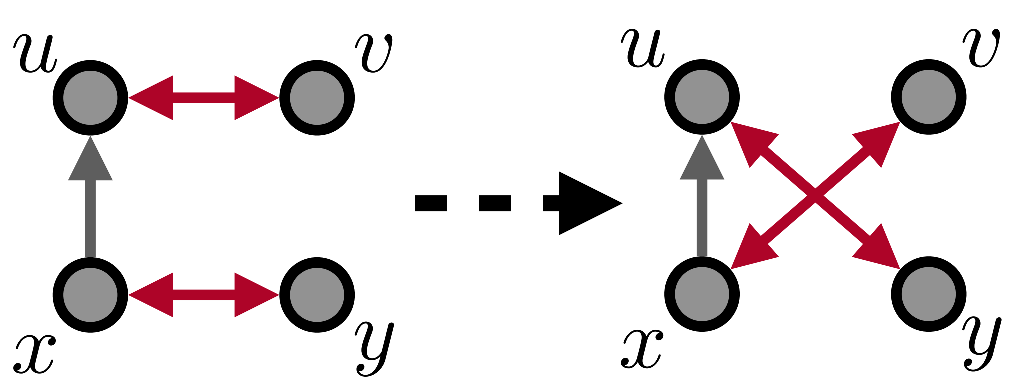

Generalized CFG (gCFG): degree-preserving rewiring & holding the number of reciprocal connections for each cell

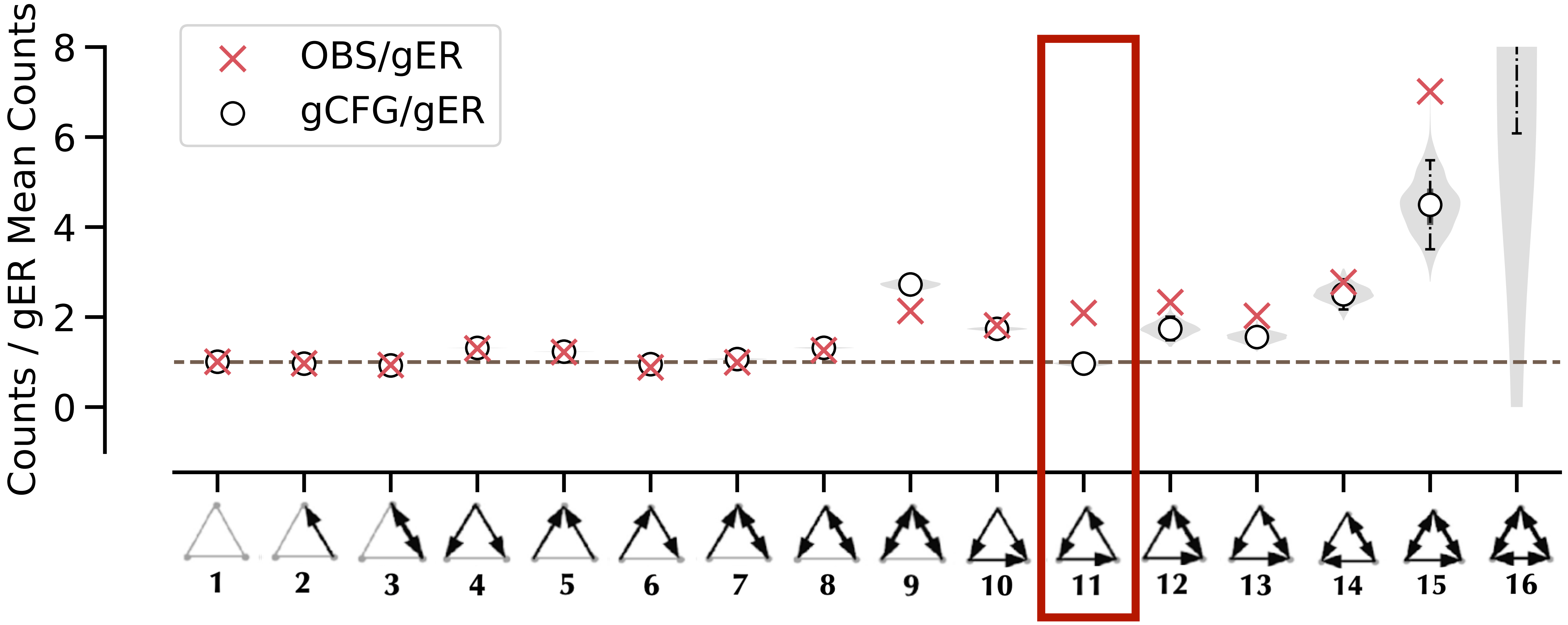

Recurrence metric #1: 3-unicycle coefficient

3-unicycle coefficient

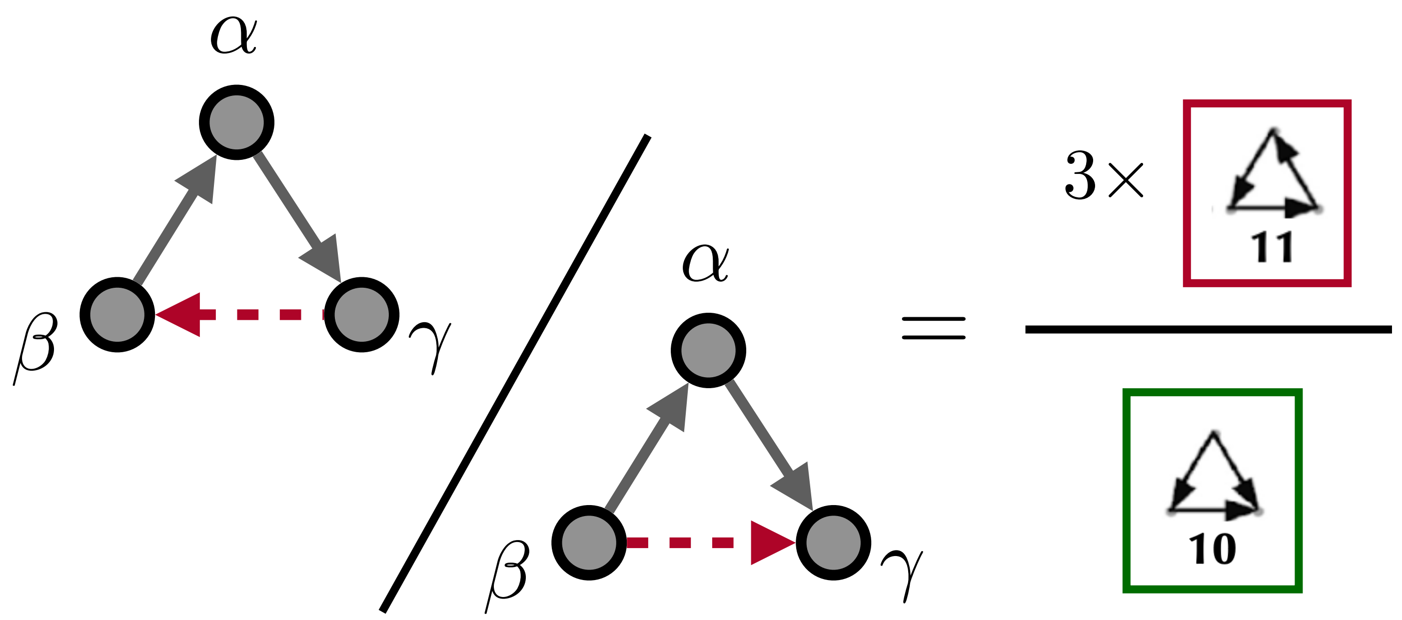

$$U_3 = \frac{\texttt{Pr}[\gamma \overset{\rightarrow}{\not\leftarrow} \beta | \beta \overset{\rightarrow}{\not\leftarrow} \alpha \wedge \alpha \overset{\rightarrow}{\not\leftarrow} \gamma]}{\texttt{Pr}[\beta \overset{\rightarrow}{\not\leftarrow} \gamma | \beta \overset{\rightarrow}{\not\leftarrow} \alpha \wedge \alpha \overset{\rightarrow}{\not\leftarrow} \gamma]}$$

Recurrence metric #2: 3-cycle coefficient

3-cycle coefficient

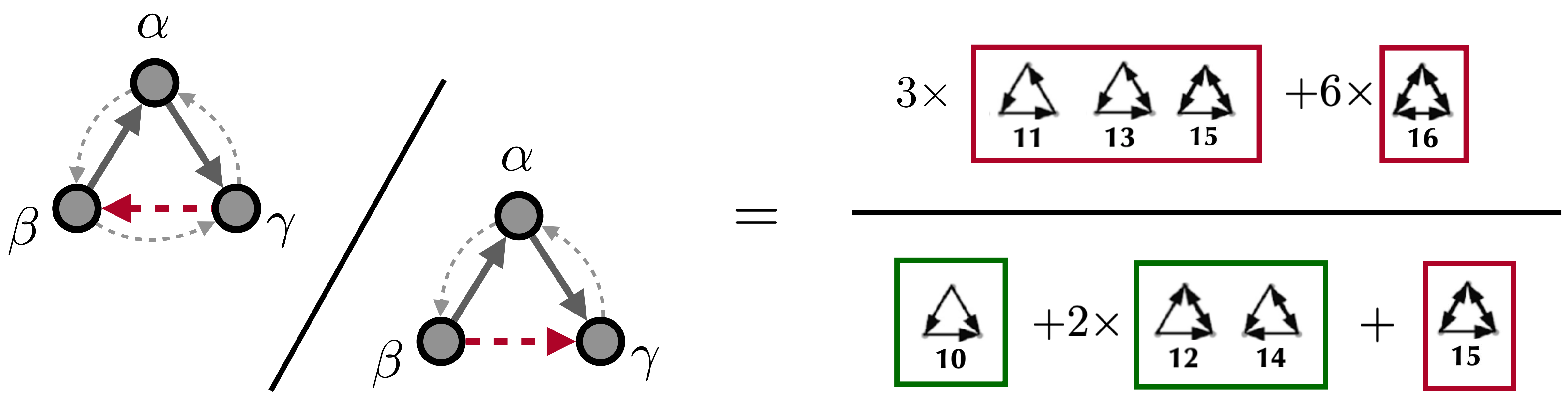

$$C_3 = \frac{\mathtt{Pr}[\gamma \rightarrow \beta | \beta \rightarrow \alpha \wedge \alpha \rightarrow \gamma]}{\mathtt{Pr}[\beta \substack{\rightarrow \\ \not\leftarrow} \gamma | \beta \rightarrow \alpha \wedge \alpha \rightarrow \gamma]}$$

modO is much more recurrent than random graphs

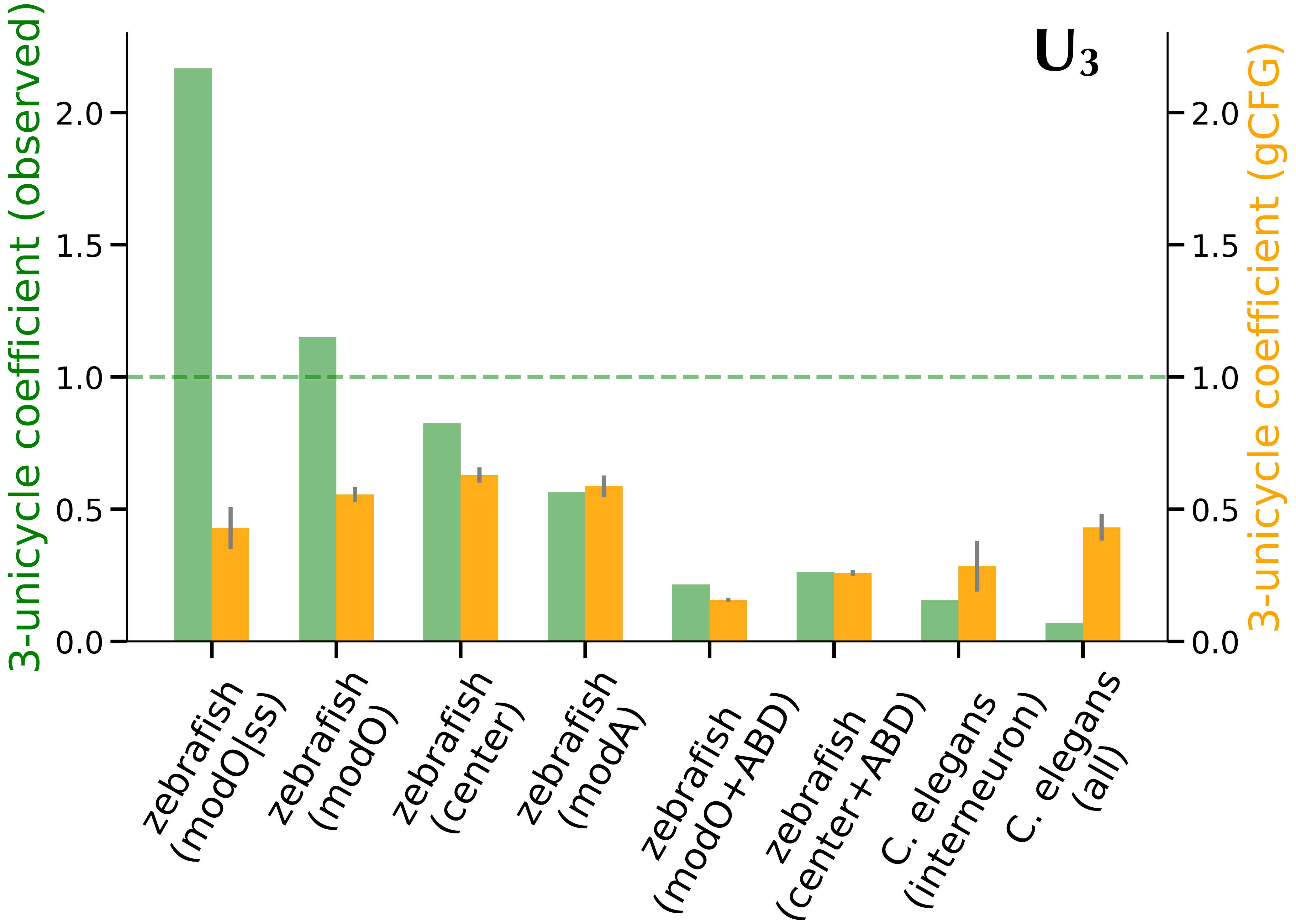

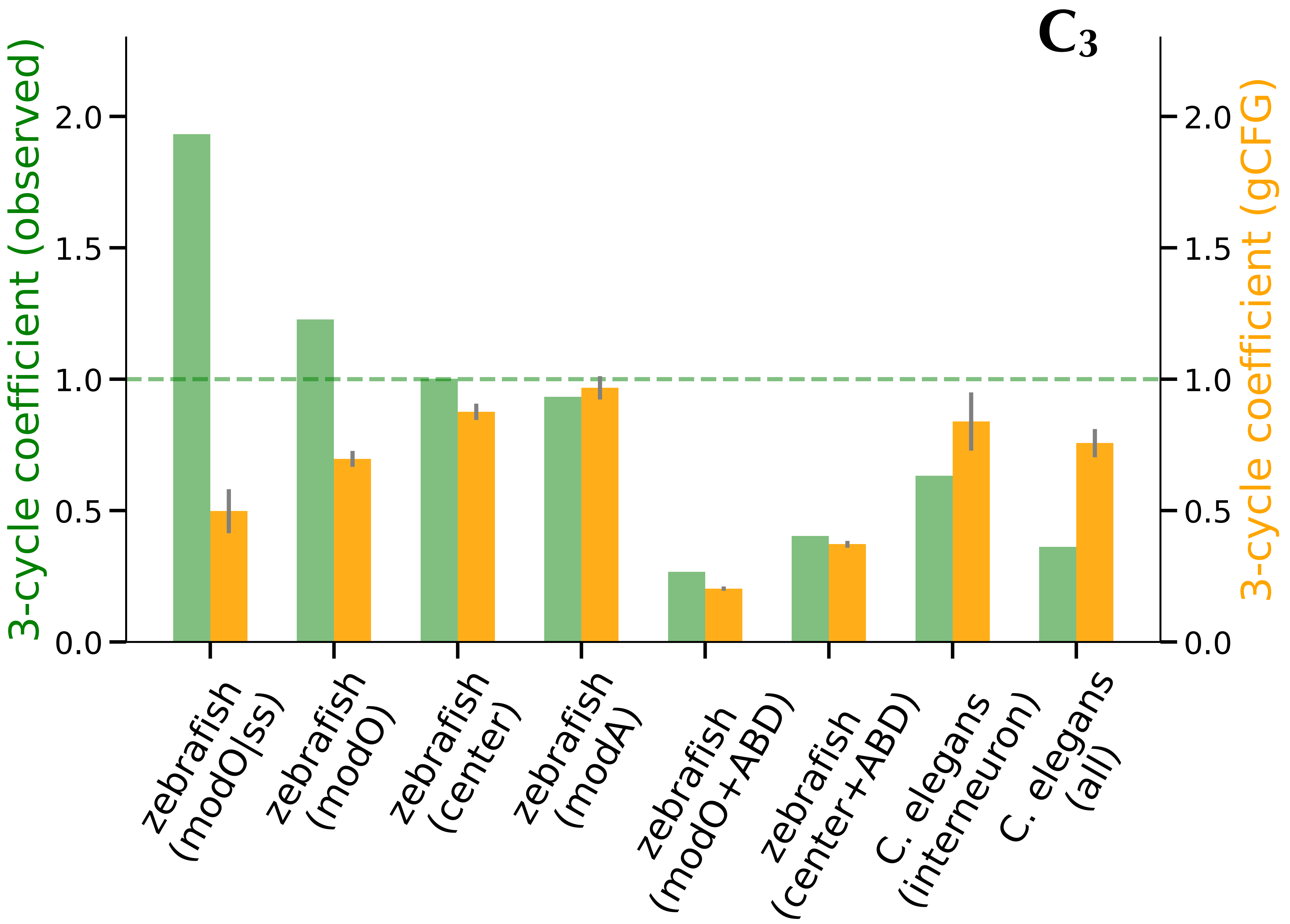

DC-SBM discovers a 3-block structure in modO

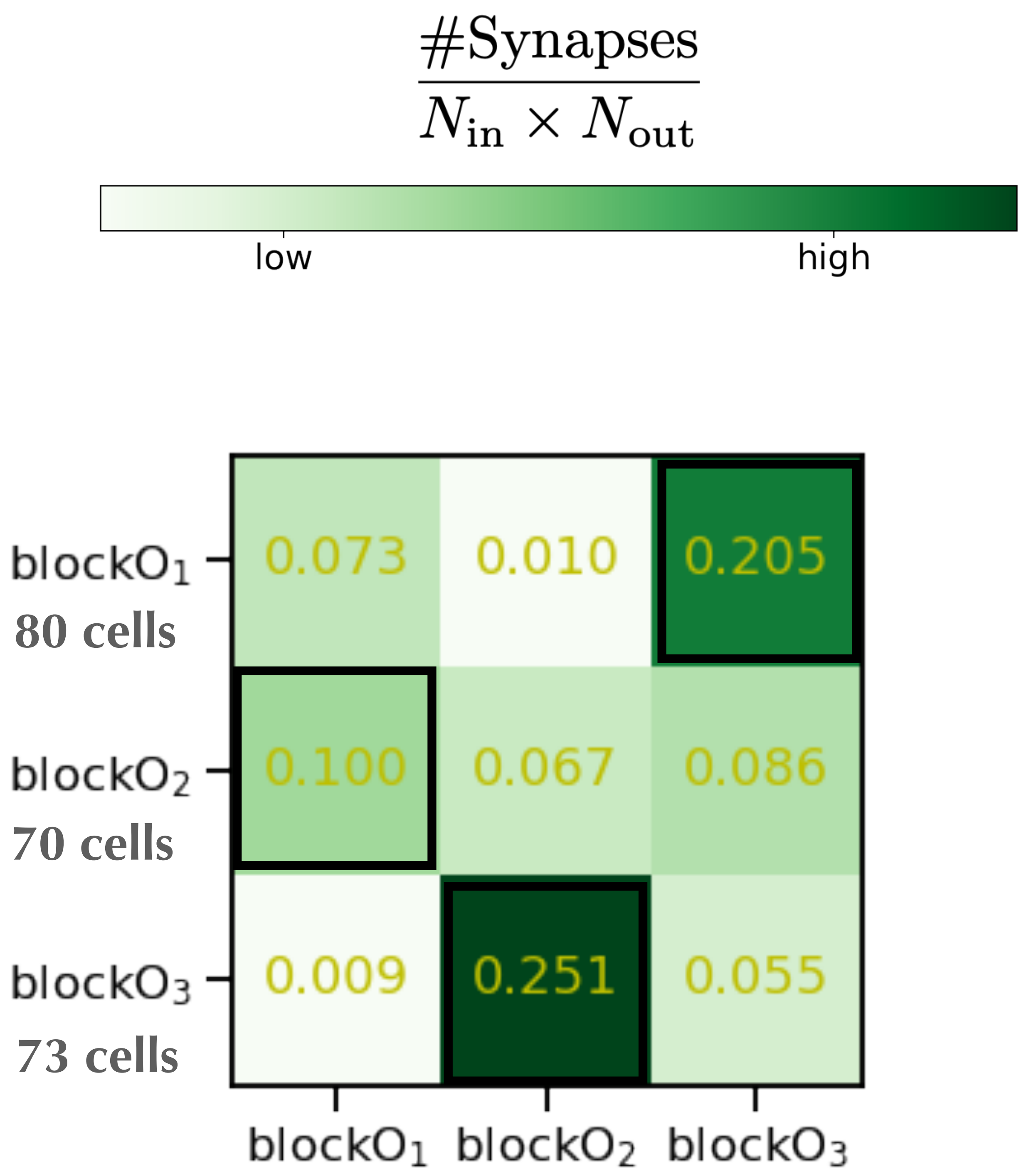

	blockO$_1$	blockO$_2$	blockO$_3$
blockO$_1$ 80 cells	0.073	0.010	0.205
blockO$_2$ 70 cells	0.100	0.067	0.086
blockO$_3$ 73 cells	0.009	0.251	0.055

87.2% 3-unicycles comes from this 3-block structure

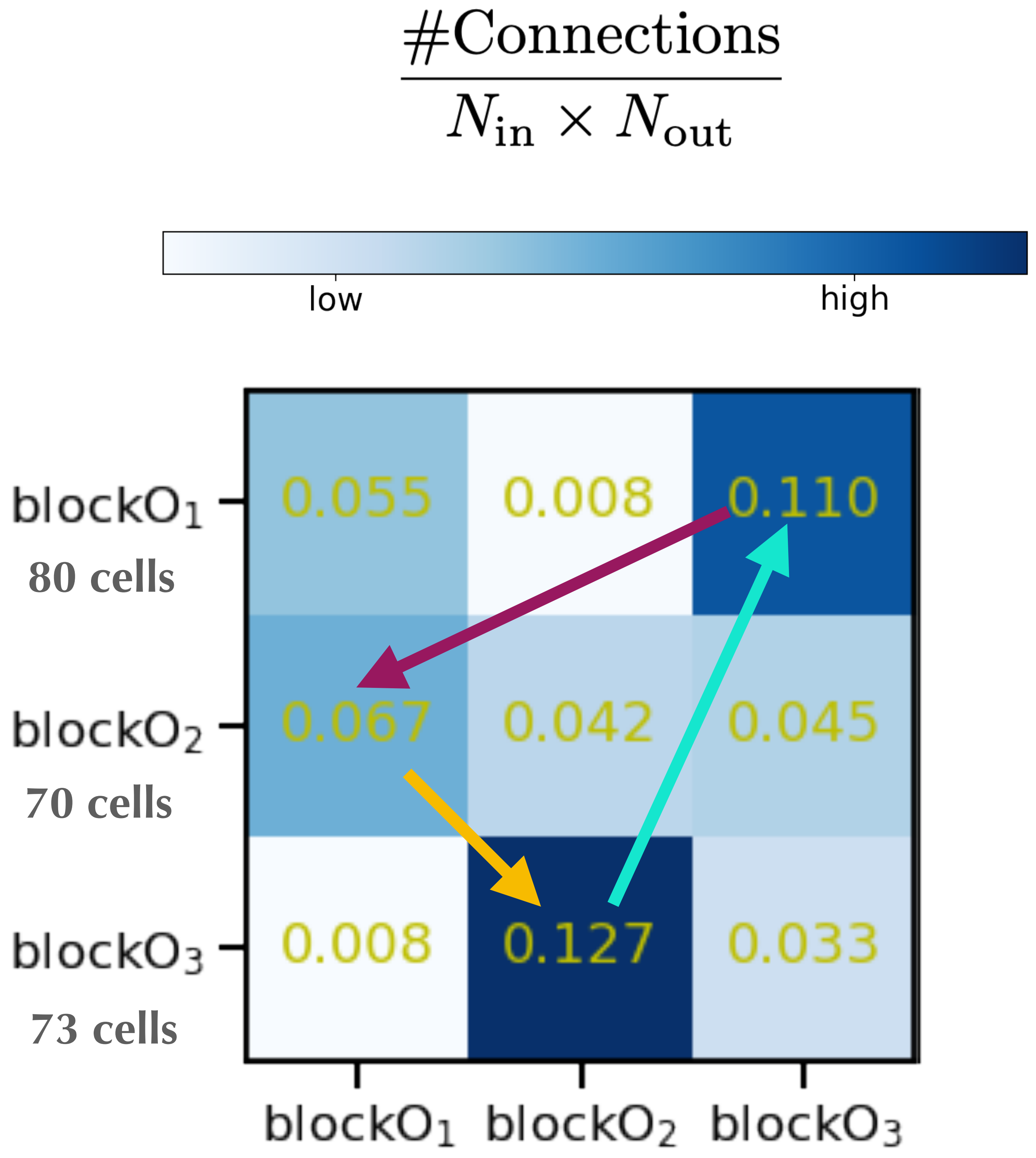

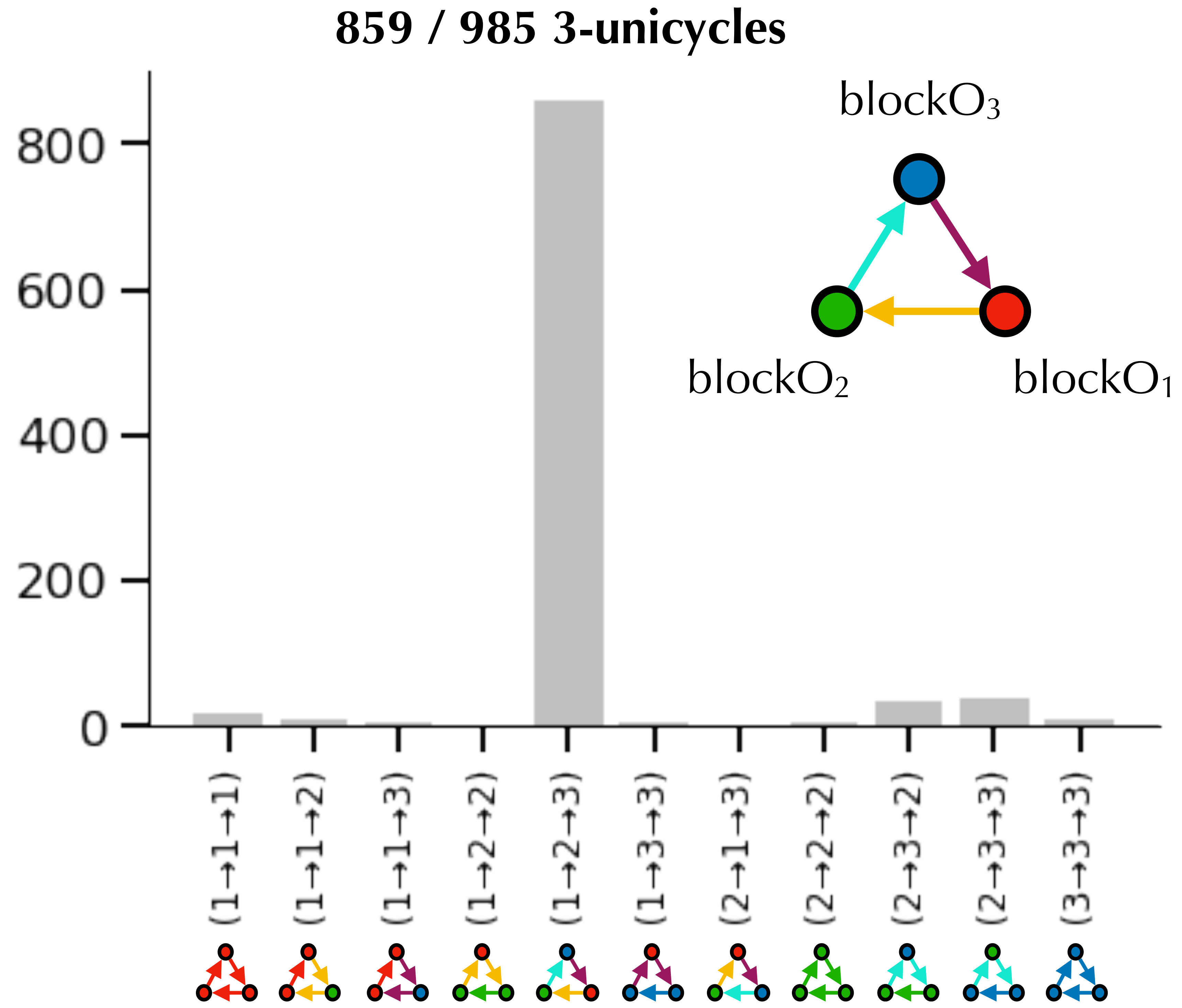

Identifying saccadic neurons by tracing the axons of presynaptic partners of ABD neurons

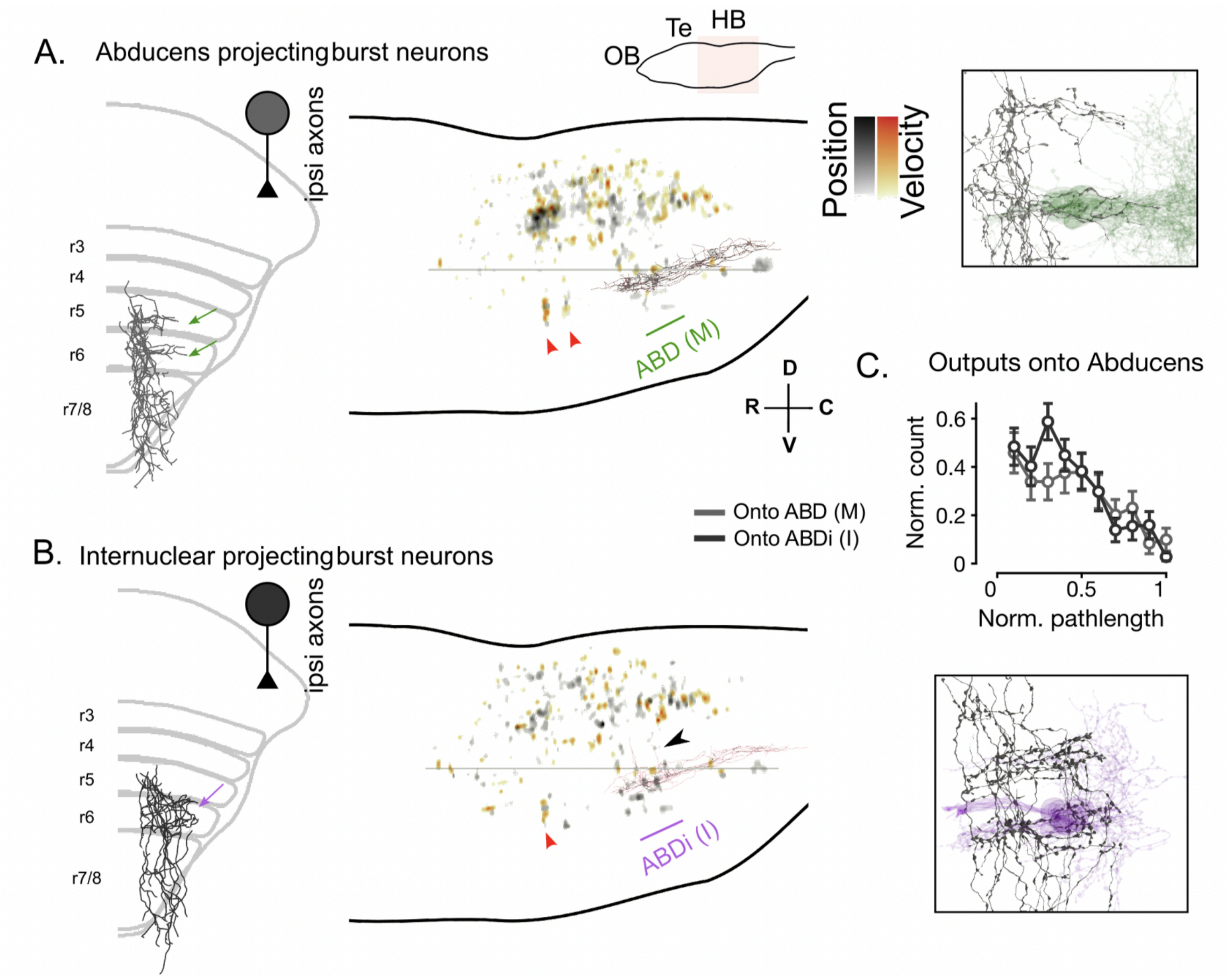

Identifying of inhibitory burst neurons by lateral axons and overlap with GABAergic clusters

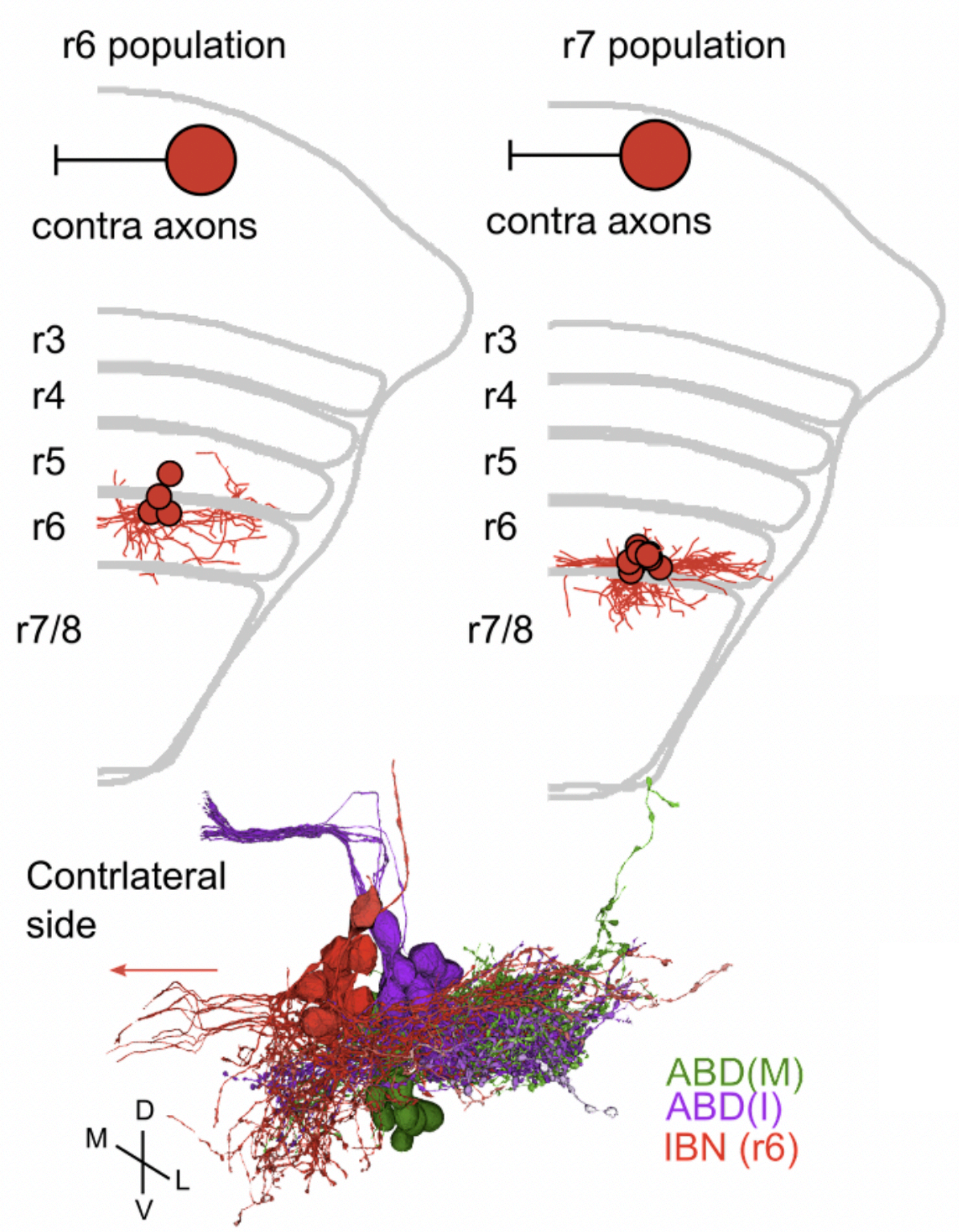

Inhibitory Burst Neurons (IBN)

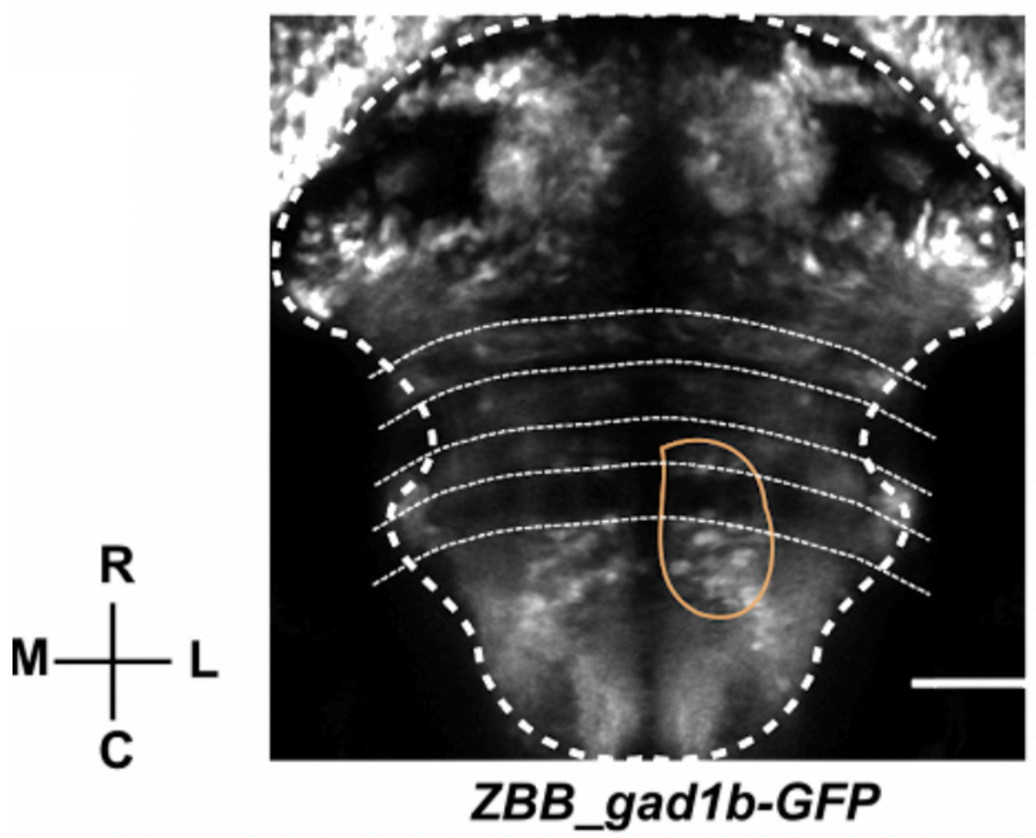

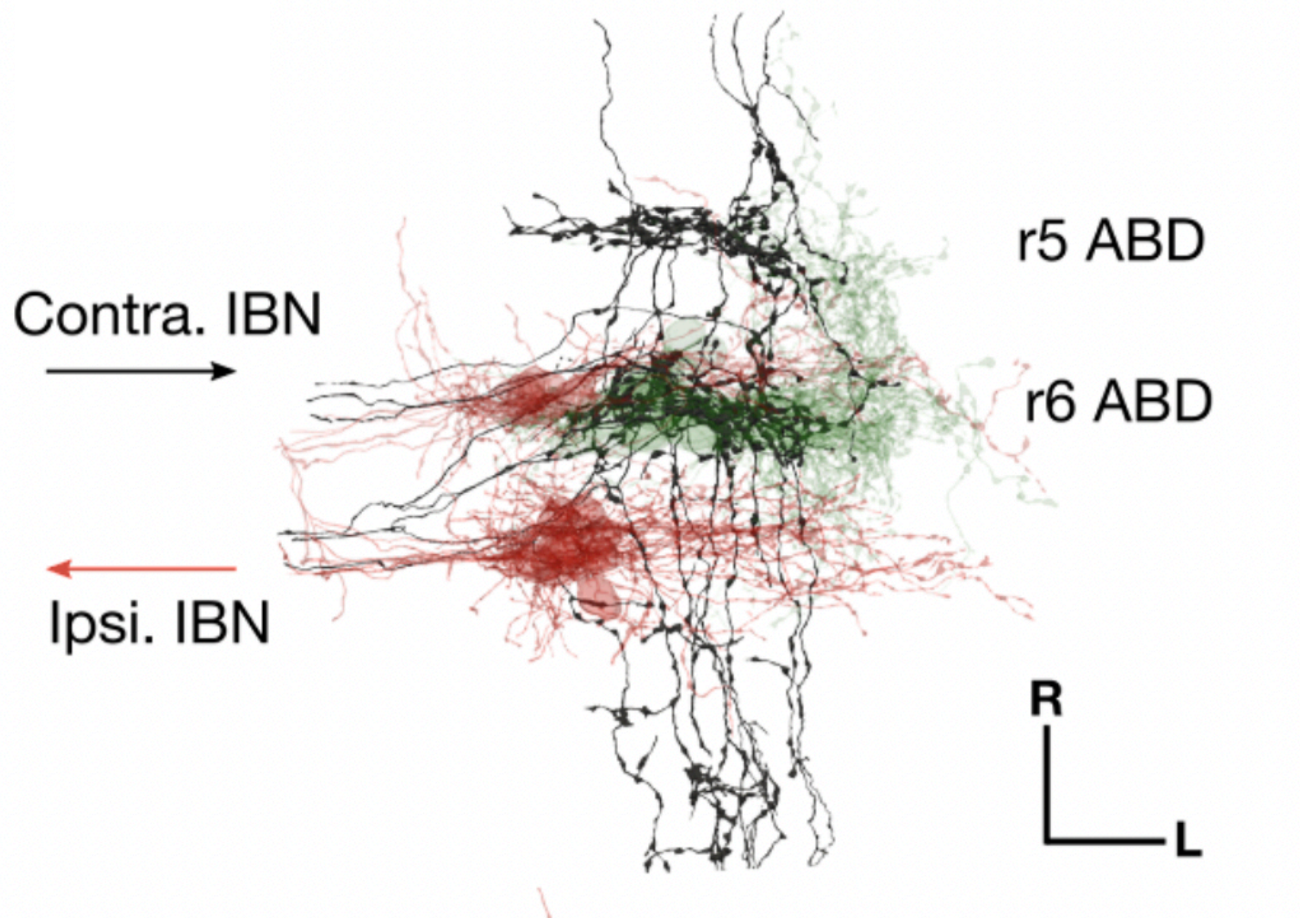

3 cyclic blocks are selective to the inputs

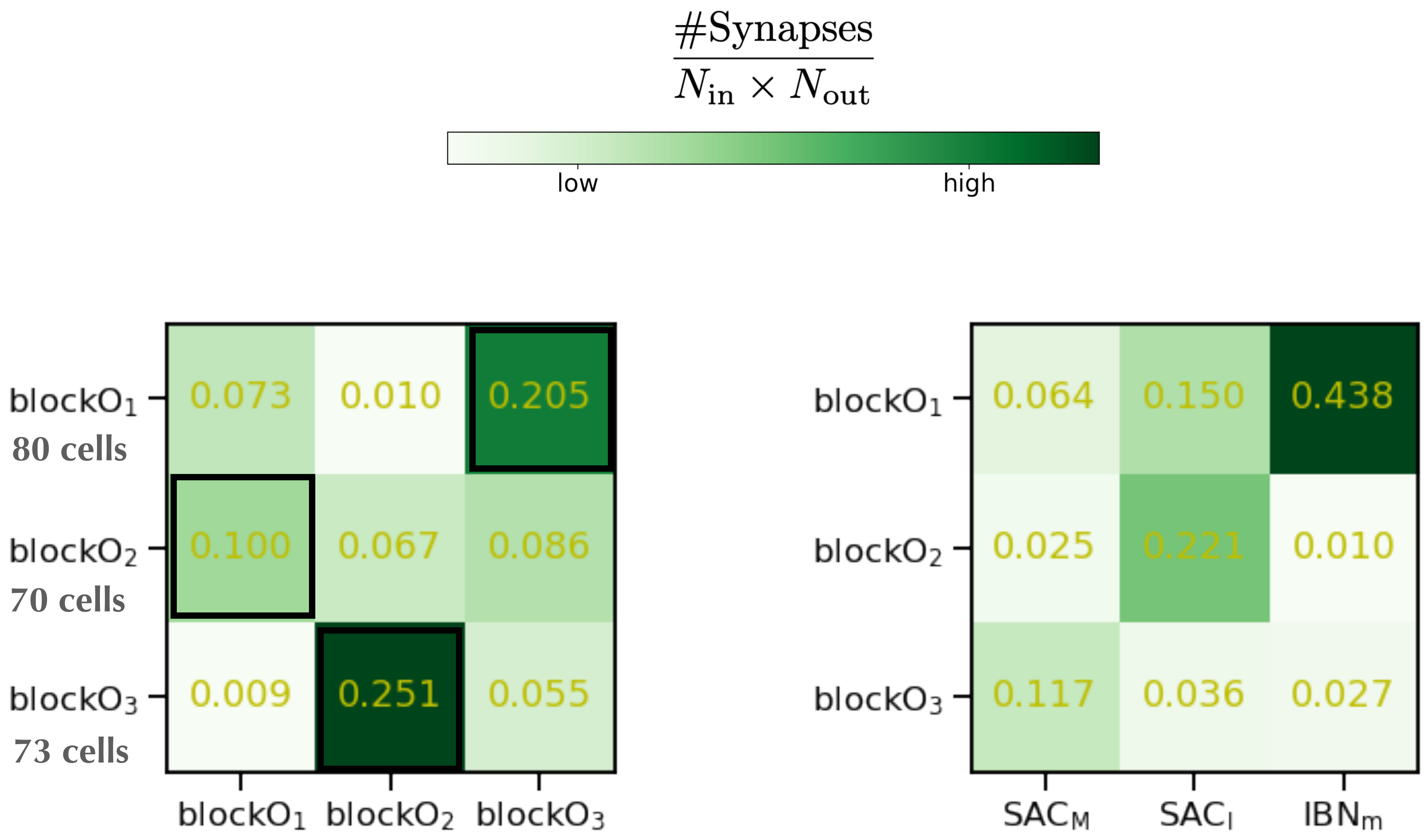

	blockO_1	blockO_2	blockO_3
blockO_1 80 cells	0.073	0.010	0.205
blockO_2 70 cells	0.100	0.067	0.086
blockO_3 73 cells	0.009	0.251	0.055

	SAC_M	SAC_l	IBN_m
blockO_1	0.064	0.150	0.438
blockO_2	0.025	0.221	0.010
blockO_3	0.117	0.036	0.027

Axonal-dendritic overlaps can explain the cyclic block structure

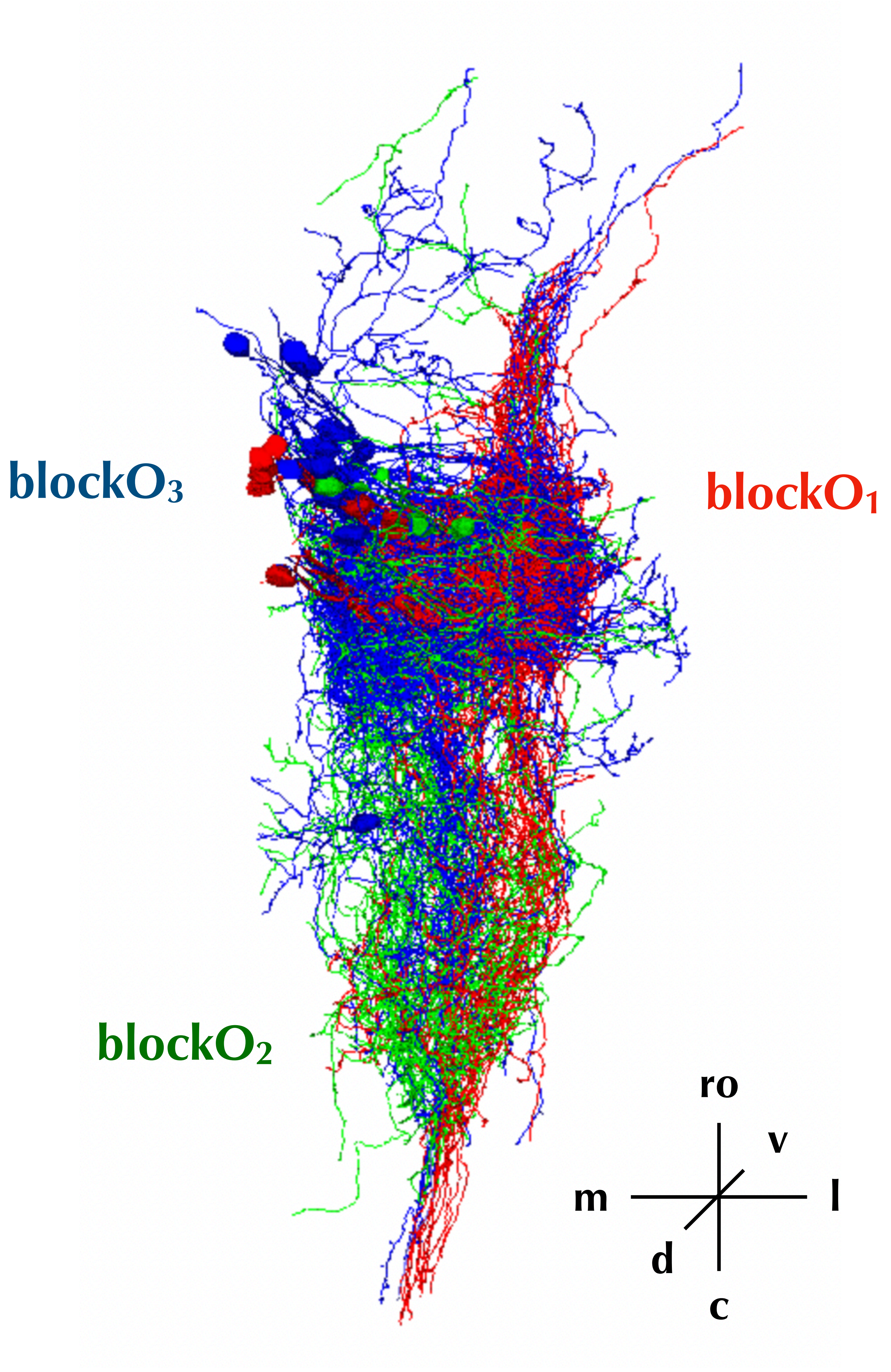

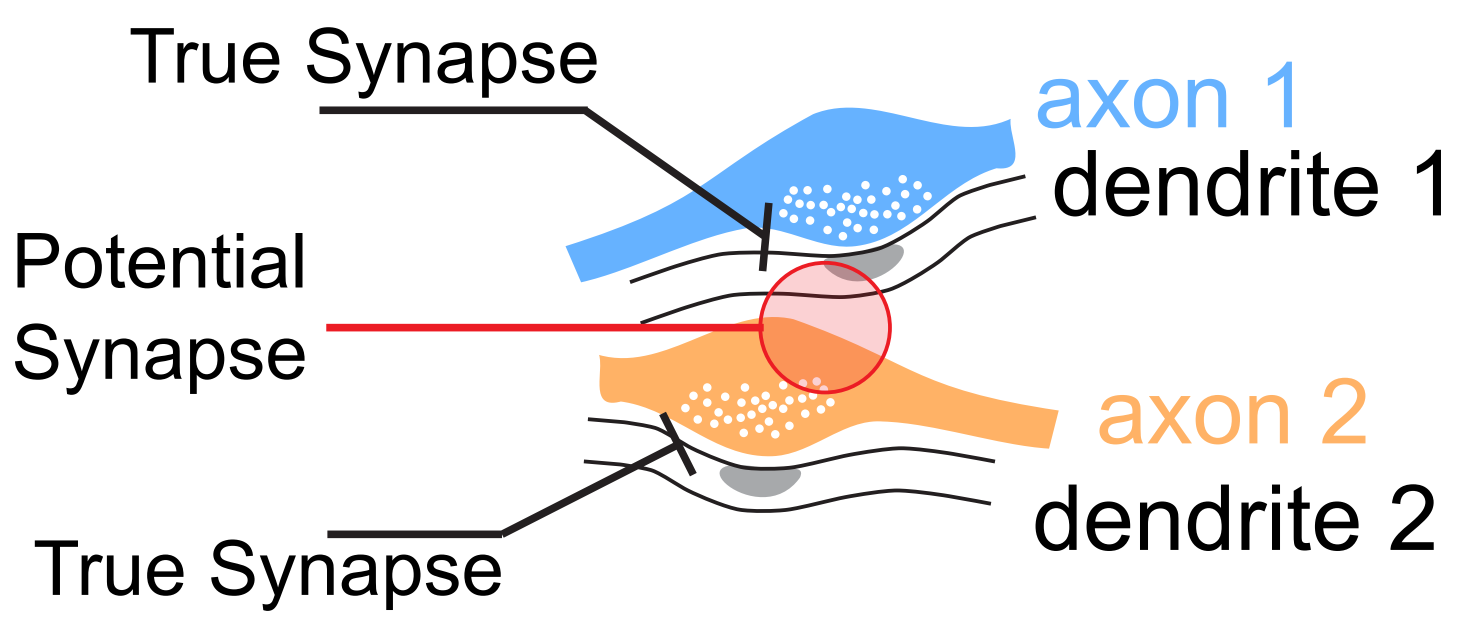

Potential synapses distance ≤ 2μm

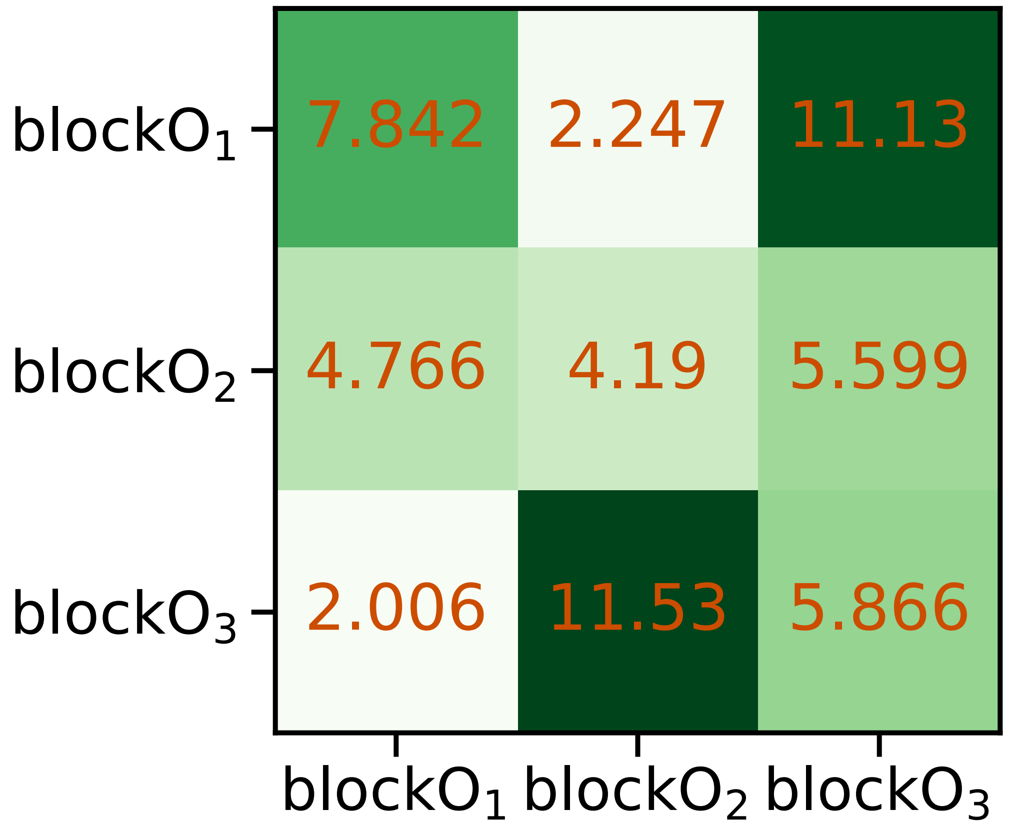

	blockO₁	blockO₂	blockO₃
blockO₁	7.842	2.247	11.13
blockO₂	4.766	4.19	5.599
blockO₃	2.006	11.53	5.866

Potential synapses distance ≤ 5μm

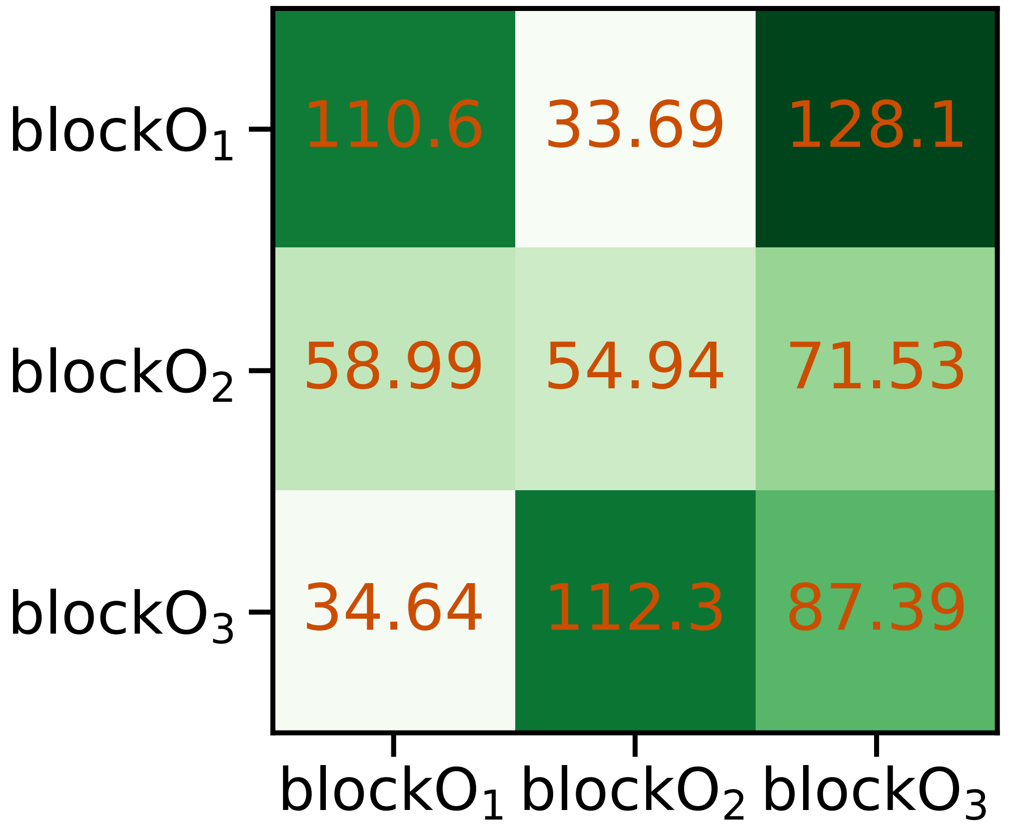

	blockO₁	blockO₂	blockO₃
blockO₁	110.6	33.69	128.1
blockO₂	58.99	54.94	71.53
blockO₃	34.64	112.3	87.39

Potential synapses distance ≤ 10μm

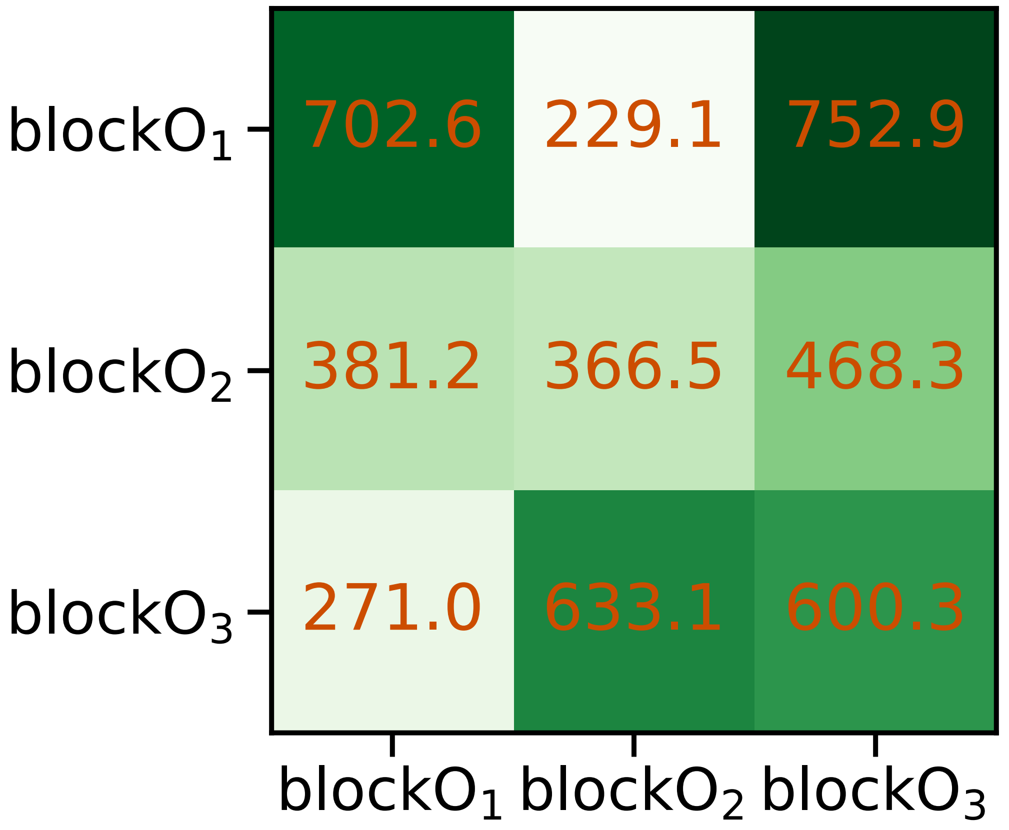

	blockO₁	blockO₂	blockO₃
blockO₁	702.6	229.1	752.9
blockO₂	381.2	366.5	468.3
blockO₃	271.0	633.1	600.3

What could be the potential function of cellular 3-cycles?

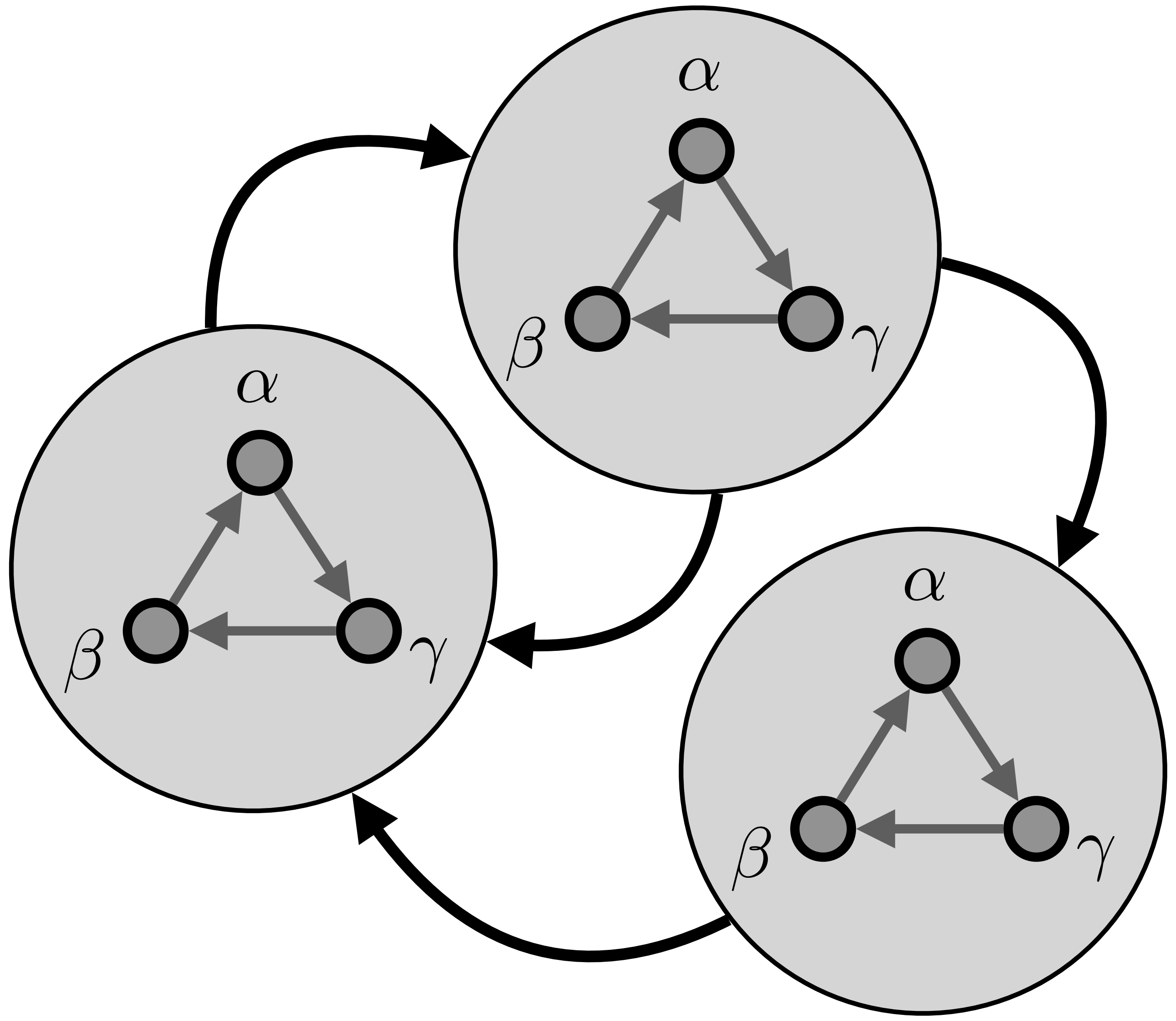

Each unit has a longer effective cellular time constant

Embedding 3-cycle units in the larger network lowers the need for tight tuning globally. (Koulakov et al. 2002)

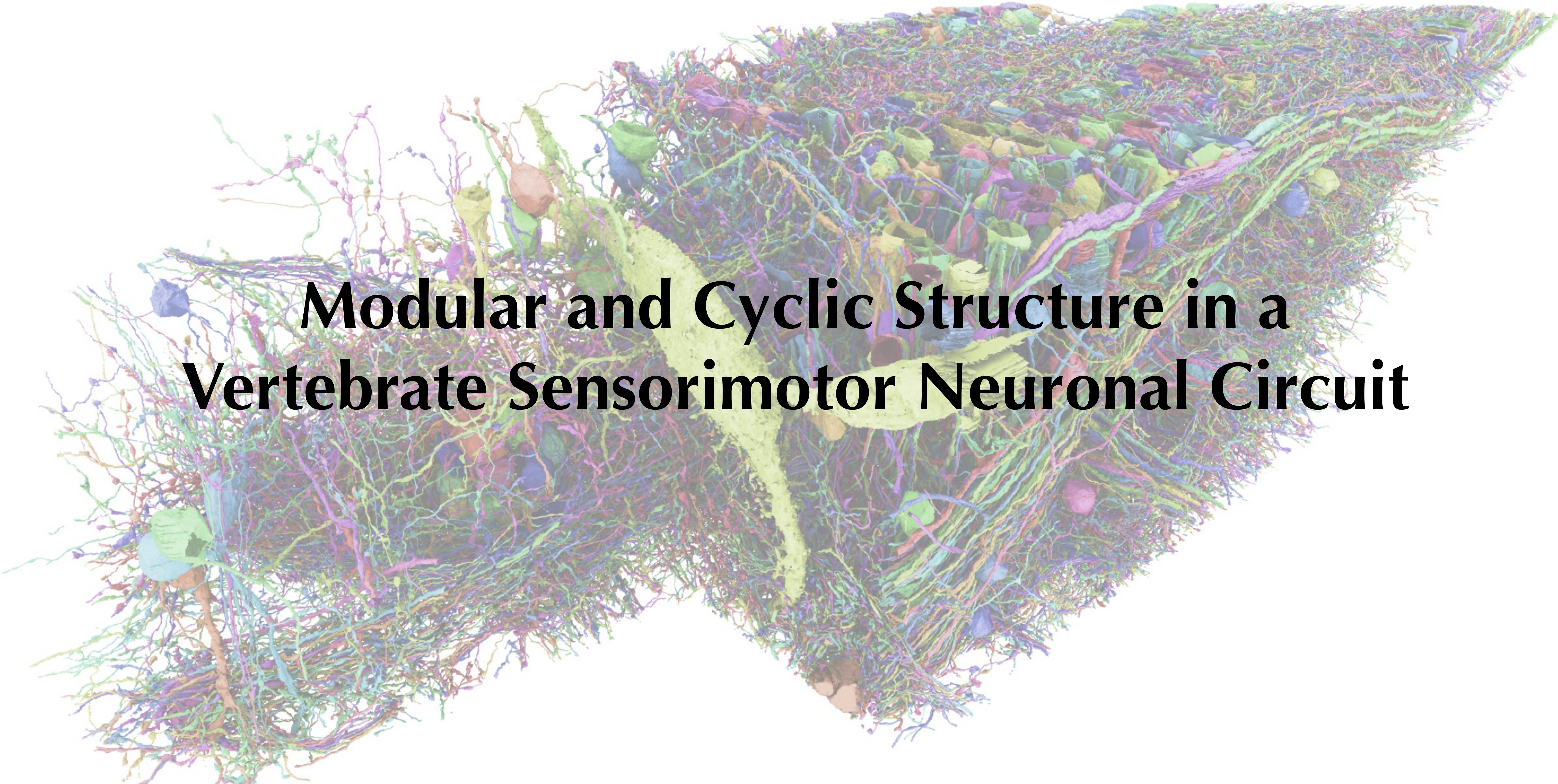

Modular and Cyclic Structure in a Vertebrate Sensorimotor Neuronal Circuit

“Tony” Runzhe Yang

Dr. Ashwin Vishwanathan

Prof. Emre Aksay

Prof. Mark Goldman

Prof. Sebastian Seung

Supplementary Slides

Rapid transition and long persistence of horizontal eye position

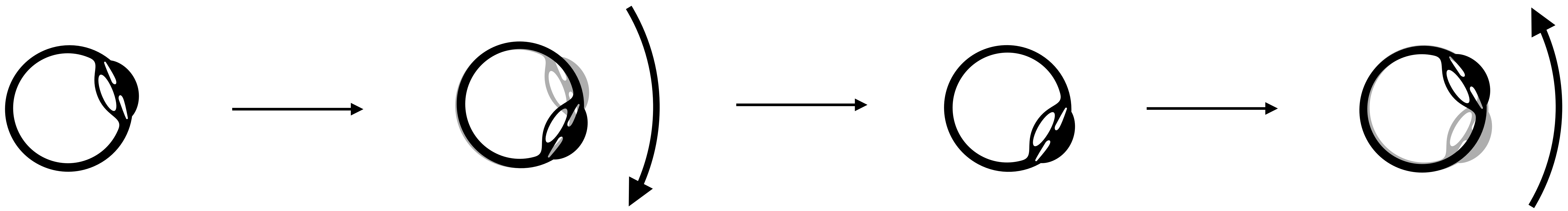

saccade
~100 msec

fixation
1 sec~min

the brain is able to remember horizontal eye positions between two fast movements.

Neural integrators encode eye position as persistent neural activity

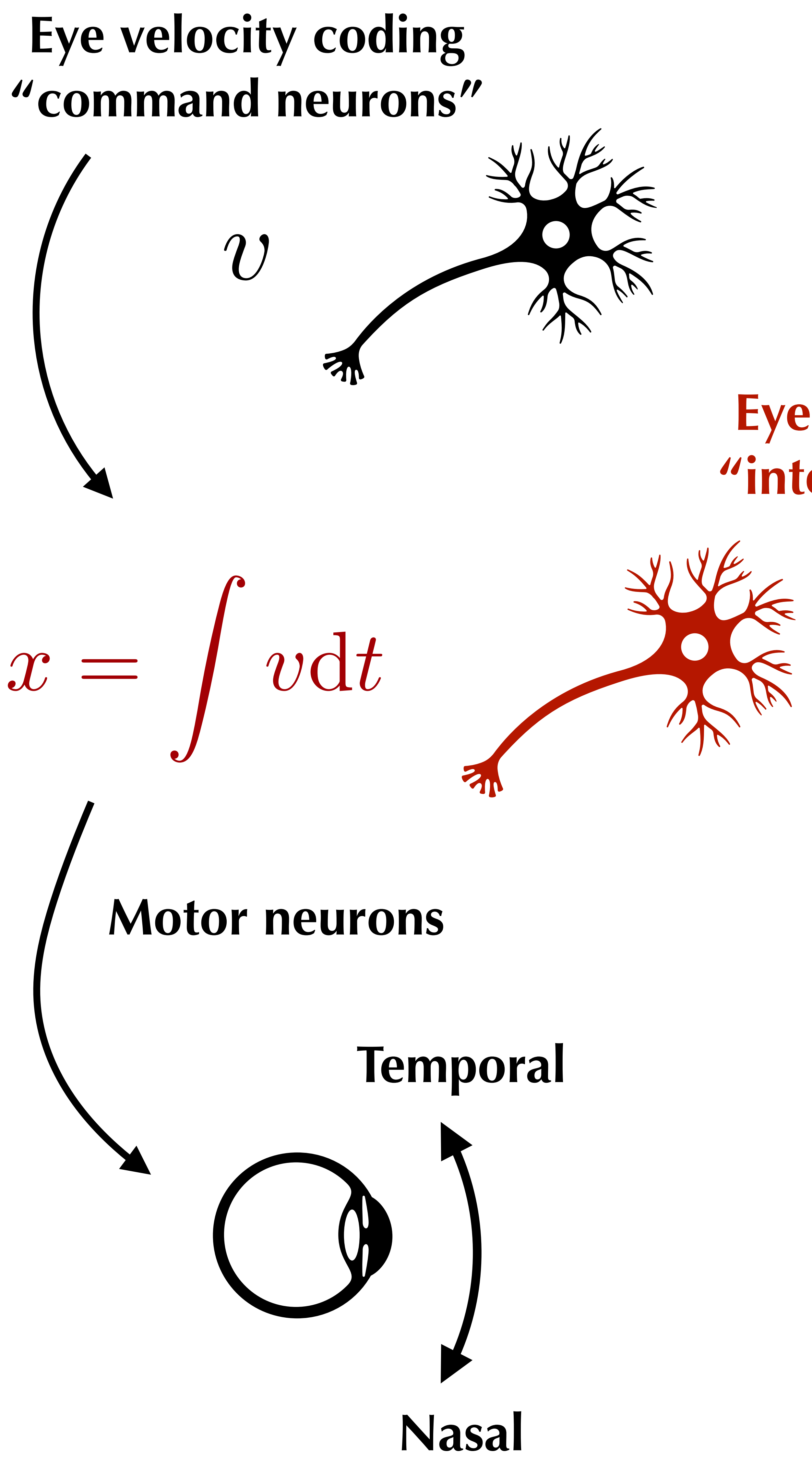

Eye velocity coding
“command neurons”

v

$$x = \int v\mathrm{dt}$$

Eye position coding
“integrator neurons”

Motor neurons

Temporal

Nasal

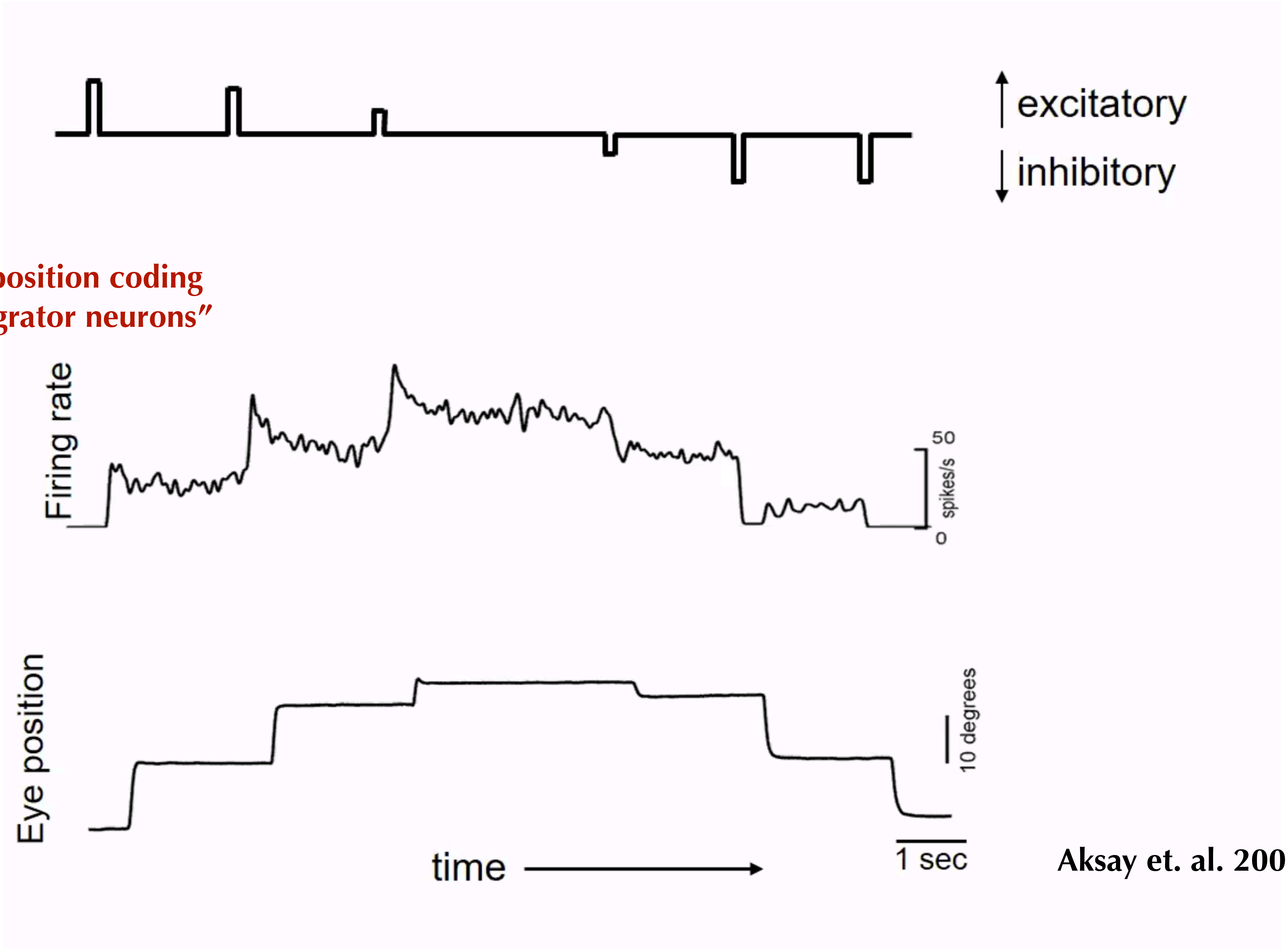

Aksay et. al. 2001

The line attractor model requires recurrent connections

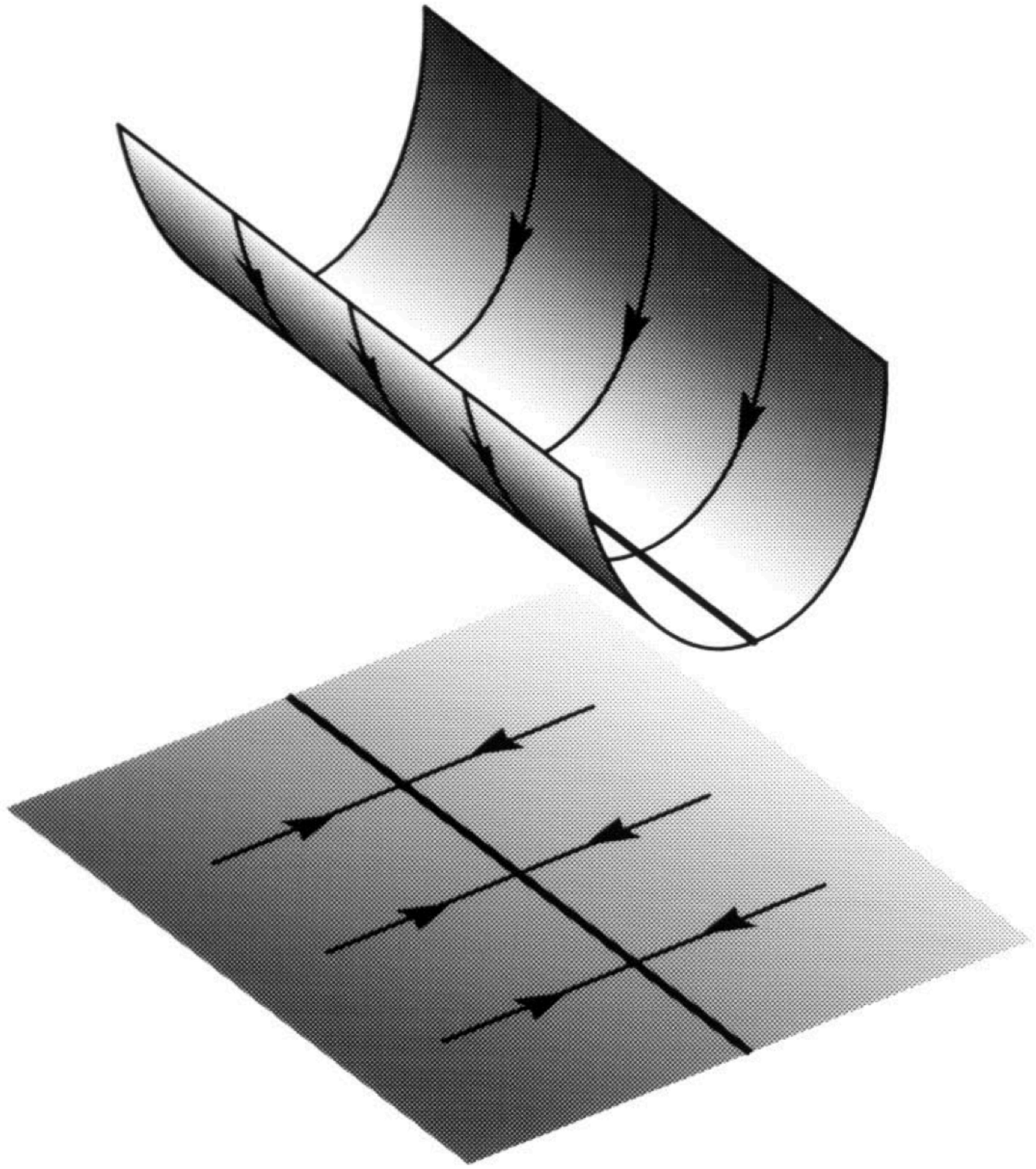

Seung 1996

$$v_i \approx g_i u_i + v_i^p.$$

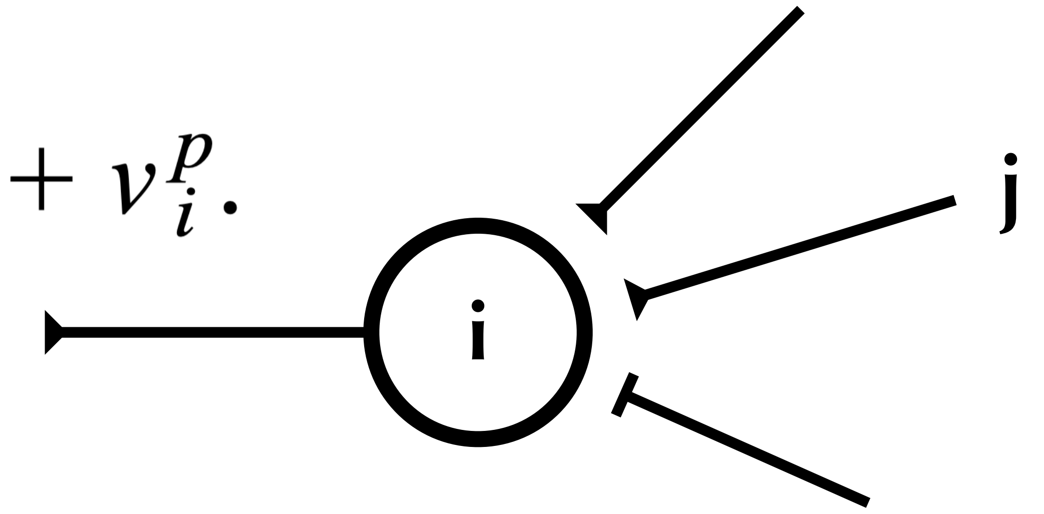

time scale 150ms

presynaptic firing rate

$$\tau_s \frac{du_i}{dt} + u_i = \sum_{j=1}^{N} T_{ij} v_j + h_i.$$

total postsynaptic current

synaptic strength

input from the vestibular afferents

synaptic weight matrix

$$W_{ij} = g_i T_{ij}$$

$$v_i = \sum_{j=1}^{N} W_{ij} v_j + f_i.$$

"force" on neuron *i*

$$f_i = g_i h_i + v_i^p$$

The oculomotor diagram

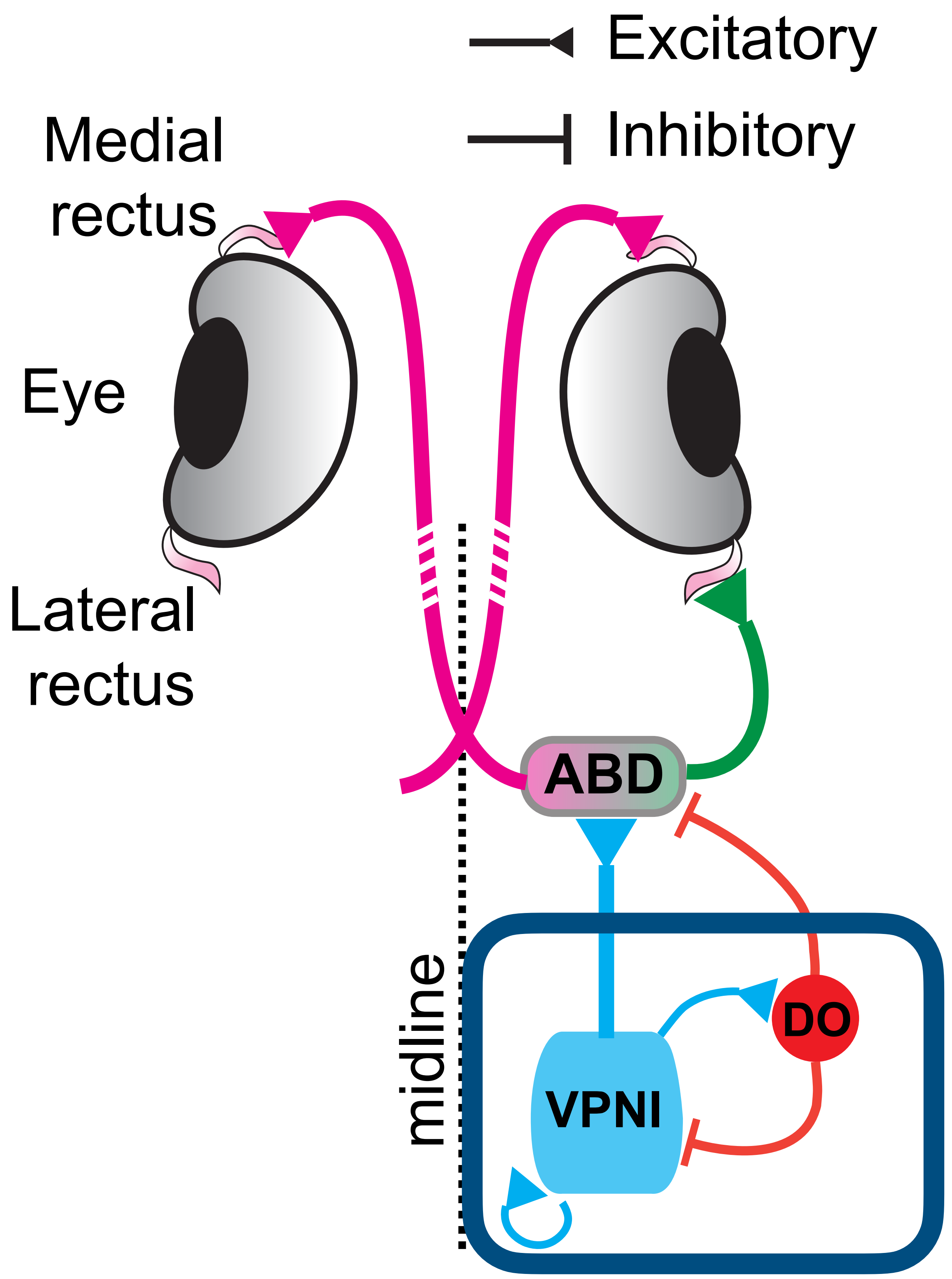

Oculomotor Module

Most cellular 3-cycles are among integrator neurons

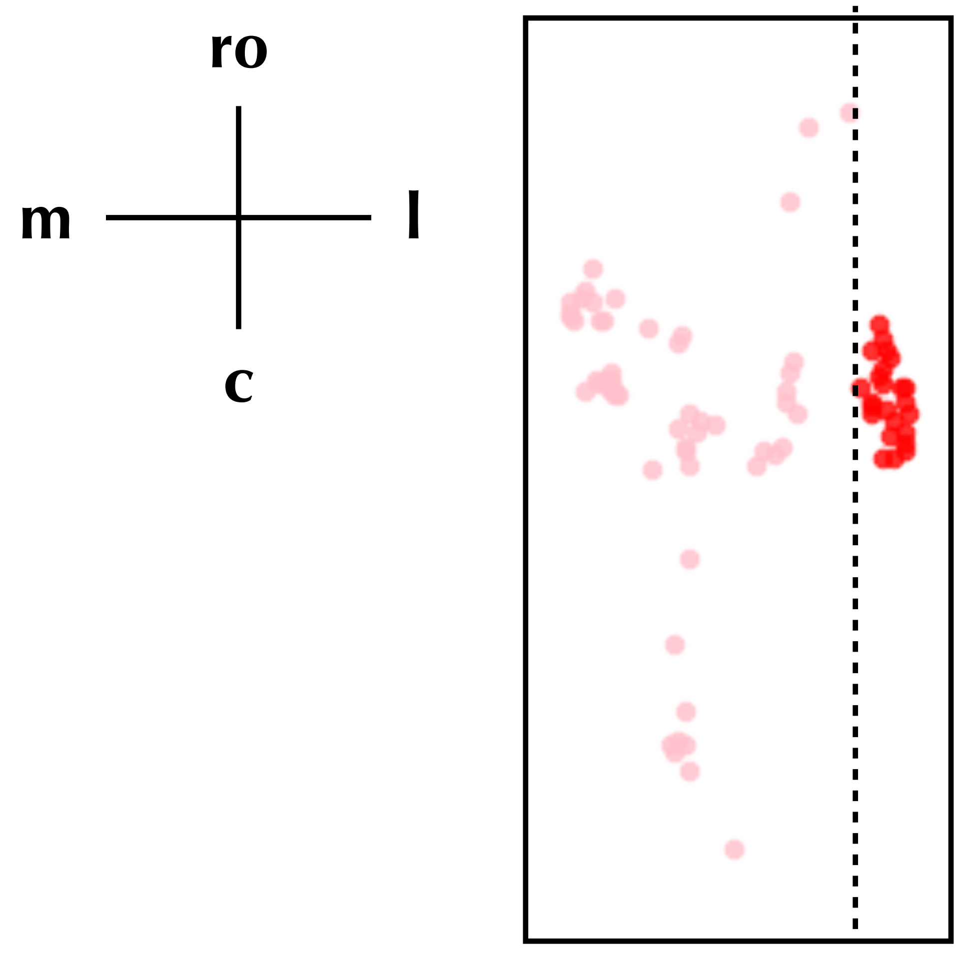

blockO_1 somata

Inferred DO neurons

Inferred integrator neurons

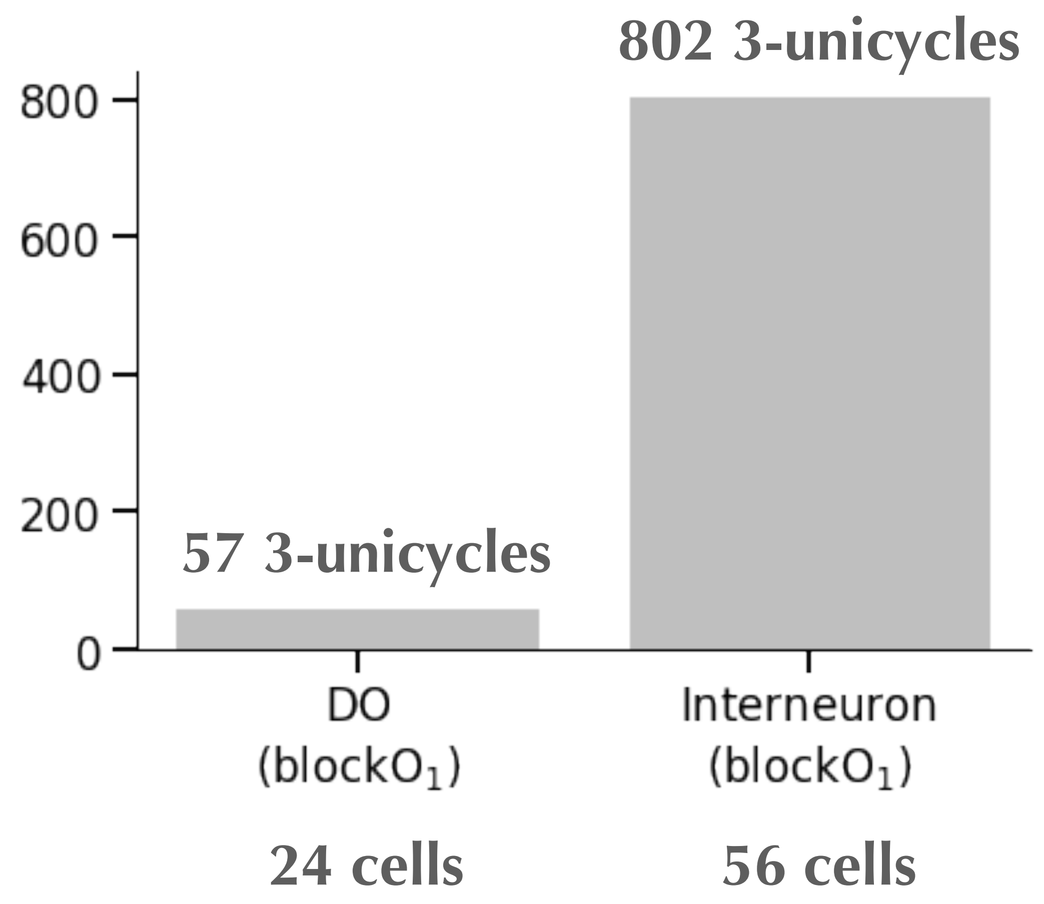

Wiring diagram of 3-block modO

Intra-block connections

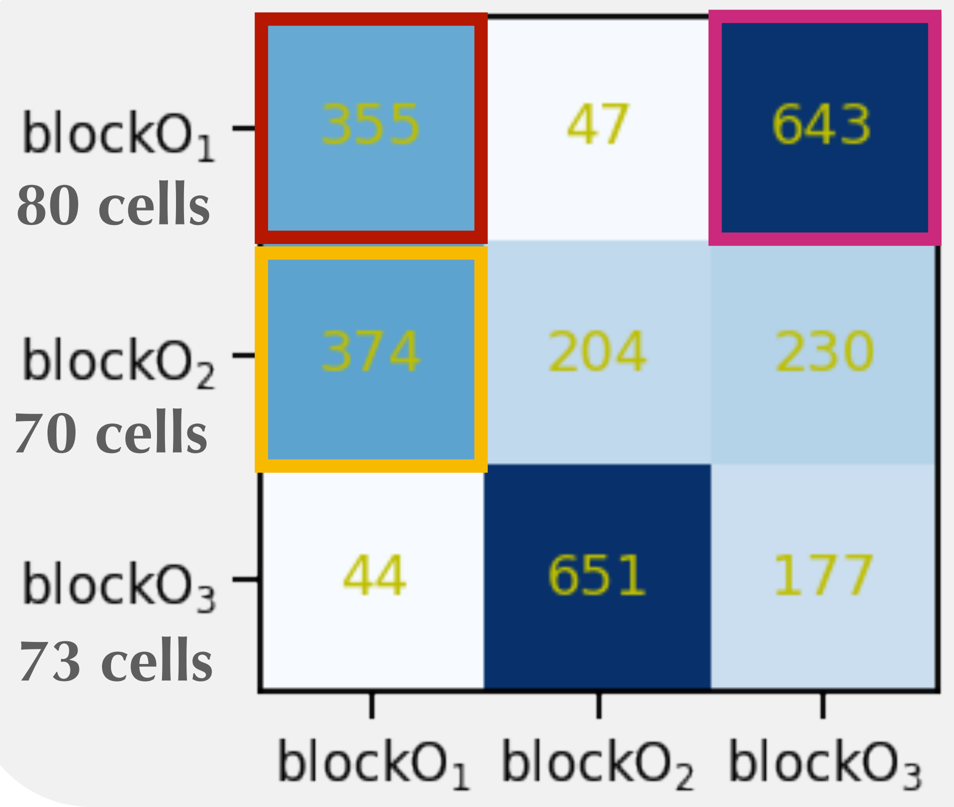

	blockO_1	blockO_2	blockO_3
blockO_1 80 cells	355	47	643
blockO_2 70 cells	374	204	230
blockO_3 73 cells	44	651	177

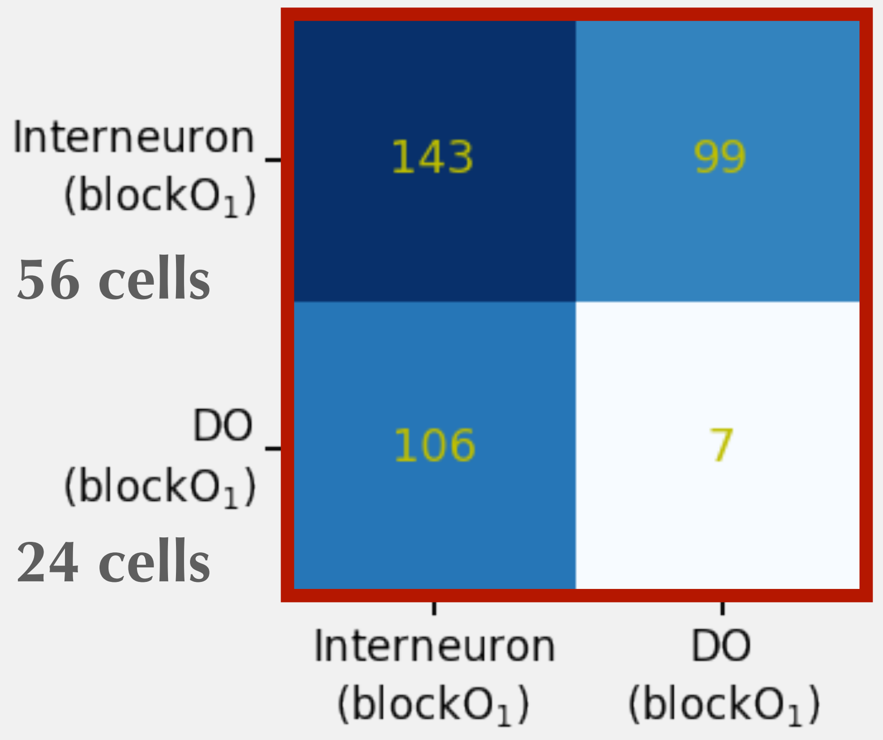

	Interneuron (blockO_1)	DO (blockO_1)
Interneuron (blockO_1) 56 cells	143	99
DO (blockO_1) 24 cells	106	7

Inputs to blockO_1

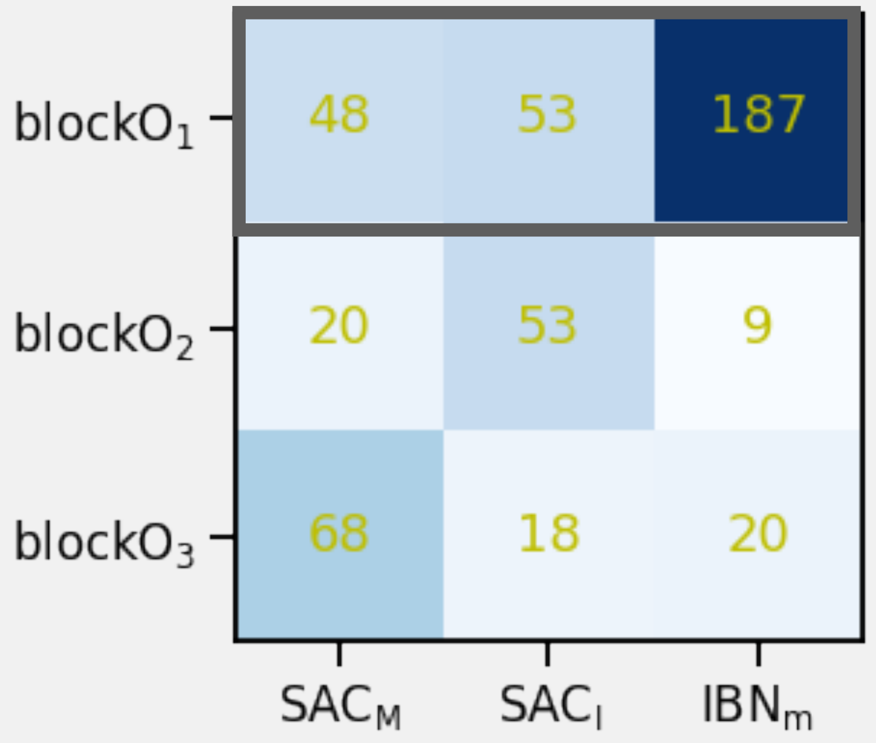

	SAC_M	SAC_l	IBN_m
blockO_1	48	53	187
blockO_2	20	53	9
blockO_3	68	18	20

	blockO_3	SAC_M	SAC_l	IBN_m
Interneuron (blockO_1)	518	47	52	187
DO (blockO_1)	125	1	1	0

Outputs from blockO_1

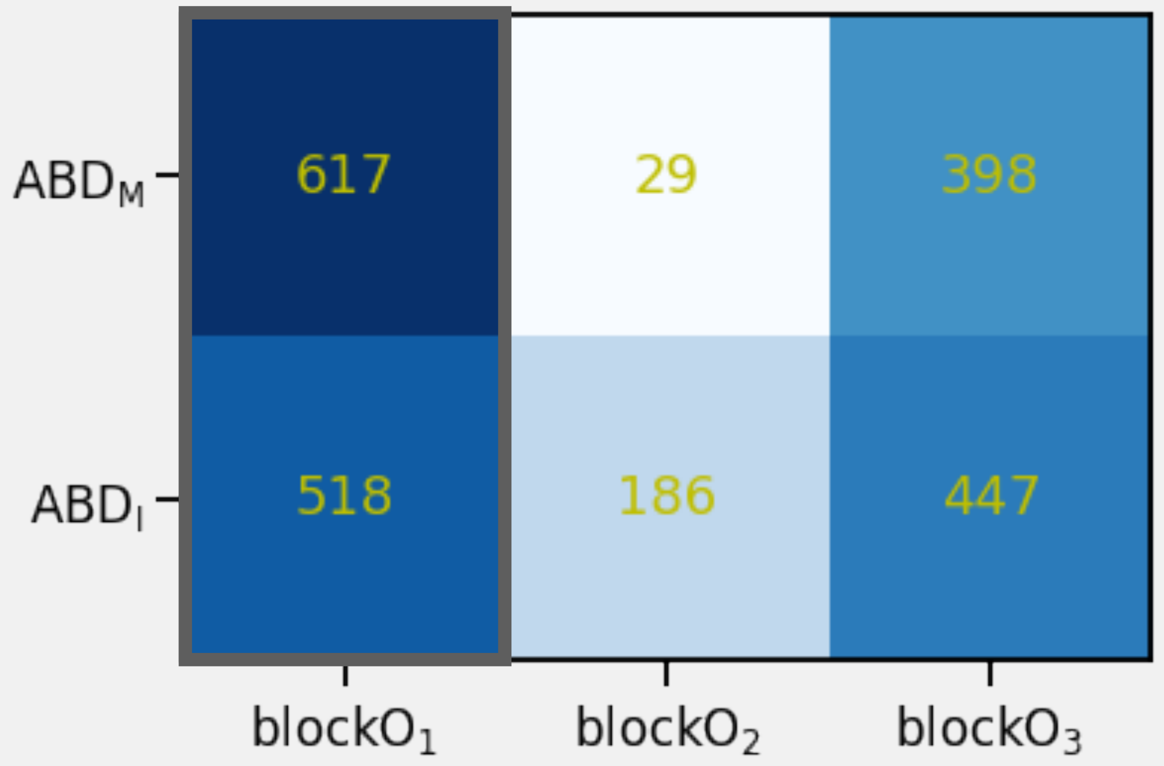

	blockO_1	blockO_2	blockO_3
ABD_M	617	29	398
ABD_l	518	186	447

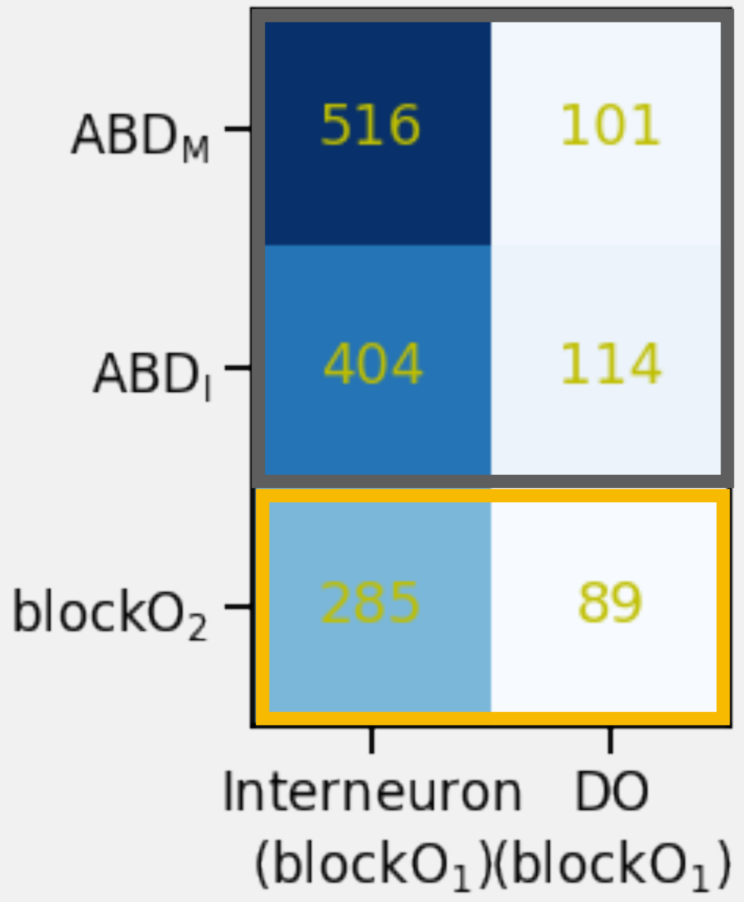

	Interneuron (blockO_1)	DO (blockO_1)
ABD_M	516	101
ABD_l	404	114
blockO_2	285	89

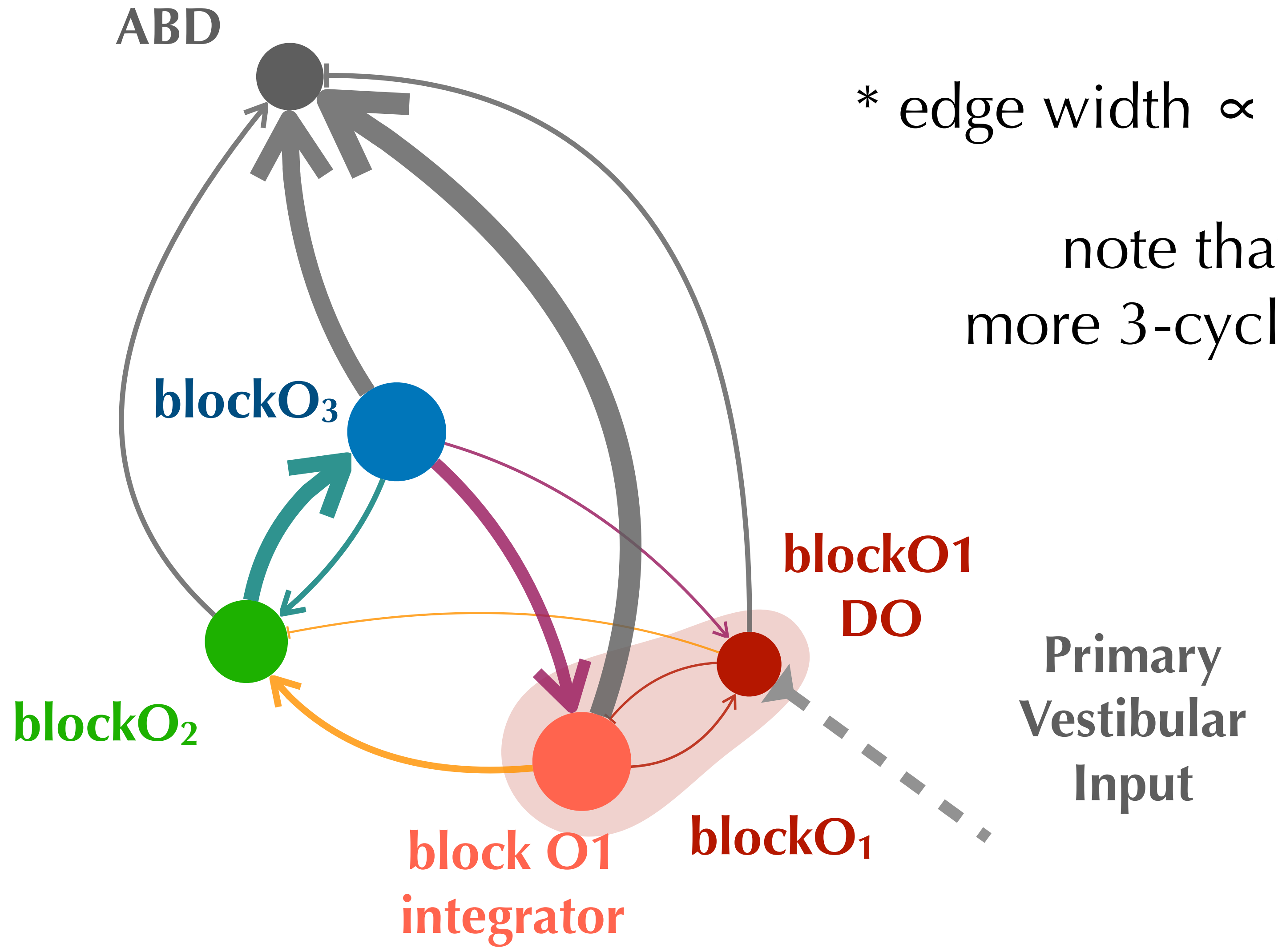

* edge width ∝ number of connections

note that we have much more 3-cycles than expectation

What could be the potential function of cellular 3-cycles?

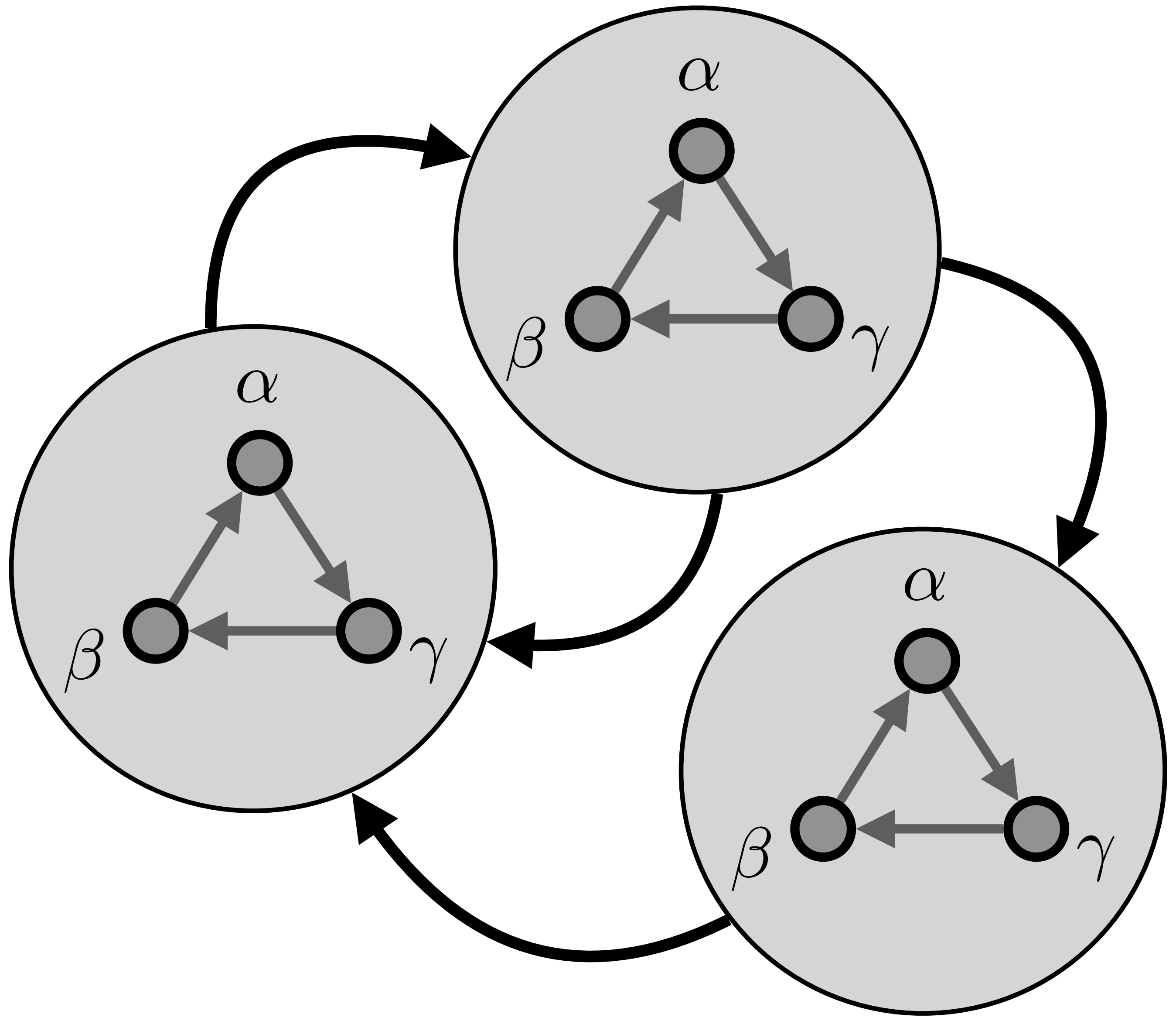

Each unit has a longer effective cellular time constant

Embedding 3-cycle units in the larger network lowers the need for tight tuning globally. (Koulakov et al. 2002)